NASA CONTRACTOR REPORT

NASA CR-883

NASA CR-883

FACILITY FORM 602

N[redacted]39
(ACCESSION NUMBER)
95
(PAGES)
(NASA CR OR TMX OR AD NUMBER)
(THRU)
1
(CODE)
31
(CATEGORY)

LUN[redacted]

Photog[redacted]

Prepared b[redacted]
THE BOE[redacted]
Seattle, W[redacted]
for Langley[redacted]

NATIONAL [redacted] TON, D. C. • OCTOBER 1967

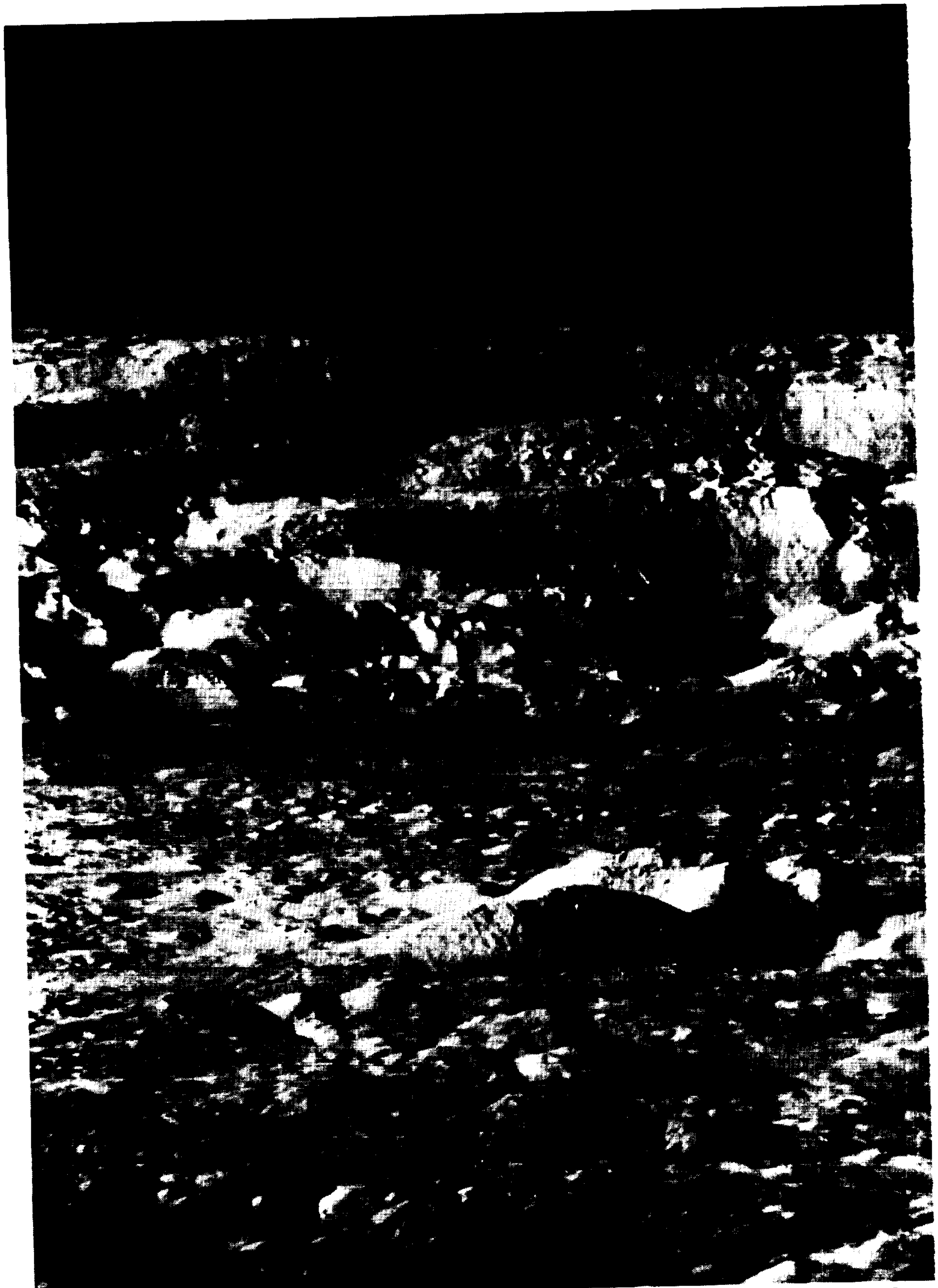

THE CRATER COPERNICUS – Photo taken by NASA-Boeing Lunar Orbite
November 23, 1966, 00:05:42 GMT, from a
of 150 miles.

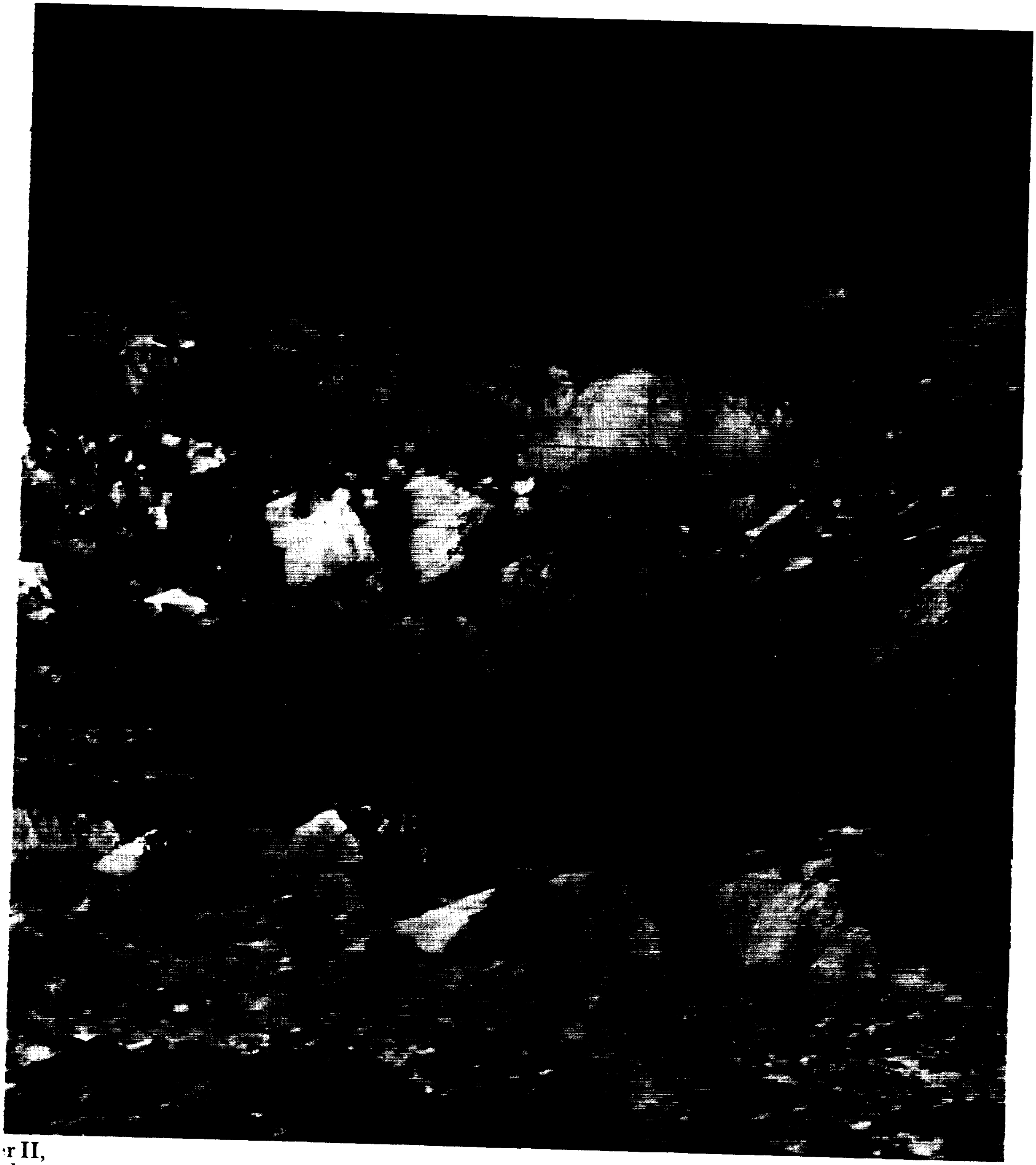

·r II,
distance

NASA CR-883

LUNAR ORBITER II

Photographic Mission Summary

Distribution of this report is provided in the interest of information exchange. Responsibility for the contents resides in the author or organization that prepared it.

Issued by Originator as Document No. D2-100752-1

Prepared under Contract No. NAS 1-3800 by
THE BOEING COMPANY
Seattle, Wash.

for Langley Research Center

NATIONAL AERONAUTICS AND SPACE ADMINISTRATION

For sale by the Clearinghouse for Federal Scientific and Technical Information
Springfield, Virginia 22151 – CFSTI price $3.00

CONTENTS

FIGURES

TABLES

ILLUSTRATIONS

PRECEDING PAGE BLANK NOT FILMED.

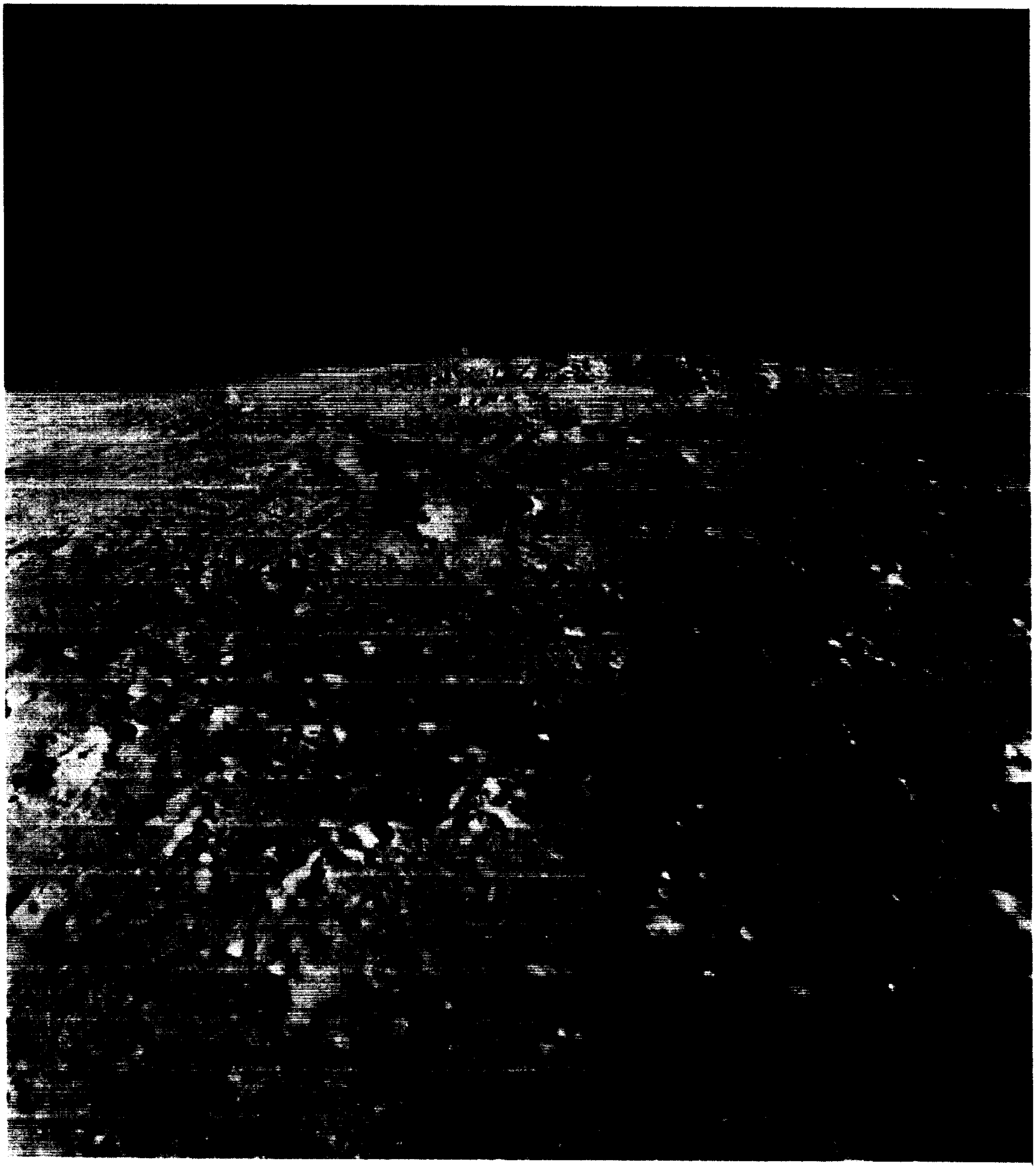

Wide-Angle Frame 162 – Site IIS-12

Looking north toward the crater Copernicus

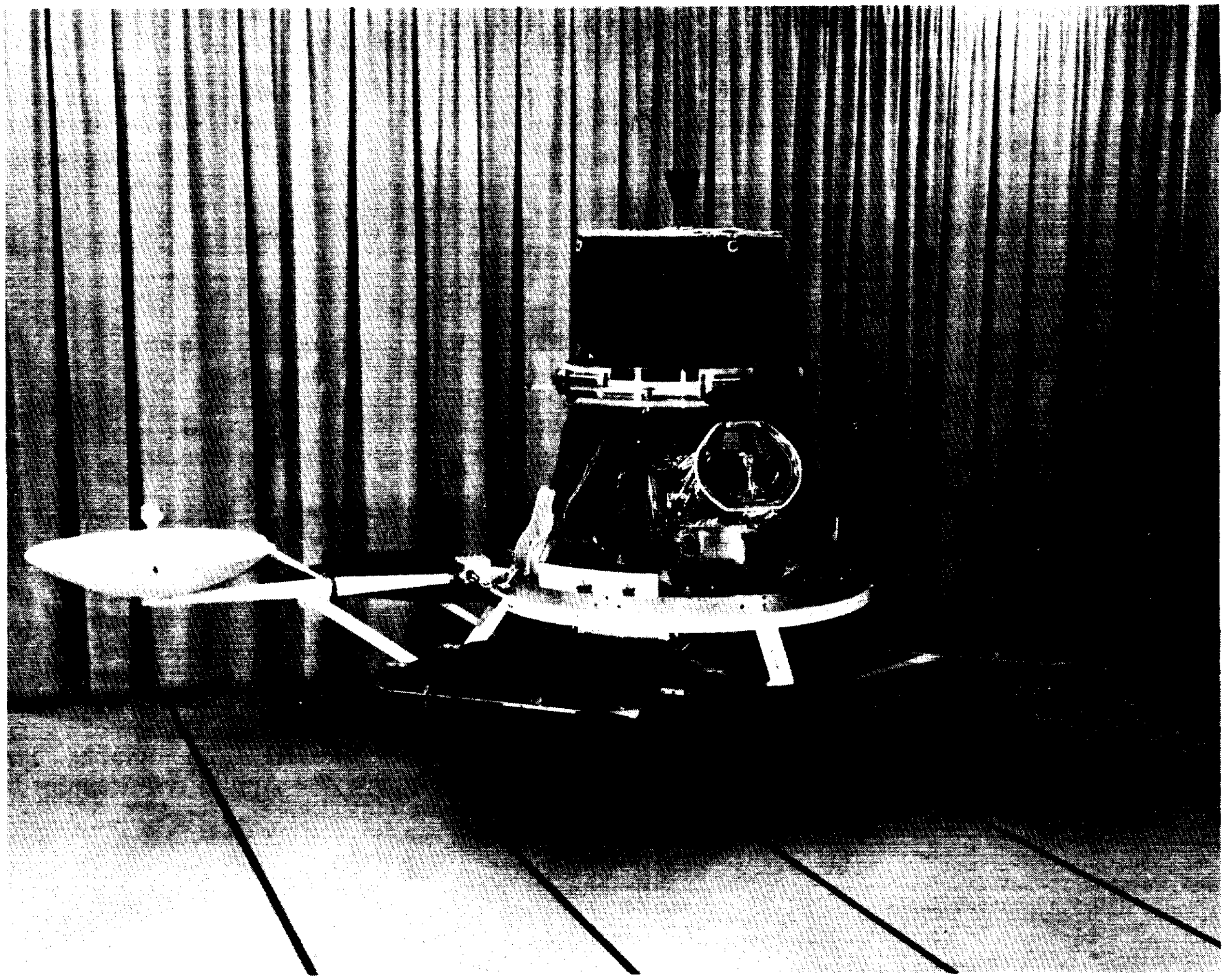

The Lunar Orbiter Spacecraft

LUNAR ORBITER II

1.0 PHOTOGRAPHIC MISSION SUMMARY

The second of five Lunar Orbiter spacecraft was successfully launched from Launch Complex 13 at the Air Force Eastern Test Range by an Atlas-Agena launch vehicle at 23:21 GMT on November 6, 1966. Tracking data from the Cape Kennedy and Grand Bahama tracking stations were used to control and guide the launch vehicle during Atlas powered flight. The Agena-spacecraft combination was maneuvered into a 100-nautical-mile-altitude Earth orbit by the preset on-board Agena computer. In addition, the Agena computer determined the maneuver and engine-burn period required to inject the spacecraft on the cislunar trajectory 20 minutes after launch. Tracking data from the down-range stations and the Johannesburg, South Africa station were used to monitor the entire boost trajectory.

Shortly after spacecraft separation the deployment sequences were completed, the Sun acquired, and the spacecraft was acquired by the Deep Space Network tracking stations.

Canopus was acquired during the first attempt 9 hours after launch. The single midcourse maneuver was executed 44 hours after launch. The spacecraft velocity control engine was ignited 92.5 hours after launch to inject the spacecraft into an elliptical lunar orbit with a perilune of 196 km. After 33 orbits the spacecraft velocity was reduced to transfer to the photographic orbit with a perilune of 49.7 km.

The first of 13 primary and 17 secondary photo sites was photographed on November 18, 11 days and 16 hours after launch. A total of 184 primary-site photos were taken on 22 orbits. The 27 secondary-site photos were taken on 18 orbits. During the 7 days required to photograph the selected sites, portions or all of 49 telephoto and 45 wide-angle photos were read out and transmitted to the stations during the priority readout period. The photographic phase of the mission was completed on November 26 when the desired film processing was completed, the Bimat web cut, and the final readout period initiated.

Readout and examination of photos continued in a routine manner for the next 11 days and 72 readout periods. On December 7 the traveling-wave-tube amplifier failed to turn on. Repeated attempts to reactivate the amplifier were unsuccessful and the photographic mission was terminated midway through the readout of Site IIP-1. The combined priority and final readout provided 100% of the wide-angle coverage of this site. Portions of six of the remaining eight telephoto frames to be read out at the time of the failure were obtained during priority readout.

All the primary sites were photographed by near-vertical photography (except Site IIP-5, where a small roll maneuver was required to obtain the desired coverage). Secondary-site photography included vertical, oblique, and convergent telephoto stereo photography.

During the photographic mission the spacecraft recorded three hits by the micrometeoroid detectors mounted on the periphery of the engine deck. An additional possible hit was indicated by a change in temperature detected by a thermistor mounted on the tank deck.

All mission objectives were satisfactorily accomplished, except for the reconstruction of a small area of Primary Site IIP-1 photographs. This mission completes the Apollo requirement for two area-search missions.

Wide-Angle Frame 215 – Site IIS-17

Looking north – shows ray structure in Oceanus Procellarum.

1.1 INTRODUCTION

The Lunar Orbiter program was formalized by Contract NAS1-3800 on May 7, 1964, as one of the lunar and planetary programs directed by the NASA headquarters Office of Space Sciences and Applications. The program is managed by the Langley Research Center, Hampton, Virginia, with The Boeing Company as the prime contractor. Lunar Orbiter is the third in a succession of unmanned missions to photograph the Moon and to provide lunar environmental data to support the Apollo manned lunar landing mission.

The three successful Ranger flights each provided a series of photographs of decreasing area and increasing resolution (to a fraction of a foot) as each spacecraft approached and impacted the Moon. The Surveyor provides detailed information on lunar surface characteristics (with resolution in millimeters) in the immediate area of each successful soft landing. Surveyor contributes small-scale relief and soil mechanics data limited to the line of sight surrounding the landing site.

The Lunar Orbiter prime mission is to photograph large areas at a resolution level adequate to provide information for selection and verification of suitable landing sites for manned Apollo vehicles and unmanned Surveyor vehicles. Monoscopic coverage at approximately 1-meter resolution and stereoscopic photographs at approximately 8-meter resolution at a nominal altitude of 46 km are to be obtained of each primary photo site.

1.1.1 PROGRAM DESCRIPTION

The Lunar Orbiter system design was based on the requirement to photograph specific target sites within an area of interest bounded by ± 10-degree latitude and ± 60-degree longitude. Types of photo missions within the primary region are classified as:

- Single-site search and examination;
- Large-area search;
- Spot photos;
- Combinations of above.

Designated areas of scientific interest and landmarks for Apollo navigation outside of the primary area may also be photographed.

Lighting conditions and altitude must be adequate for detection of:

- Features equivalent to a cone having a 2-meter base diameter and 0.5-meter height;
- An area 7 by 7 meters of 7-degree slope (When sloped in a direction to provide maximum contrast with surrounding area).

The original plan required that each of the five missions (during the 1966 to 1967 period) provide topographic information of at least 8,000 square kilometers at nominal 1-meter resolution and approximately 40,000 square kilometers at nominal 8-meter resolution. This coverage can be obtained by single photographs or by 4-, 8-, or 16-exposure sequences in either of two automatic sequencing modes (nominal 2 or 8 seconds between exposures).

In addition to the five flight spacecraft, three ground test spacecraft are included in the comprehensive ground test and flight program. The ground test spacecraft were used for the qualification test program, mission simulation testing in an environmental space chamber, and performance demonstration and tests of spacecraft compatibility with ground support facilities.

Additional program requirements include the collection of selenodetic data which can be used to improve the definition of the lunar gravitational field, and knowledge of the size and shape of the Moon. Radiation intensity and micrometeoroid impact measurements are also to be obtained to further define the lunar environment.

At the completion of each photographic mission (approximately 30 to 35 days after launch), the spacecraft may remain in lunar orbit for an extended period to obtain additional tracking data, continue environmental monitoring, and conduct scientific experiments.

The Lunar Orbiter I mission provided extensive moderate-resolution coverage of the nine primary Apollo sites, as well as area photographs of eight proposed site areas for the Lunar Orbiter II mission. Mission I provided a wealth of terrain data for evaluation and redesign of Mission II. Mission I primary sites were located along a southern latitude band within the established Apollo zone of interest (± 5° latitude and ± 45° longitude).

Mission II sites were located along a northern latitude band in the Apollo zone. The combination of these two missions supports the Apollo requirement of at least two Lunar Orbiter site search missions.

1.1.2 PROGRAM MANAGEMENT

Successful accomplishment of Lunar Orbiter program objectives requires the integrated and cooperative efforts of government agencies, private contractors, numerous subcontractors, and the worldwide data collection system of the NASA Deep Space Network. The functional relationship and responsibilities of these organizations are shown in Figure 1.1-1.

As the prime contractor, Boeing is responsible to the Lunar Orbiter Project Office of the NASA-Langley Research Center for the overall project management and implementation of the complete operating system. Boeing is also responsible for the establishment – with and through the NASA-Langley Research Center – of effective working relationships with all participating government agencies.

The NASA Lewis Research Center supports the Lunar Orbiter program by providing the Atlas-Agena launch vehicle and associated services that are necessary to: (1) ensure compatibility of the spacecraft with the launch vehicle; and (2) launch and boost the spacecraft into the proper cislunar trajectory.

The Air Force Eastern Test Range (AFETR) provides facilities, equipment, and support required to test, check out, assemble, launch, and track the spacecraft and launch vehicle. The AFETR also controls the Atlas launch vehicle trajectory and monitors Agena performance through cislunar injection, separation, and retrofire to ensure orbital separation. Appropriate instrumentation facilities, communications, and data recorders are provided at downrange and instrumentation ships to ensure the availability of data for boost trajectory control, acquisition by the Deep Space Network (DSN), and postmission analysis.

The Deep Space Network (DSN) is managed by the Jet Propulsion Laboratory. This network, consisting of the Space Flight Operations Facility (SFOF) and the Deep Space Stations

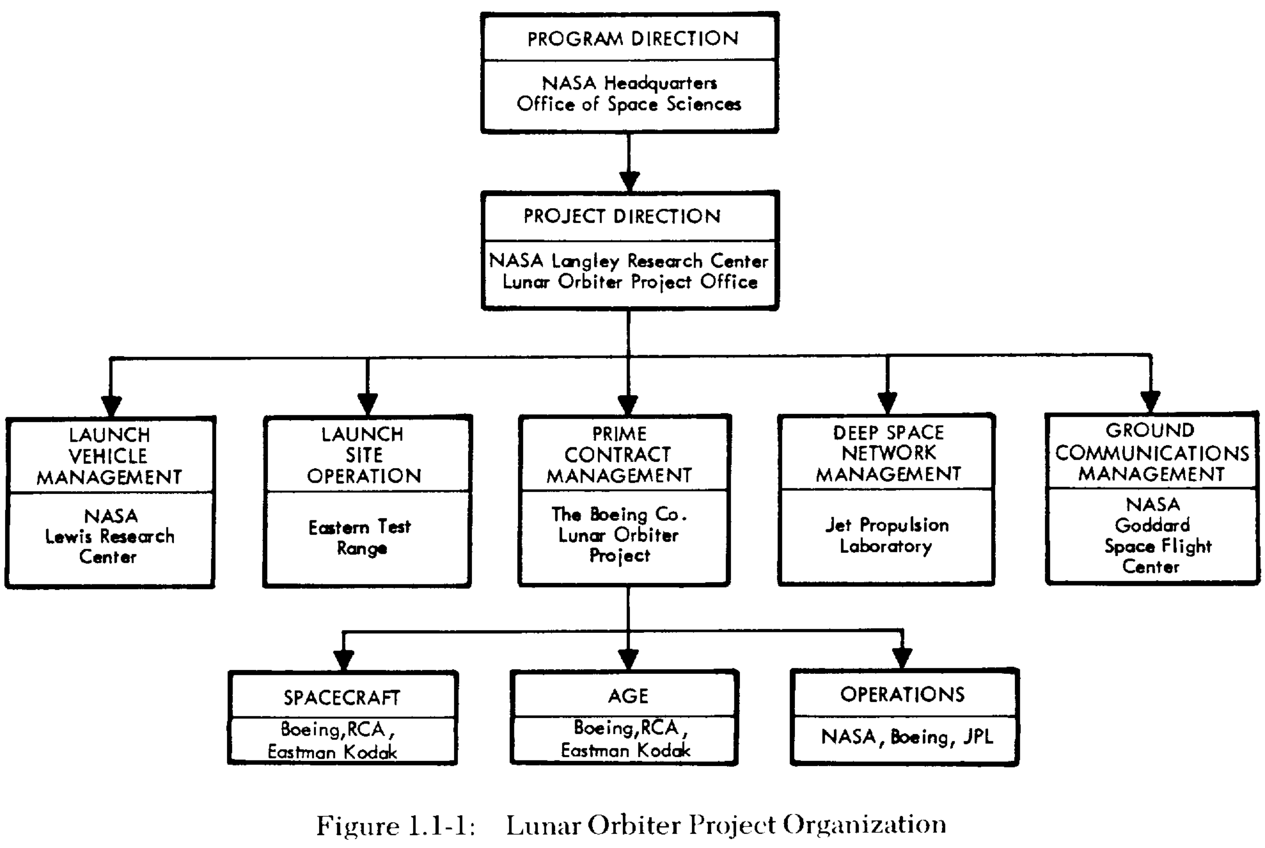

Figure 1.1-1: Lunar Orbiter Project Organization

(DSS), provides two-way communications with the spacecraft, data collection, and data processing. Facilities are provided for operational control which interface with Lunar Orbiter mission-peculiar equipment. Support is also provided in terms of personnel, equipment calibration, and housekeeping services.

Goddard Space Flight Center is the agency responsible for the worldwide network of communication lines necessary to ensure prompt distribution of information between the several tracking stations and the Space Flight Operations Facility during the mission and mission training periods.

1.1.3 PROGRAM OBJECTIVES

The prime project objective of the Lunar Orbiter mission is to secure topographic data regarding the lunar surface for the purpose of extending our scientific knowledge, and selecting and confirming landing sites for Apollo. To accomplish the objective, high-resolution photographic data covering specified areas on the lunar surface and moderate-resolution photographic data coverage of extensive areas are necessary.

Other objectives are to secure information concerning the size and shape of the Moon, the properties of its gravitational field, and lunar environmental data.

Selection of the photo sites for each Lunar Orbiter mission is based on Apollo constraints and preferences as modified to reflect the knowledge gained by preceding missions. The present Apollo constraints and preferences indicate that a minimum of two Lunar Orbiter site search missions are required. Lunar Orbiter I photographed a series of primary sites located along a southern latitude band within the ± 5-degree latitude and ± 45-degree longitude Apollo zone.

Landing sites are desired at a number of locations to fulfill the exploration and scientific objectives of the Apollo program and to provide an adequate launch window. The topography of an Apollo landing site must be smooth enough for an Apollo landing module (LM) landing and the approach terrain must be reasonably level to allow satisfactory LM landing radar performance. The surface resolution requirement to enable the selection of suitable sites for Apollo landings is approximately 1 meter.

The selenodetic and environmental mission data objectives require no special instrumentation. Tracking data obtained throughout the mission produce the basic data required to satisfy the selenodetic objectives. Micrometeoroid detectors mounted on the periphery of the spacecraft and radiation detectors mounted internally monitor the lunar environmental data on each flight for transmission to the ground stations.

1.1.3.1 Mission II Objectives

Specific objectives for Mission II were defined by NASA as follows:

"Primary:

- To obtain, from lunar orbit, detailed photographic information of various lunar areas, to assess their suitability as landing sites for Apollo and Surveyor spacecraft, and to improve our knowledge of the Moon.

Secondary:

- To provide precision trajectory information for use in improving the definition of the lunar gravitational field.
- To provide measurements of micrometeoroid flux and radiation dose in the lunar environment, primarily from spacecraft performance analysis."

The objectives and ground rules for Lunar Orbiter II stipulated that the primary sites to be photographed shall have promise of being acceptable Apollo landing sites considering location, topography, and soil mechanics. The sites shall also provide some engineering geology data to support the extrapolation of Surveyor data. Also included in the Lunar Orbiter II photographic mission was the impact area of Ranger VIII. Lunar Orbiter II photo sites were located along a northern latitude band within the Apollo zone, whereas Lunar Orbiter I sites were along a southern latitude band.

Site selection for Lunar Orbiter II included the assignment of either a primary or secondary photo site for each of the 211 available frames of photography. Film-set photo required to minimize the effects of known photo subsystem characteristics were used to photograph secondary sites. Information obtained from the Lunar Orbiter I photos was used in the evaluation and selection of Mission II sites.

Table 1.1-1: Primary and Secondary Photo Site Coverage					
	Location		Photo Coverage		
Site No.	Longitude	Latitude	Orbits	Exposures Per Orbit	Total Frames
IIP-1	36°55'E	4°10'N	1	16	16
IIP-2	34°00'E	2°45'N	1	8	8
IIP-3	21°20'E	4°20'N	2	8	16
IIP-4	15°45'E	4°45'N	1	8	8
IIP-5(Ranger 8)	24°38'E	2°42'N	1	8	8
IIP-6*	24°10'E	0°45'N	2	8	16
IIP-7	2°00'W	2°10'N	2	8	16
IIP-8*	1°00'W	0°05'N	3	8	24
IIP-9	13°00'W	1°00'N	1	8	8
IIP-10	27°10'W	3°28'N	2	8	16
IIP-11	19°55'W	0°05'S	2	8	16
IIP-12	34°40'W	2°25'N	2	8	16
IIP-13	42°20'W	1°30'N	2	8	16
			Comments		
IIS-1			Immediately after IIP-1		
IIS-2	35°25'E		Convergent telephoto stereo (two orbits)		
IIS-3 - 5	Farside		Vertical and oblique		
IIS-6	4°30'E	4°15'N			
IIS-7	1°00'W	0°05'N	Oblique of IIP-8 looking south		
IIS-8	12°50'E	0°30'N			
IIS-9	0°30'E	2°20'N			
IIS-10.2 +	11°50'W	3°20'N	Crater Gambert C		
IIS-11	27°10'W	4°40'N			
IIS-12	20°00'W	8°00'N	Oblique of Copernicus		
IIS-13	43°50'W	3°20'N			
IIS-14	Farside		20 degrees from terminator		
IIS-15	53°W	11°N	Oblique due north		
IIS-16	54°30'W	2°40'N			
IIS-17	59°W	7°25'N	Oblique due north		

* Biased toward area photographed in Mission I
\+ Changed from a westerly oblique of Site IIP-8 during mission.

Other considerations (unchanged from Mission I) were the requirements to:

- Read out selected frames between sites for mission control.
- Sidelap for telephoto coverage between adjacent orbits using vertical photography.
- Re-examine Mission I Sites I-3 and I-5 because the desired 1-meter coverage was not obtained during Mission I and these sites were located within the Mission II illumination band.

Mission II contained 13 primary photo sites within the Apollo zone that were to be photographed with a total of 184 frames during 22 separate orbits. In addition, 17 secondary sites were identified on the near-and farsides of the Moon. Secondary photo site coverage included coverages as:

- Convergent telephoto stereo photos;
- Oblique photos (looking to north and south);
- Vertical photos.

Table 1.1-1 tabulates the location of the 17 secondary sites and the location and coverage required for each of the 13 primary photo sites.

With the exception of Secondary Sites IIS-1 and -2 (which are four frame sequences taken during one and two photo passes, respectively), all secondary sites are single-frame exposures. Figure 1.1-2 graphically identifies each of the primary sites and indicates the corresponding photo orbit and altitude.

1.1.4 MISSION DESIGN

The Lunar Orbiter spacecraft was designed around its photo subsystem to ensure the maximum probability of success of the photographic mission. Similarly, the mission design maximized the probability of quality photography by placing the spacecraft over the mission target(s) in the proper attitude, altitude, and within the established lighting limitations. Launch vehicle, spacecraft, and photographic considerations were integrated into the design effort to optimize the trajectory and sequence of events to satisfy mission photographic objectives. Primary mission events as related to the Earth-Moon-Sun-spacecraft orbit geometry are shown in Figure 1.1-3.

Selection of the trajectory was based on conditions which must be satisfied, such as:

- Transit time (Earth to Moon) of approximately 90 hours;
- Initial orbit of 1850-km apolune and 200-km perilune;
- Nominal photographic altitude of 45 km;
- Orbit inclination of approximately 12 degrees at lunar equator;
- Descending-node photography for lighting;
- Posigrade orbit for visibility of injection.

Trajectory and orbit data used for mission design were based upon computations using Clarke's model of the Moon with Earth effects. The data used were the output of computer programs covering the following phases:

- Translunar Search Program;
- Translunar Orbit Description Program;
- Lunar Orbit Description Program.

Table 1.1-2 tabulates launch window characteristics for the November launch periods. The nominal sequence of events presented in the mission event sequence and time line analysis was based on a launch time approximately 30 minutes into the first launch window.

The trajectories required to accomplish the photographic objectives during these launch periods were documented in the form of:

- Targeting specifications for the booster agency;
- Tabulated trajectory data;
- Tracking and telemetry coverage plan;
- Mission error analysis;
- Alternate mission studies.

The set of orbit parameters that provided the required coverage of the photo sites determined the sequence and timing of events to obtain the desired photo coverage. Other factors that affected photo subsystem sequences included such operational or spacecraft performance limitations as:

- Start readout no sooner than 18 minutes after earthrise to ensure spacecraft acquisition and photo subsystem video adjustments;
- End readout 7 minutes before expected sunset to prepare spacecraft for Sun occultation operation;
- Interval of 14 minutes between end of processing and the start of readout to allow TWTA warmup and video adjustments;
- Interval of 2 minutes between end of readout and the start of processing to turn off readout and activate processor;
- Inhibit processing at least 5 minutes before Sun occultation (to prevent processing on battery power only);
- Advance one frame every 8 hours to avoid film set;
- Process two frames every 15 hours to avoid Bimat stick;
- Process two frames every 4 hours to reduce Bimat dryout;
- Read out as many frames as possible between photo passes to support the near-real-time mission operation and control functions.

The nominal planned sequence of significant events from the transfer to final ellipse (end of Orbit 45) to the completion of film processing and "Bimat cut" command (Orbit 103) is shown in Figure 1.1-4. The ordinate covers the period of one complete orbit (3 hours, 28 minutes, 25 seconds) and the abscissa covers successive orbits during the mission. Time progresses from the bottom to the top; the time at the top of any orbit is identical to the bottom of the next orbit. Three bands are shown in the figure which represent the periods when the Earth, the Sun, and the star Canopus are not visible to the spacecraft. The bar charts at the top represent the

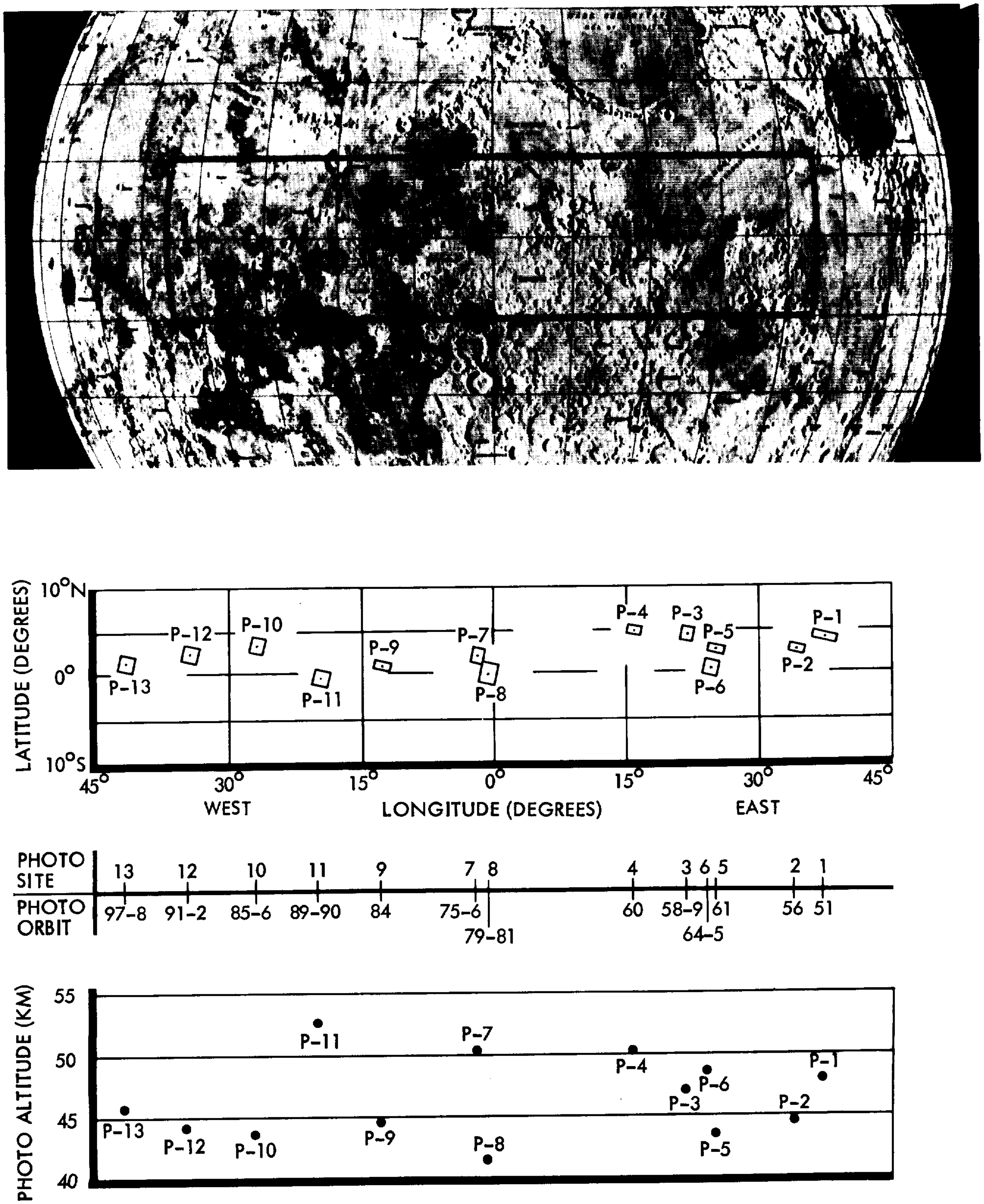

Figure 1.1-2: Primary Photo Site Distribution

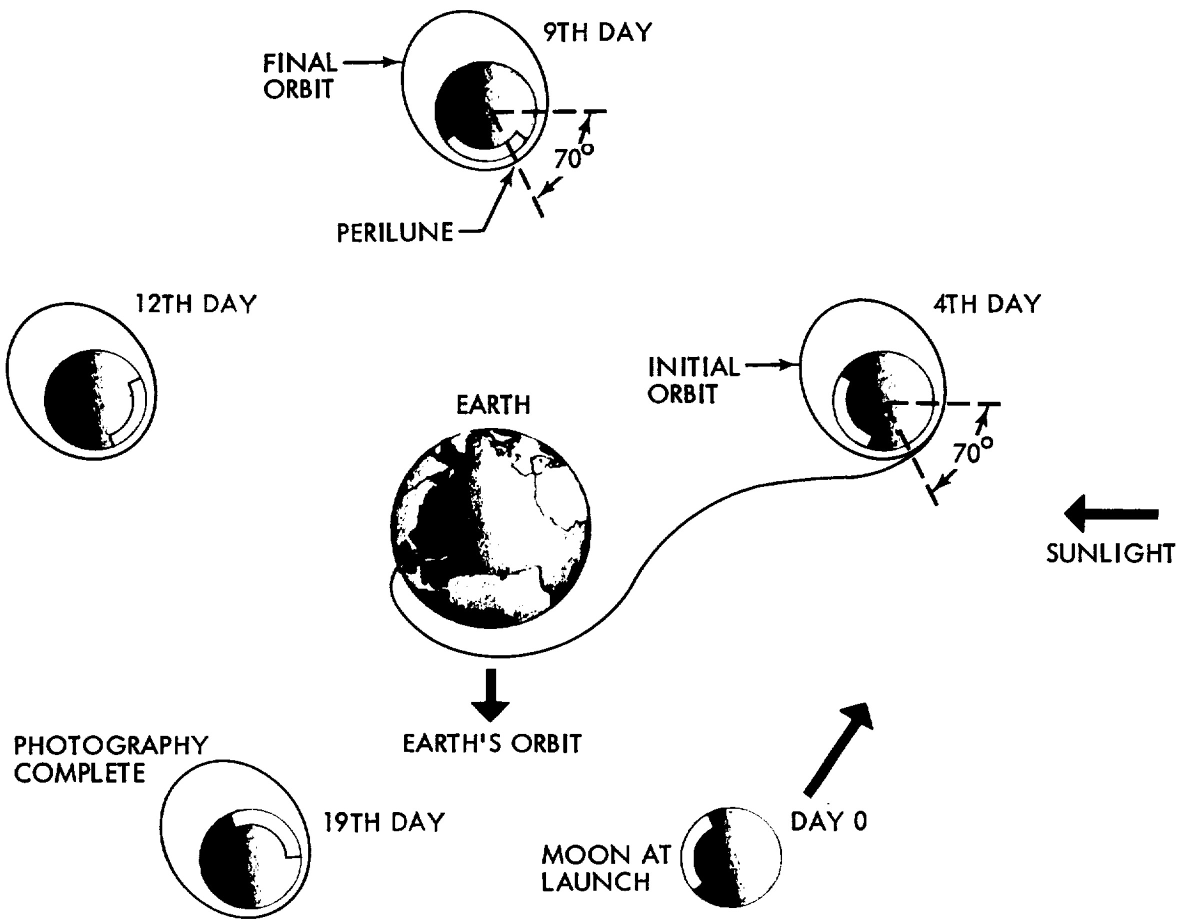

Figure 1.1-3: Sun-Earth-Moon-Spacecraft Relationships

Table 1.1-2: Launch Window Summary				
	Launch Time(GMT)		Launch Azimuth(deg)	
Launch Date	Start	Stop	Start	End
Nov. 6-7	22:58	1:35	90	114
Nov. 8	0:21	2:58	87	111
Nov. 9	0:48	3:59	78	102
Nov. 10	1:03	4:55	69	93
Nov. 11	1:56	5:53	66	87

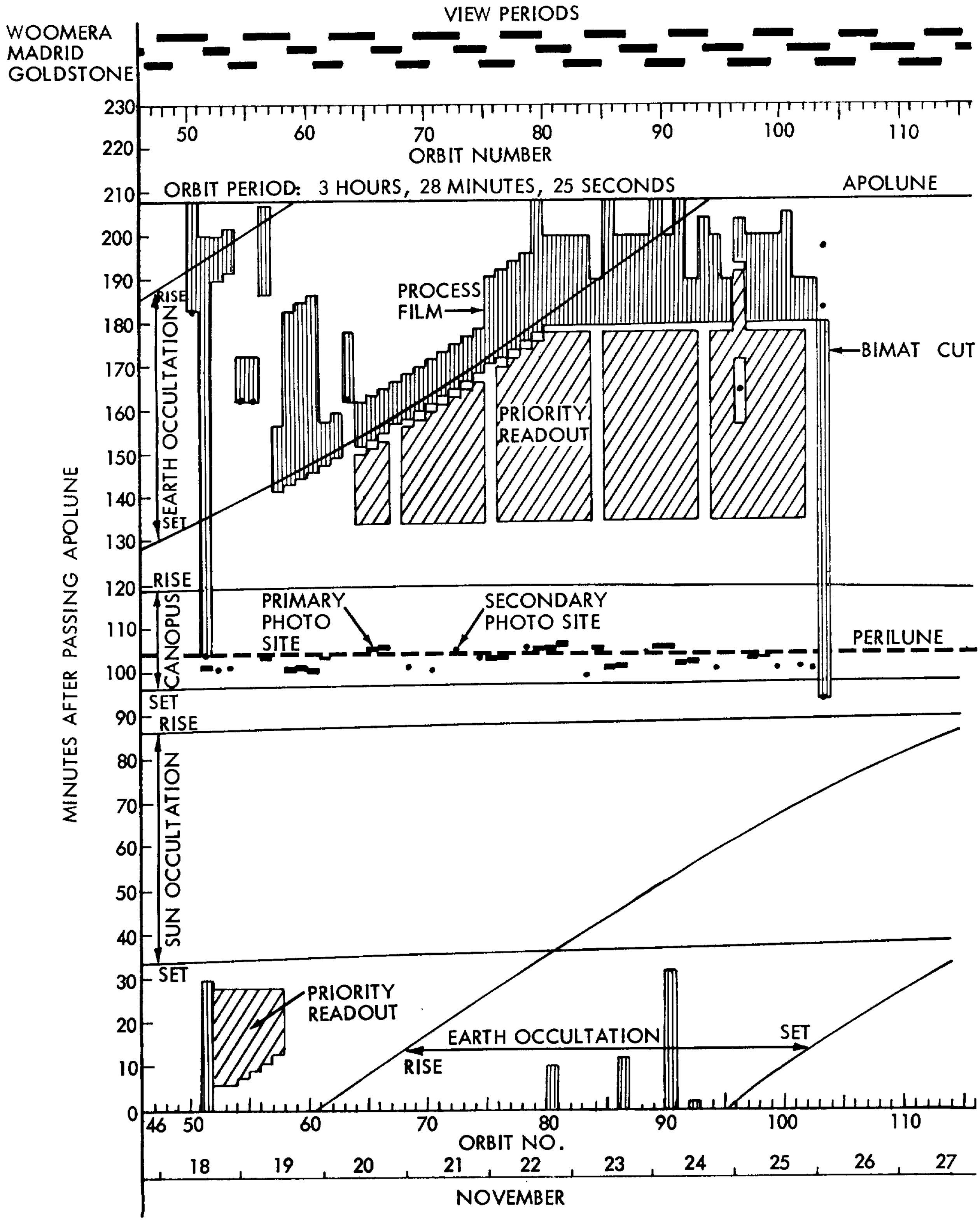

Figure 1.1-4: Planned Photo Period Sequence of Events

approximate viewing periods of the three primary Deep Space Stations. The figure also shows where the photos were taken with respect to time from orbit perilune as well as the times allotted to film processing and priority readout.

Figure 1.1-5 shows spacecraft exposure numbers of each photo and the sequence of primary and secondary photo sites. The shaded portions indicate the wide-angle photos read out in the priority mode. The partial frame readouts for telephoto coverage on either or both sides of the wide-angle photos are not shown.

1.1.5 FLIGHT VEHICLE DESCRIPTION

The Lunar Orbiter spacecraft is accelerated to injection velocity and placed on the cislunar trajectory by the Atlas-Agena launch vehicle. Figure 1.1-6 shows the general configuration of the complete launch vehicle.

Spacecraft Description – The 380-kilogram (853-pound) Lunar Orbiter spacecraft is 2.08 meters (6.83 feet) high, spans 5.21 meters (17.1 feet) from the tip of the rotatable high-gain dish antenna to the tip of the low-gain antenna, and measures 3.76 meters (12.4 feet) across the solar panels. Figure 1.1-7 shows the spacecraft in the flight configuration with all elements fully deployed (the mylar thermal barrier is not shown). Major components are attached to the largest of three deck structures which are interconnected by a tubular truss network. Thermal control is maintained by controlling emission of internal energy and absorption of solar energy through the use of a special paint covering the bottom side of the deck structure. The entire spacecraft periphery above the large equipment-mounting deck is covered with a highly reflective aluminum-coated mylar shroud, providing an adiabatic thermal barrier. The tank deck is designed to withstand radiant energy from the velocity control engine to minimize heat losses in addition to its structural functions. Three-axis stabilization is provided by using the Sun and Canopus as primary angular references, and by a three-axis inertial system when the vehicle is required to operate off celestial references, during maneuvers, or when the Sun and/or Canopus are occulted by the Moon.

The spacecraft subsystems (as shown in the block diagram of Figure 1.1-8) have been tailored around a highly versatile "photo laboratory" containing two cameras, a film supply, film processor, a processing web supply, an optical electronic readout system, an image motion compensation system (to prevent image smear induced by spacecraft velocity), and the control electronics necessary to program the photographic sequences and other operations within the photo subsystem. Operational flexibility of this photo subsystem includes the capability to adjust key system parameters (e.g., number of frames per sequence, time interval between frames, shutter speed, line-scan tube focus) by remote control from the ground.

The influence of constraints and requirements peculiar to successful operation in lunar orbit are apparent in the specific design selected.

- A three-axis stabilized vehicle and control system were selected to accommodate the precise pointing accuracies required for photography and for accurate spacecraft velocity-vector corrections during midcourse, lunar orbit injection, and orbit-transfer maneuvers.

- The spacecraft is occulted by the Moon during each orbit, with predictable loss of communication from Earth. Since spacecraft operations must continue behind the Moon, an on-board command system with a 128-word memory was provided to support up to 16 hours of automatic operation. It can be interrupted at virtually any time during radio communication to vary the stored sequences or introduce real-time commands. The selected programmer design is a digital data processing system containing register, precision clock, and comparators, to permit combining 65 spacecraft control functions into programming sequences best suited to spacecraft operations required during any phase of the mission.

- The communications system high-gain antenna was provided with a $\pm$ 360-degree rotation capability about the boom axis to accommodate pointing errors introduced by the Moon's rotation about the Earth.

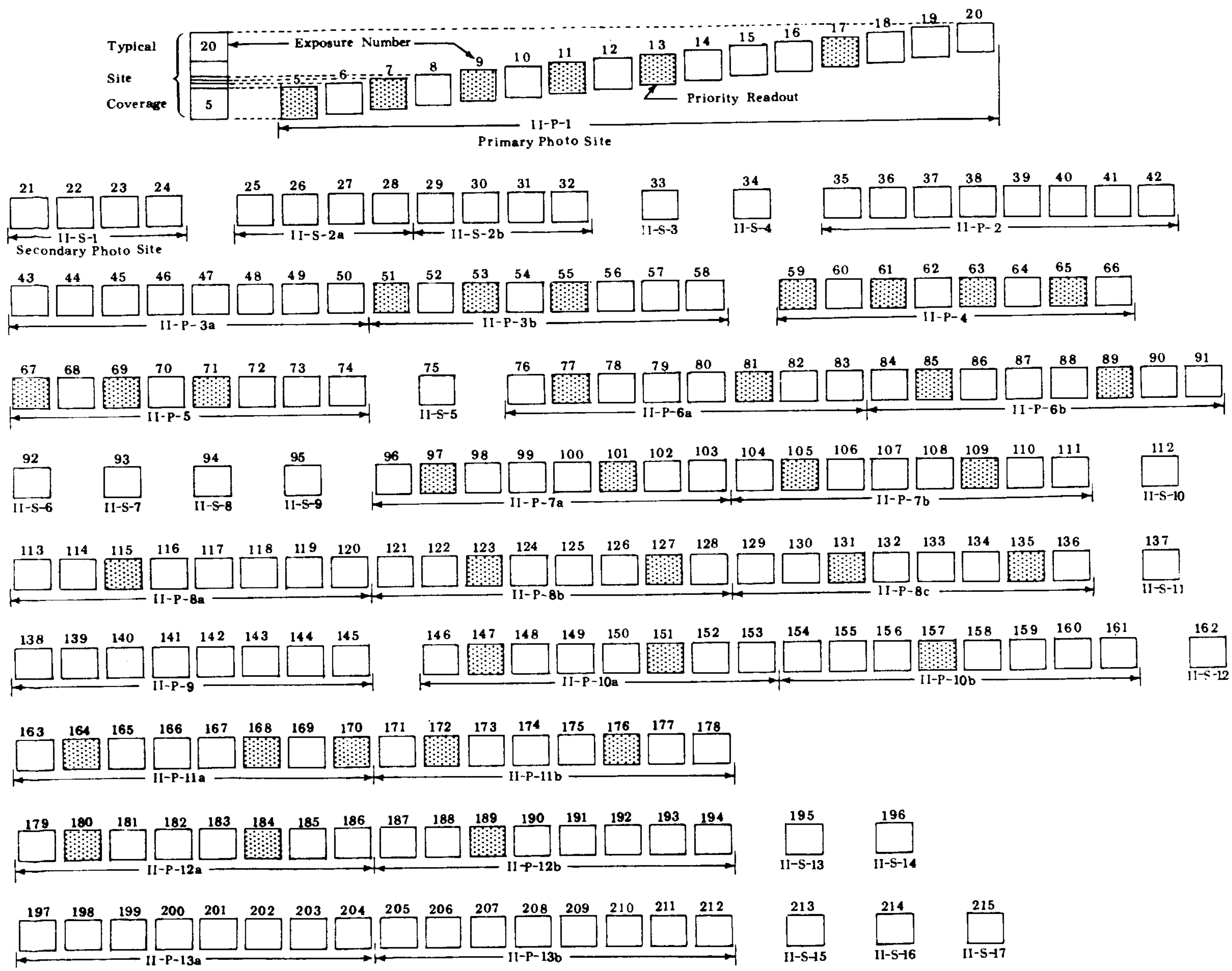

Figure 1.1-5: Exposure Sequences and Wide-Angle Priority Readout

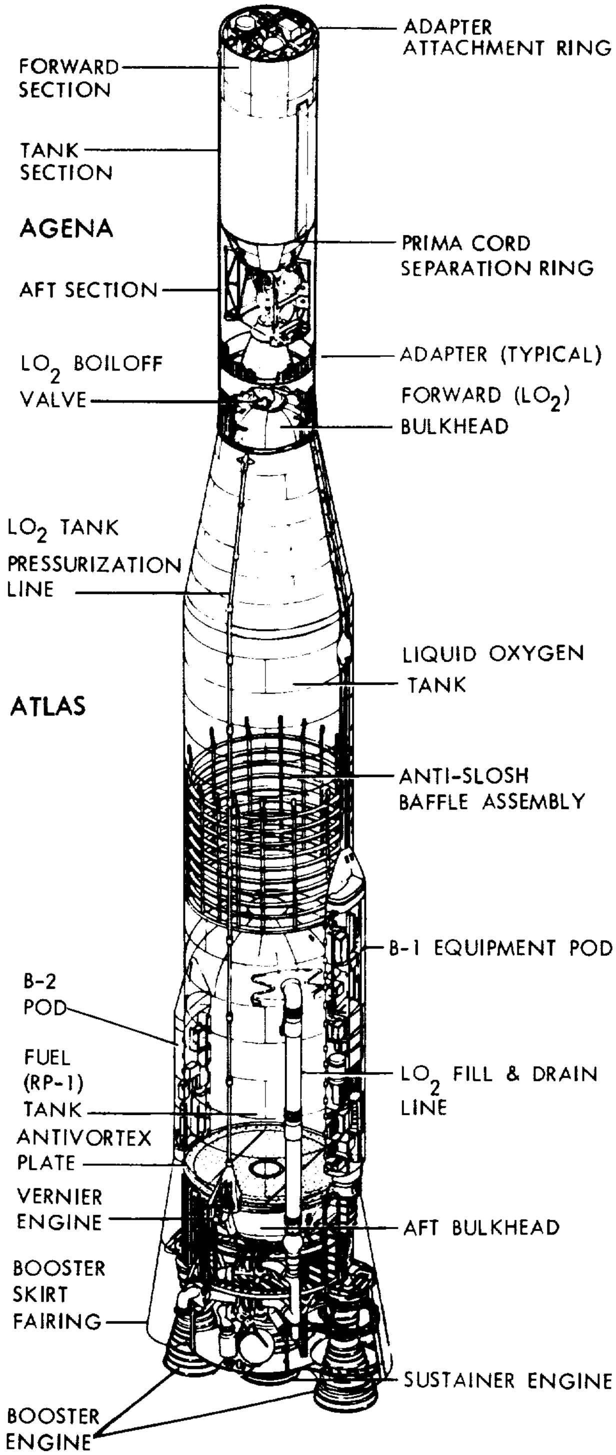

Figure 1.1-6: Launch Vehicle

- Two radiation detectors were provided to indicate the radiation dosage levels in the critical unexposed film storage areas. One detector measured the exposure seen by the unexposed film remaining in the shielded supply spool, the second, the integrated radiation exposure seen by undeveloped film in the camera storage looper. The data from these detectors allow the selection of alternate mission plans in the advent of solar flare activity.

The overall operation of taking the lunar pictures, processing the film, and readout and transmission of the photo video data within the spacecraft is shown in schematic form in Figure 1.1-9. In addition, the photo reconstruction process at the Deep Space Stations and the reassembly process at Eastman Kodak, Rochester, New York, are also shown.

Significant changes from the spacecraft basic configuration (defined in more detail in NASA Report CR 782, Lunar Orbiter I Photographic Mission Summary – Final Report) based on the performance of Mission I, include:

- Revised the photo subsystem to make it generally less susceptible to electromagnetic interference and in particular to make the telephoto camera focal-plane shutter operate properly.
- Incorporated more reliable transistors in the shunt power regulator.
- Painted low-gain antenna and solar panels to reduce glint in Canopus tracker.
- Painted the equipment mounting deck with S-13G coating to reduce the rate of paint degradation and subsequent spacecraft heating.
- Eliminated noise spikes in the inertial reference unit.
- Added thermal coating coupons.
- Modified the photo subsystem Bimat-cut timing.

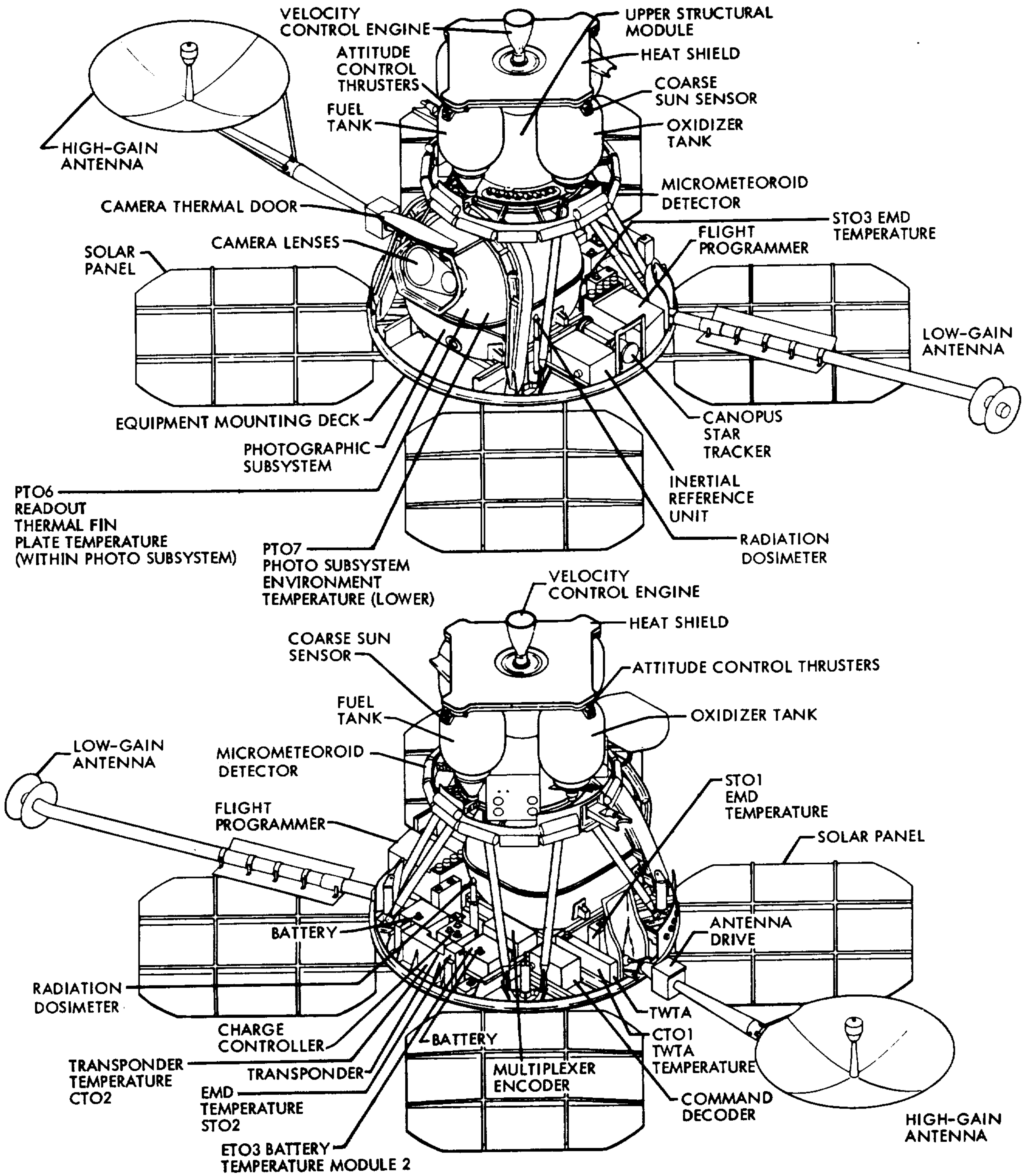

NOTE: SHOWN WITH THERMAL BARRIER REMOVED

Figure 1.1-7: Lunar Orbiter Spacecraft

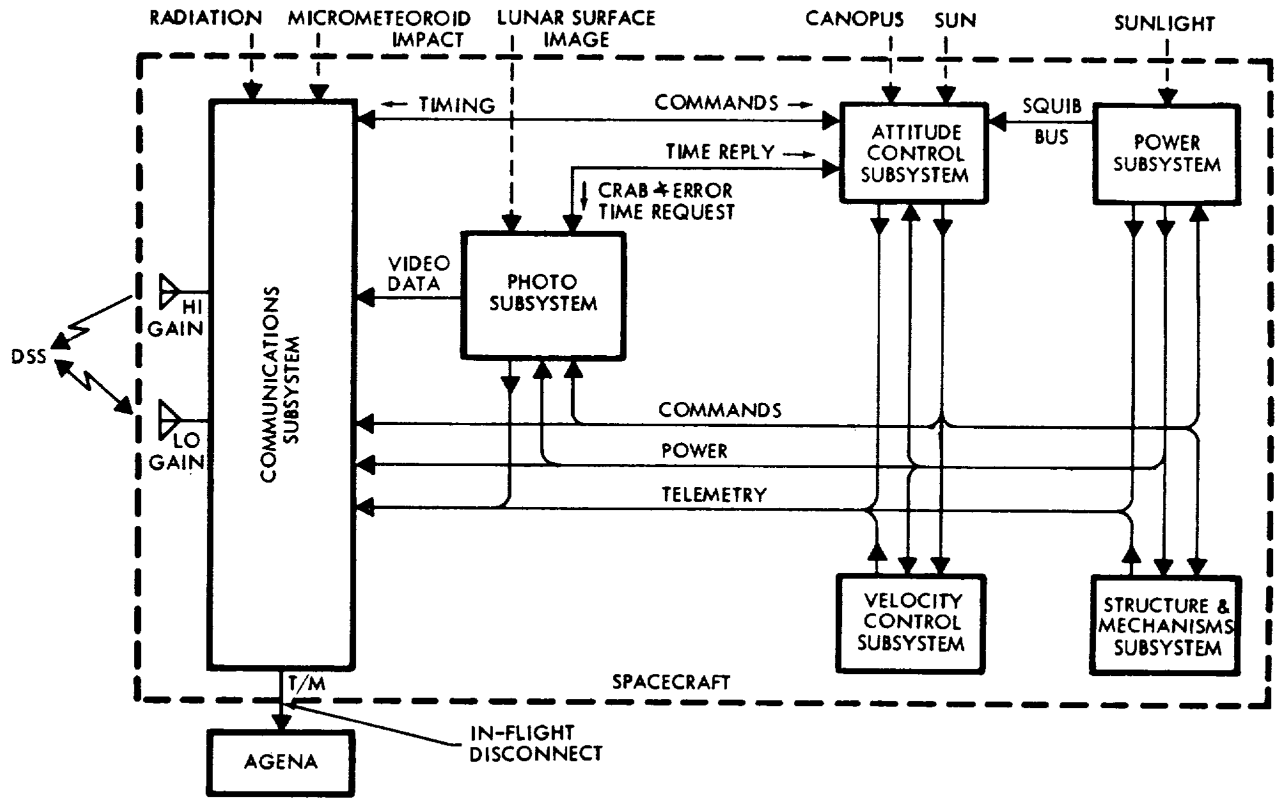

Figure 1.1-8: Lunar Orbiter Block Diagram

LAUNCH VEHICLE

The Atlas-Agena combination is a two-and-a-half-stage vehicle.

Two interconnected subsystems are used for Atlas guidance and control – the flight control (autopilot) and radio guidance subsystems. Basic units of the flight control subsystem are the flight programmer, gyro package, servo control electronics, and hydraulic controller. The main ground elements of the radio guidance subsystem are the monopulse X-band position radar, continuous-wave X-band doppler radar (used to measure velocity), and a Burroughs computer. The airborne unit is a General Electric Mod III-G guidance package which includes a rate beacon, pulse command beacon, and decoder. The radio guidance subsystem interfaces with the flight control (autopilot) subsystem to complete the entire guidance and control loop. All engines of the SLV-3 Atlas are ignited and stabilized prior to launch commitment.

The upper stage is an Agena space booster and includes the spacecraft adapter. It is adapted for use in the Lunar Orbiter mission by inclusion of optional and "program-peculiar" equipment. Trajectory and guidance control is maintained by a preset on-board computer. The Agena engine is ignited twice: first to accelerate the Agena-Lunar Orbiter combination to the velocity required to achieve a circular Earth orbit, and second to accelerate the spacecraft to the required injection velocity for the cislunar trajectory.

The Agena Type V telemetry system includes an E-slot VHF antenna, a 10-watt transmitter, and individual voltage-controlled oscillators for IRIG standard channels 5 through 18 and channel F. Channels 12 and 13 are used to transmit spacecraft vibrational data during the launch phase. Channel F contains the complete spacecraft telemetry bit stream during the launch phase.

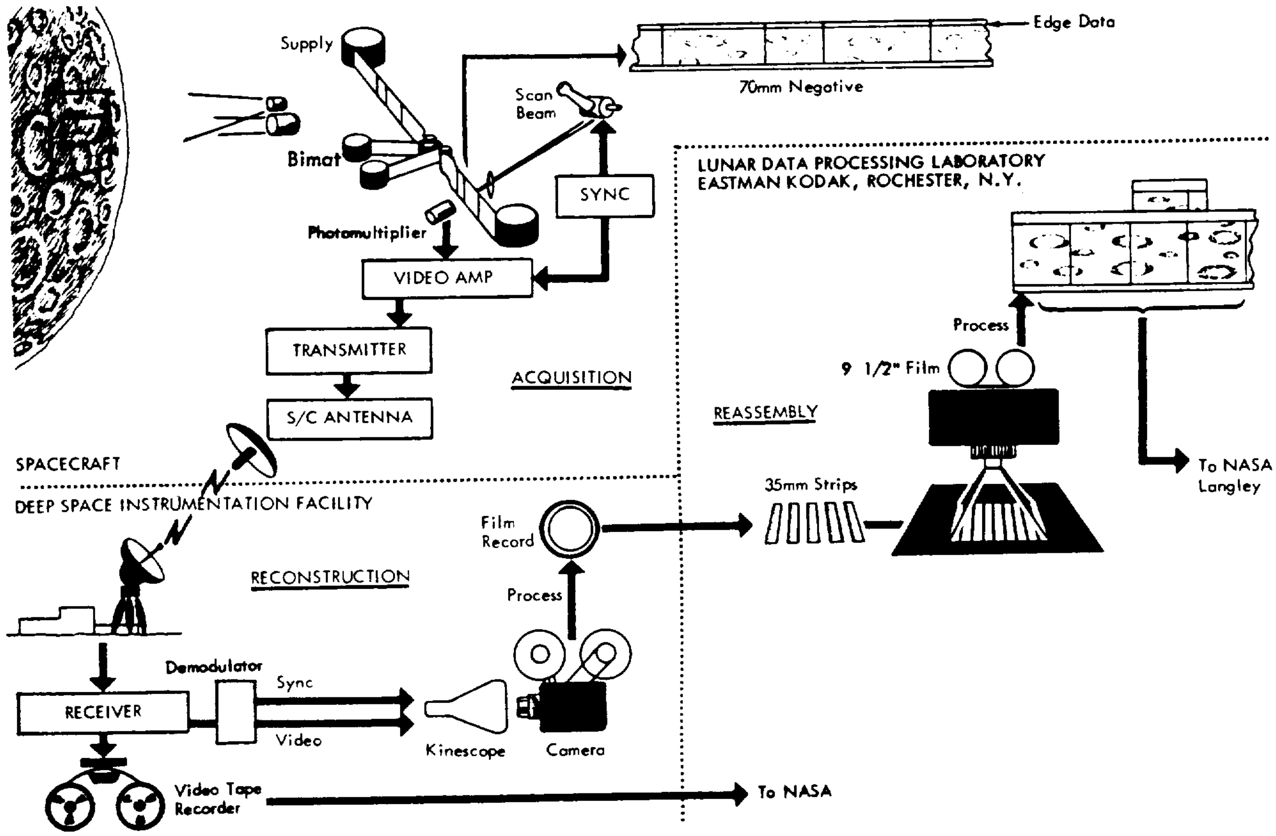

Figure 1.1-9: Photographic Data Acquisition, Reconstruction, and Reassembly

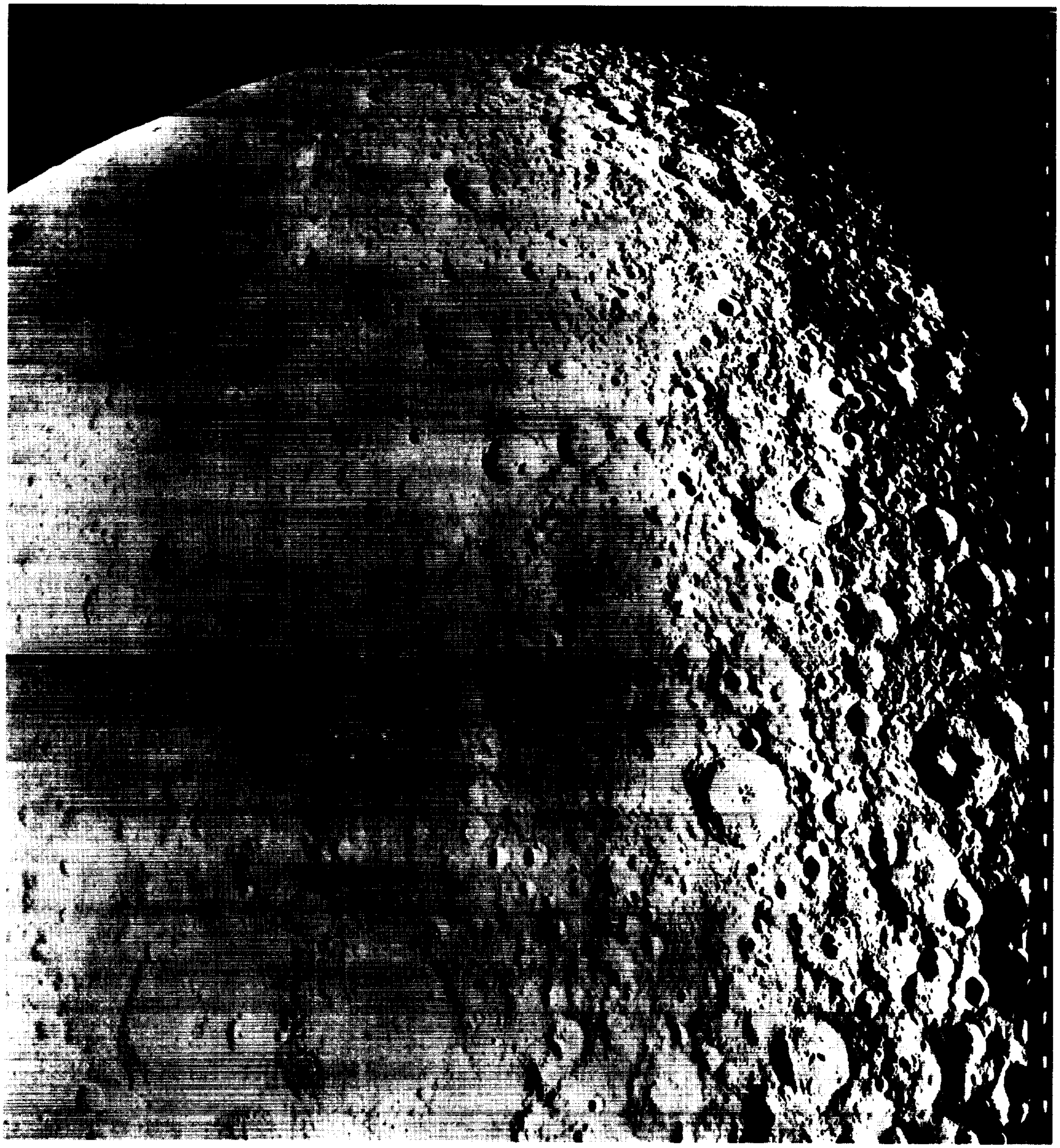

Wide-Angle Frame 34 — Site IIS-4

Looking north on farside

1.2 LAUNCH PREPARATION AND OPERATIONS

Lunar Orbiter II mission preparation began with arrival of the spacecraft at ETR, where it was assembled, tested, and readied for launch. The Atlas-Agena boost vehicle and the Lunar Orbiter spacecraft each received quality acceptance tests at the individual contractor's plants prior to delivery to the AFETR. Early planning included the dissemination of information to the launch agency for proper programming of the Atlas-Agena system for the projected launch days. Atlas, Agena, and Lunar Orbiter spacecraft activities at AFETR were integrated so that all systems were properly checked out to support the scheduled launch date. Lunar illumination requirements, Earth-Moon geometry, and Sun-Moon relationships required that these plans be geared to use the available launch windows.

Control of the launch was delegated to the Lewis Research Center, supported by the downrange stations and appropriate instrumentation ships located in the Atlantic and Indian Oceans. Upon acquisition of the spacecraft by the Deep Space Network tracking stations, control of the Lunar Orbiter mission was passed from the AFETR to the Space Flight Operations Facility at Pasadena, California.

The following sections summarize the activities and performance prior to acquisition by the Deep Space Network.

1.2.1 LAUNCH VEHICLE PREPARATION

The SLV-3 Atlas, Serial Number 5802, arrived at ETR on August 30, 1966. Receiving inspection and normal premission testing of the SLV-3 were accomplished at Hangar J. On September 13, the SLV-3 was erected on Launch Complex 13. The first of two booster flight acceptance composite tests (B-FACT) was conducted on October 6. The dual propellant loading test took place on October 11, followed by the booster adapter mating on October 14. The second B-FACT was accomplished on October 18. Figure 1.2-1 summarizes the separate launch preparation and testing of the Atlas, Agena, and Lunar Orbiter, as well as the combined tests in the launch area.

The following problems were encountered and corrected during normal testing procedures.

- The vernier engine oxidizer bleed valves failed to reseat properly following pressurization and venting of the engine start tanks.
- The booster gas generator igniter plugs P155 and P156 were identified in the reverse order.
- Fuel leakage was detected at a sustainer fuel low-pressure duct weld joint.
- The sustainer LO_2 reference regulator and the first replacement regulator both exhibited out-of-tolerance regulation characteristics.
- A second-stage oil evacuation chamber valve drive motor malfunctioned.
- The B2 hydraulic accumulator pressure loss was out of tolerance.
- A calibration and conditioning system amplifier on the helium booster tank was defective.
- Two gyros in the flight control system were rejected.
- A rate beacon in the guidance system overheated because the blower was inoperable.
- Two transducers gave incorrect measurements.

The Agena, Serial Number 6631, arrived at Hangar E on August 29 for receiving inspection and functional checkout. The Agena was mated to the Atlas on October 25. Standard prelaunch checkout and tests revealed the following problems, which were corrected.

- Three O-rings were removed and replaced.
- A fuel valve had excessive leakage.
- Several oil leaks were detected.
- A C-band beacon exhibited decreasing output power.

The joint flight acceptance composite test was completed without the spacecraft on October 31.

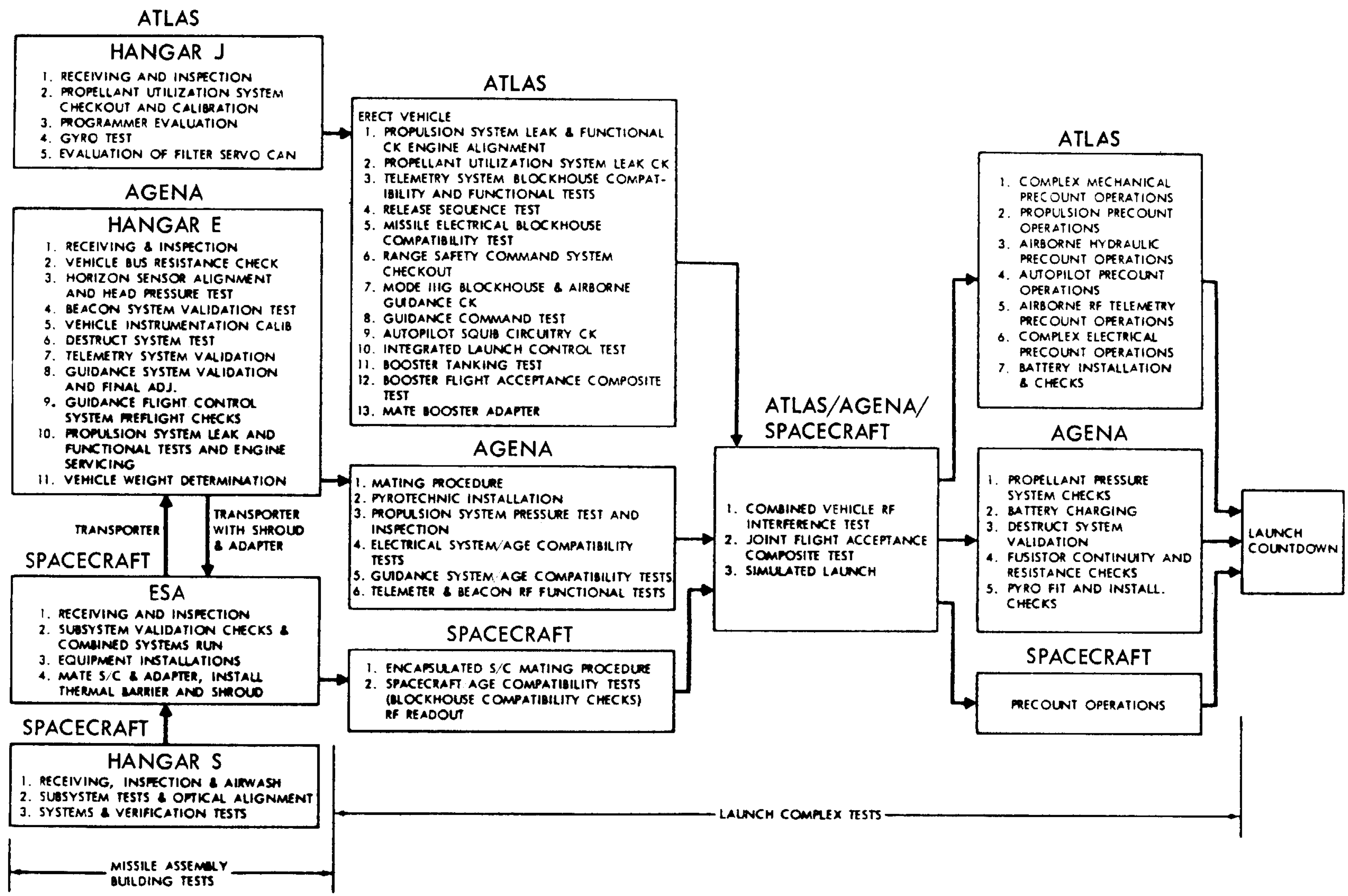

Figure 1.2-1: Launch Operations Flow Chart

1.2.2 SPACECRAFT PREPARATION

Lunar Orbiter Spacecraft 5 arrived at Cape Kennedy on June 10, 1966, to serve as backup for the first mission. The spacecraft was inspected and tested in Hangar S, then was taken to the explosive safe area (ESA) and prepared for fueling. On July 30 it was determined that the spacecraft would not be needed to further support Mission I and it was placed in storage for the second mission.

On August 26 Spacecraft 6 arrived at Cape Kennedy for testing as a backup to Spacecraft 5.

Spacecraft 5 was removed from storage for modification and retest on August 30. Retest was necessary because of the time that had elapsed since previous testing to support Mission I was completed. Limited modifications were also required as a result of experience gained from Mission I.

All tests were completed successfully at Hangar S. On October 17 the spacecraft was transferred to the explosive safe area 5/6 for final testing, installation of ordnance, loading of the photo subsystem, fueling, and final weight and balance checks. Prior to the final move to Launch Pad 13 on October 31, the thermal barrier and nose fairing (shroud) were installed around the spacecraft.

The major problems encountered and corrected during prelaunch testing and checkout at ETR are noted here.

- The transponder was found to have a 9-db gain in carrier power when switching to Mode 2 operation. The allowable tolerance was 5 ± 1.3 db. A mismatch between the transponder and the modulation selector was indicated and the transponder was replaced.
- The inertial reference unit (IRU) roll gyro output voltage was low and the unit was replaced.
- The star tracker star map output voltage was not compatible with the calibration curves furnished with the star tracker test set. The test set was found to have shifted output levels. The star tracker was reinstalled and the retest was satisfactory, using a different test set.
- The spacecraft power transistor panel contained old-type transistors with wire leads. A panel with more reliable transistors was substituted.
- The equipment mounting deck was given an additional coat of paint due to the higher than expected degradation of the paint on the previous flight.
- Three micrometeoroid detectors were found to have the Beryllium-copper detector exposed. The questionable detectors were replaced.
- The fuel, oxidizer, and nitrogen tank pressures dropped after loading. The apparent pressure loss was due to the lowering of the spacecraft temperature preparatory to loading the photo subsystem. Therefore, an additional "topping off" of the nitrogen tank was required.
- A gas leak was detected in the photo subsystem shell. The minute hole was easily patched on the inside with fiberglas cloth. Pressure and leak tests verified the adequacy of the corrective action.

1.2.3 LAUNCH COUNTDOWN

Following matchmate of the encapsulated spacecraft to the Agena on October 31, tests were run to verify the proper mating of the spacecraft and the Agena vehicle. Upon demonstration of compatibility between van and spacecraft, blockhouse and spacecraft, and DSIF-71 and spacecraft, the vehicle was held ready for simulated launch on November 3, 1966.

The simulated launch began as planned at 10:36 EST (T-460 minutes), and terminated at 18:54 EST. There were 34 minutes of unplanned hold time and a planned recycle to T-7 minutes at T-19 seconds. The following problems were encountered.

- A liquid-oxygen regulator on the Atlas failed, necessitating replacement.
- A small leak developed in the Atlas fuel system, which was repaired by replacement of seals.
- The Atlas roll gyro saturated due to the 11-degree roll program called for in launch plan "C." A 5-degree test program was satisfactorily substituted.

- The Agena C-band beacon exhibited low output power and was replaced.

- The spacecraft Canopus tracker star map voltage was noisy due to light leaks in the air conditioning exhaust vent in the shroud.

- The spacecraft traveling-wave-tube amplifier showed a decrease in power output which was caused by a change in the voltage standing wave ratio due to reflections.

On November 6, the launch countdown started at T-530 minutes. The only deviations from schedule were:

- A late acquisition of two-way lock between the spacecraft and DSIF-71 at Cape Kennedy telemetry station (TEL-2);

- A noisy takeup reel contents telemetry point was cleared by advancing approximately 1 foot of film from the readout looper to the takeup reel.

- A special check was made of the Atlas sustainer engine liquid-oxygen reference regulator output pressure to verify that the regulator had not drifted out of tolerance.

Liftoff occurred on schedule at 23:21:00:195 GMT with favorable weather conditions.

A simplified countdown sequence for the spacecraft and supporting functions is shown in Figure 1.2-2.

1.2.4 LAUNCH PHASE

The launch phase covers performance of the Lunar Orbiter B flight vehicle from liftoff through spacecraft separation from the Agena and subsequent acquisition of the spacecraft by the Deep Space Network.

1.2.4.1 Flight Vehicle Performance

Analysis of vehicle performance, trajectory, and guidance data indicated that all launch vehicle objectives were satisfactorily accomplished. Atlas objectives were to:

- Place the upper stage in the proper coast ellipse as defined by the trajectory and guidance equations;

- Initiate upper stage separation;

- Start the Agena primary timer;

- Jettison the spacecraft shroud;

- Start the secondary timer commands of the launch vehicle.

The Agena objectives were to:

- Inject the spacecraft into a lunar-coincident transfer trajectory within prescribed orbit dispersions;

- Perform Agena attitude and retromaneuvers after separation to ensure noninterference with spacecraft performance.

All of these objectives were accomplished.

Table 1.2-1 provides a summary of planned and actual significant events during the ascent trajectory. All times are referenced to the liftoff time of 23:21:00.195 GMT, Nov. 6, 1966.

Atlas Performance

Atlas SLV-3 (Serial Number 5802) performance was satisfactory throughout the flight. All engine, propulsion, and propellant utilization functions were within tolerances. Calculations based on performance parameters indicated that approximately 1,323 pounds of liquid oxygen and 766 pounds of fuel remained at SECO. This was equivalent to 7.4 seconds of additional engine burn time.

Vehicle stability was maintained throughout all phases of powered flight by the Atlas flight-control system. The programmed roll and pitch maneuvers and other commanded maneuvers were satisfactorily executed. Performance data indicated that the vehicle angular displacements and rates at vernier engine cutoff (VECO) were negligible.

Analysis of ground recorded and telemetry data indicated that both the Mod III-A ground station and Mod III-G airborne guidance equipment performed satisfactorily. All discrete and steering commands were properly transmitted by the ground station, received by the beacon, and decoded and executed by the flight-control system. Beacon track was maintained until launch plus 384.0 seconds, when the received signal strength decreased to the noise level.

Table 1.2-1: Ascent Trajectory Event Times

Event	Times (+sec) Nominal	Times (+sec) Actual
Liftoff (2-inch motion)		23:21:00:195GMT
Booster Engine Cutoff Discrete	129.0	127.993
Booster Flight Lock-in Dropout		128.108
Booster Jettison Conax Valve Command		131.104
Start Agena Secondary Timer Discrete		269.739
Sustainer Engine Cutoff Discrete	287.2	290.683
Sustainer Engine Cutoff Relay		290.690
Start Agena Primary Timer	290.6	292.766
Vernier Engine Cutoff Discrete	307.5	313.997
Vernier Engine Cutoff Relay		314.002
Jettison Shroud	309.5	316.500
Initiate Separation Discrete	311.5	318.204*
Agena First-Burn Ignition (90% P_c)	364.9	367.0
Agena First-Burn Cutoff	516.8	522.0
Agena Second-Burn Ignition (90% P_c)	1196.9	1199.1
Agena Second-Burn Cutoff	1283.6	1287.0
Spacecraft Agena Separation		1452.4

* Event initiated by autopilot programmer backup signal at sustainer engine cutoff plus 27.5 seconds.

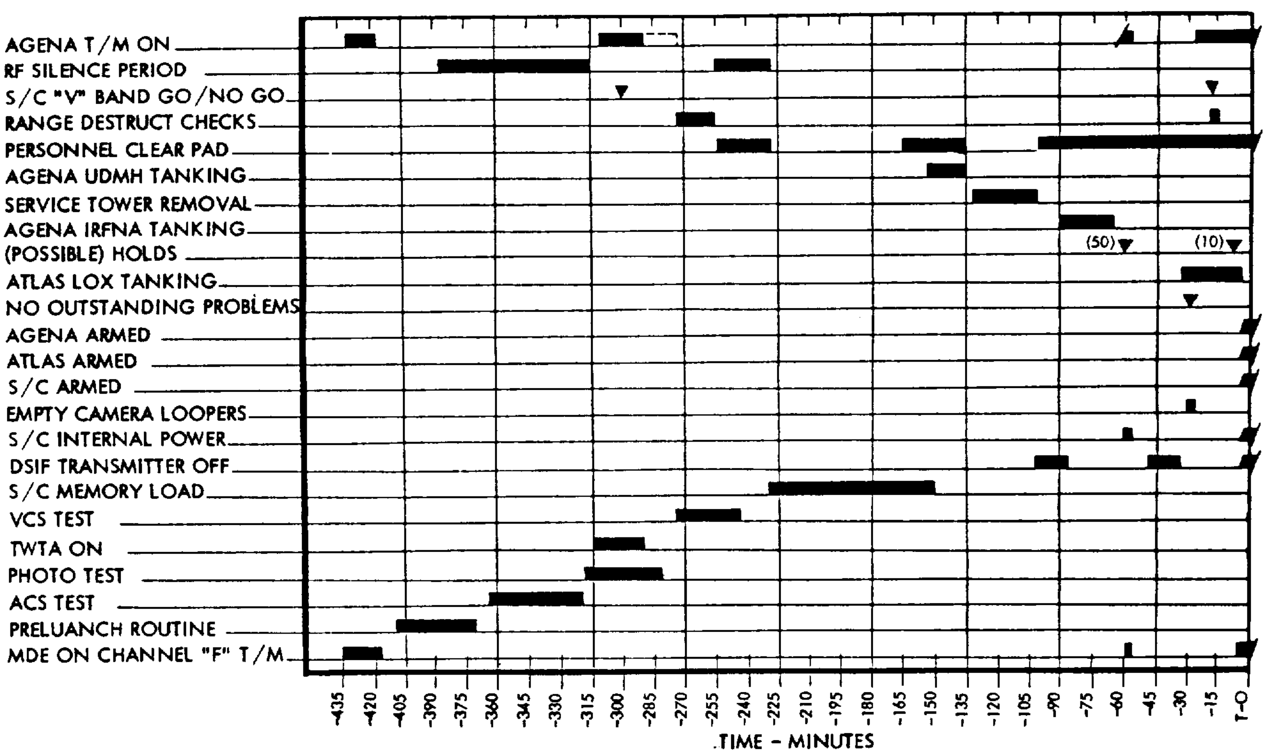

Figure 1.2-2: Master Countdown Sequence

Evaluation of all recorded data (vehicle performance telemetry, ground system monitoring, and tracking data) indicated that all components of the Atlas launch vehicle and ground supporting system operated properly throughout all phases of Atlas powered flight.

The following coast-ellipse parameters and insertion parameters at VECO+2 seconds were obtained from the guidance system data:

● Semimajor axis	14,511,985 feet
● Semiminor axis	12,706,681 feet
● Velocity magnitude	18,509 feet per second
● Velocity to be gained	+0.62 foot per second
● Filtered yaw velocity	+6.43 feet per second
● Filtered altitude rate minus desired altitude rate	+21.72 feet per second

Agena Performance

Agena D (Serial Number 6631) performance was satisfactory during the flight.

The primary sequence timer started approximately 2.2 seconds later than nominal, therefore all timer-controlled functions were proportionately delayed. Average chamber pressure during the first burn period was 504.6 psia, which produced a calculated thrust of 15,945 pounds. The total propellant flow rate was computed as 54.53 pounds per second, producing a specific impulse of 292.4 lb-sec/lb. The first burn period lasted 155.2 seconds and the second burn duration was 87.9 seconds.

Agena computer performance was satisfactory in controlling the attitude during the Earth orbit period and controlling the cislunar trajectory injection maneuver.

Many of the pitch and roll maneuvers during the Atlas boost phase were sensed by the caged Agena gyros. Small disturbances were also noted at BECO; those at Atlas-Agena separation were barely visible. Inertial reference package gyro disturbances at first and at second Agena burn ignition were small and quickly damped out by hydraulic actuator motion.

Spacecraft Performance

Spacecraft performance during the period from liftoff to acquisition by the Deep Space Network was satisfactory. All separation and deployment sequences were satisfactorily completed and the Sun was automatically acquired.

1.2.5 DATA ACQUISITION

The Earth track of the Lunar Orbiter II mission is shown in Figure 1.2-3. Significant events and planned coverage of the AFETR facilities are shown on this trajectory plot.

The AFETR preliminary test report showed the data coverage presented in the following tables. A list of electronic tracking coverage from all stations is contained in Table 1.2-2 together with the type of tracking operation employed for each period. Telemetry data recording is summarized in Table 1.2-3 by recording station and telemetry frequency.

Lunar Orbiter telemetry data were recorded via Channel F of the Agena link and also via the spacecraft telemetry system. Prior to spacecraft separation, the spacecraft transmissions (2298.3 MHz) were made with the antennas in the stowed position.

Weather conditions during the launch operation were favorable. A light rain occurred at T-115 minutes, but did not delay the launch. The upper wind shears were within acceptable limits. At liftoff the following surface conditions were recorded.

● Temperature	72°F
● Relative humidity	79%
● Visibility	10 miles
● Dew point	65°F
● Surface winds	7 knots at 065 degrees
● Clouds	Cloudy skies almost overcast
● Pressure	30.170 inches of mercury

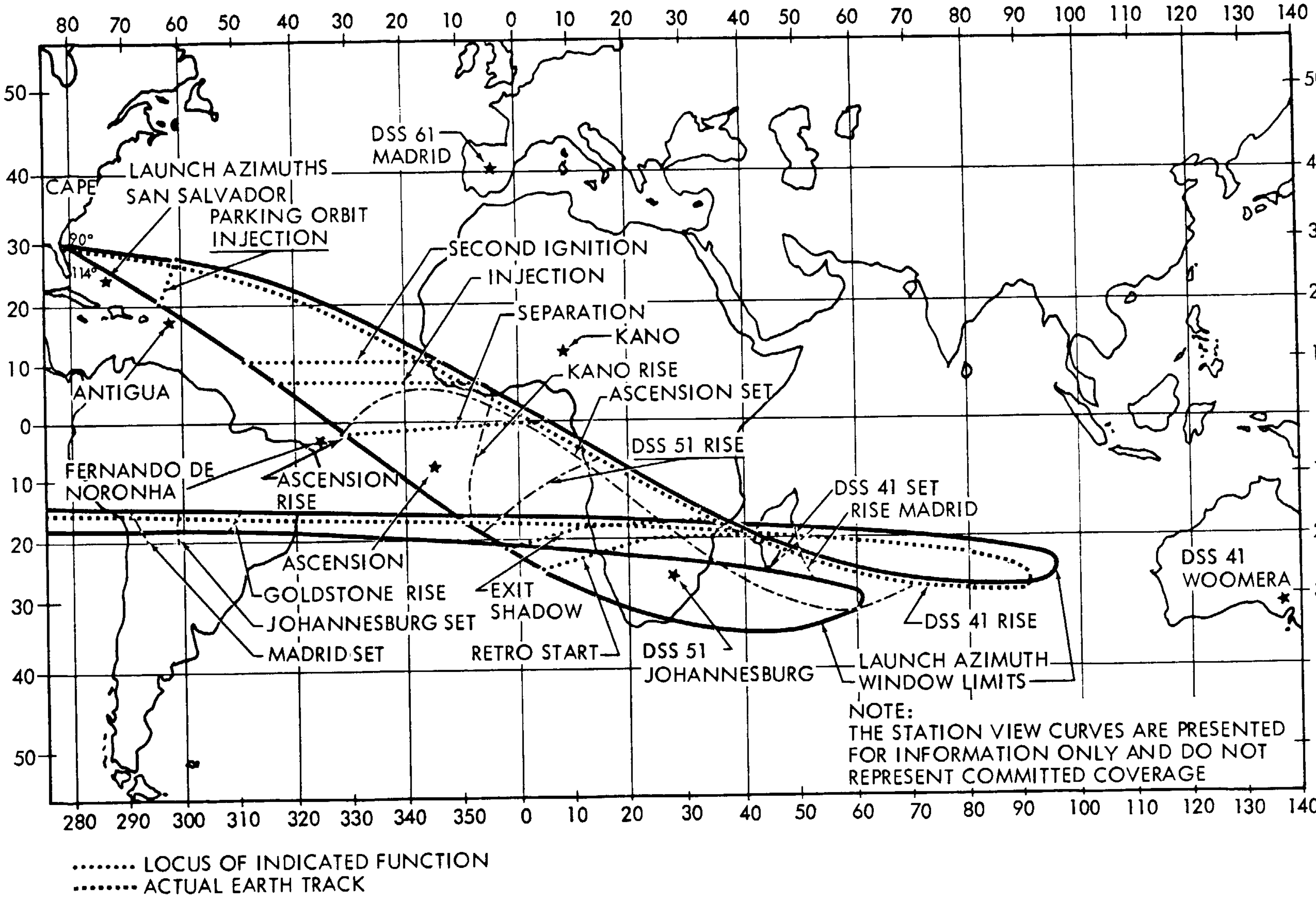

Figure 1.2-3: Earth Track for November 6-7, 1966

Table 1.2-2: AFETR Electronic Tracking Coverage

Location	Radar No.	Period of Coverage (sec) From	To	Mode of Operation
Radar				
Patrick	0.18	14	327	AB
		327	360	AS
		360	470	AB
Station 1	1.1	0	2	TV
Cape Kennedy		2	22	IR
		22	127	AS
	1.2	0	7	TV
		7	22	IR
		22	127	AS
	1.16	10	73	AS
		73	267	AB
Station 19	19.18	10	79	AS
Kennedy		79	168	AB
Space		172	174	AS
Center		174	329	AB
		329	366	AS
		366	370	AB
		372	378	AB
Station 3	3.16	68	482	AB
Grand Bahamas				
	3.18	86	465	AB
Station 7	7.18	196	606	AB
Grand Turk				
Station 91	91.18	386	736	AB
Antigua				
Station 12	12.16	--	--	(No track --
Ascension				
	12.18	--	--	below horizon)
Station 13	13.16	1610	4242	AB
Pretoria Africa				
Special Instrumentation				
Station 1	TEL ELSSE	13	110	F
Cape Kennedy		4	461	
		14	110	P
		4	467	

Mode of Operation Code:

AB = Automatic beacon track
AS = Automatic skin track
F = Flight line
IR = Infrared track
TV = Television
P = Program

Table 1.2-3: AFETR Telemetry Coverage

Location		Link (MHz) Frequency		Period of Coverage (sec) From	To
Station 1 Tel II Cape Kennedy		244.3	AGENA	-420	493
		249.9	ATLAS	-420	482
		2298.3	LUNAR ORBITER	0	130
		2298.3		140	170
Station 1 Tel IV Cape Kennedy		244.3		-420	476
		249.9		-420	476
		2298.3		0	196
Station 3 Grand Bahamas		244.3		40	515
		249.9		40	515
		2298.3		60	515
Station 4 Eleuthera		249.9		77	530
Station 7 Grand Turk		249.9		168	320
		249.9		329	498
		249.9		502	588
Station 91 Antigua		244.3		335	745
		2298.3		360	680
Station 12 Ascension		244.3		1270	1721
		244.3		1774	1813
		2298.3		1554	1664
Station 13 Pretoria, Africa		244.3		1577	8100
		2298.3		1587	1729
ARIS Uniform	Mobile Range Instrumentation Facilities	244.3		725	1139
		2298.3		785	1049
SIL 1 #490		244.3		888	1449
ARIS Whiskey		244.3		1070	1557
		2298.3		1078	1566
ARIS Yankee		244.3		1331	2793
		2298.3		1353	2800

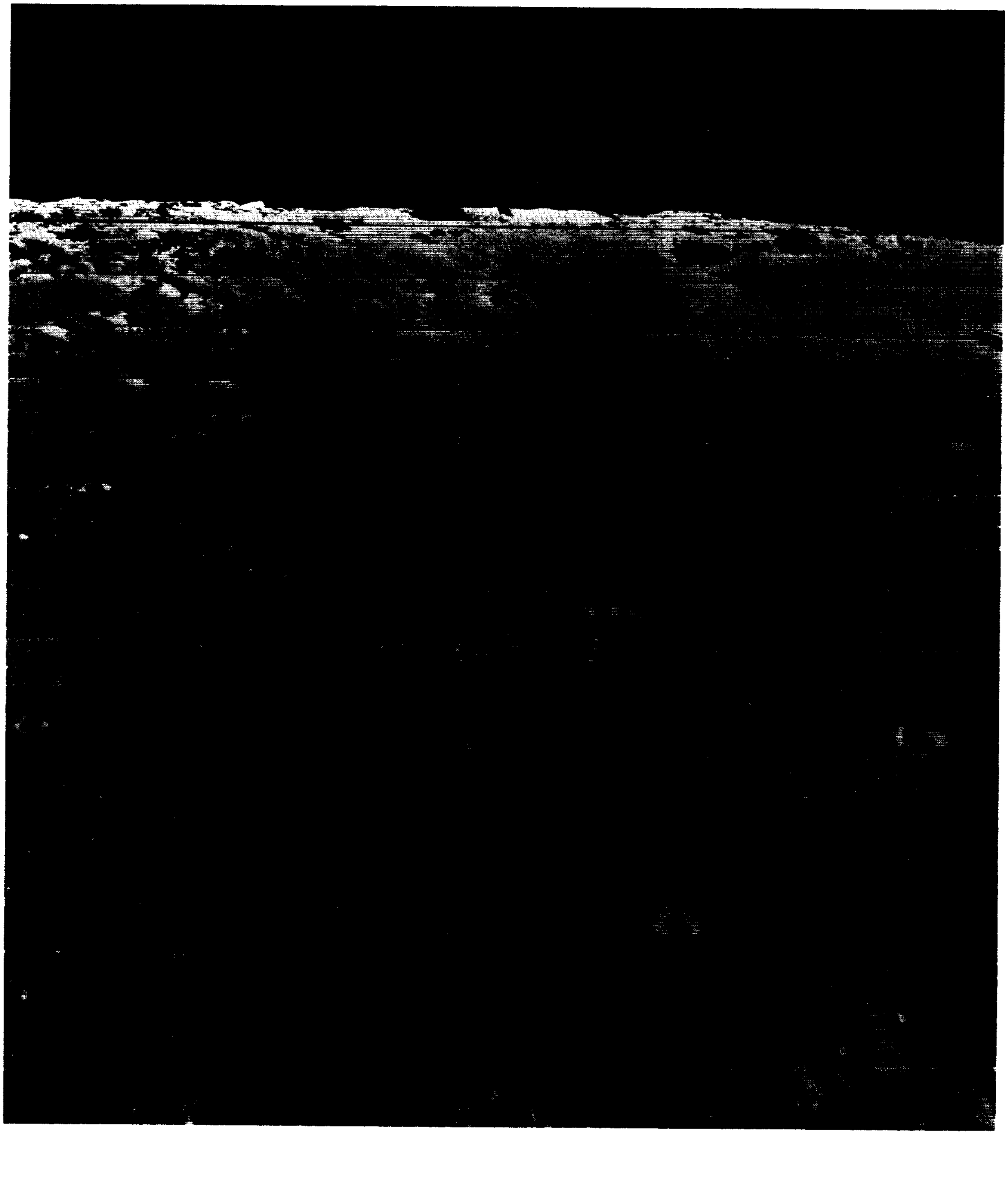

Wide-Angle Frame 93 – Site IIS-7

Looking south over Sinus Medii toward the crater Hershel

1.3 MISSION OPERATIONS

Operation and control of Lunar Orbiter II required the integrated services of a large number of specialists stationed at the SFOF facility in Pasadena, California, as well as at the worldwide Deep Space Stations. The Langley Research Center exercised management control of the mission through the mission director. Two primary deputies were employed: the launch operations director located at Cape Kennedy, and the space flight operations director located at the Space Flight Operations Facility (SFOF), Pasadena.

Launch vehicle and spacecraft performance after liftoff was monitored in the launch mission control center at ETR by the mission director. Telemetry data was used by the launch team and was relayed in real time to the SFOF through the Cape Kennedy Deep Space Station. This dissemination of spacecraft performance data to the launch and operations teams enabled efficient and orderly transfer of control from Cape Kennedy to the SFOF.

Flight control of the mission was centralized at the SFOF for the remainder of the mission. All commands to the spacecraft were coordinated by the spacecraft performance analysis and command (SPAC) and flight path analysis and command (FPAC) team of subsystem specialists and submitted to the space flight operations director for approval prior to being transmitted to the DSIF site for retransmission to the spacecraft.

Operational performance of the spacecraft and the worldwide command, control, and data recovery systems are presented in the following sections.

1.3.1 MISSION PROFILE

The Lunar Orbiter space vehicle -- consisting of Atlas SLV (Serial Number 5802), Agena D (Serial Number 6631), and Lunar Orbiter B -- was successfully launched at 23:21:00.195 GMT on November 6, 1966 from Launch Complex 13 at AFETR. Liftoff occurred at the opening of the window for November 6. The flight azimuth of 93.8 degrees required by launch plan 6C was satisfied.

Figure 1.3-1 provides a pictorial summary of the 31-day photographic mission of Lunar Orbiter II. The timing of events during the countdown and through the "start Canopus acquisition" function are referenced to the liftoff time. The remainder of the mission is referenced to Greenwich Mean Time. Photography of each of the primary sites is indicated by site and orbit number and GMT. The corresponding information for the 17 secondary sites is not shown on the chart. With one exception all of the secondary sites were photographed as planned at varying intervals between the primary sites.

Two types of photo readout periods are shown in the shaded areas. The priority readout was limited to one spacecraft frame or less by photo subsystem internal limitations and the available view periods when the Sun was visible to the spacecraft. This period was terminated upon completion of photography when the "Bimat cut" command was transmitted and executed. During the "final readout" period the readout time per orbit was limited only by the available view periods when the spacecraft was in the sunlight, and by the operating temperatures within the photo subsystem.

Also shown in Figure 1.3-1 are the major events during the powered portion of flight necessary to inject the spacecraft on the cislunar trajectory. The major spacecraft functions required to make it fully operational and attain the desired lunar orbits are also shown.

Spacecraft acquisition by the Deep Space Network occurred 51 minutes after launch and the spacecraft had acquired and locked on to the Sun. Nine hours after launch the Canopus acquisition sequence was initiated and properly completed. Approximately 44 hours after launch the midcourse maneuver and velocity change were commanded and executed with such precision that the planned second midcourse maneuver was not required.

Ninety-two and one half hours after launch the lunar injection maneuver and velocity change were executed. This maneuver placed the spacecraft in a lunar orbit having an initial apolune of 1867 km, a perilune of 196 km, a period of 216 minutes, and an orbit inclination of 11.97 degrees at the lunar equator. During the initial ellipse, the Goldstone test film was read out to the prime Deep Space Stations to verify coordination procedures and system operational readiness.

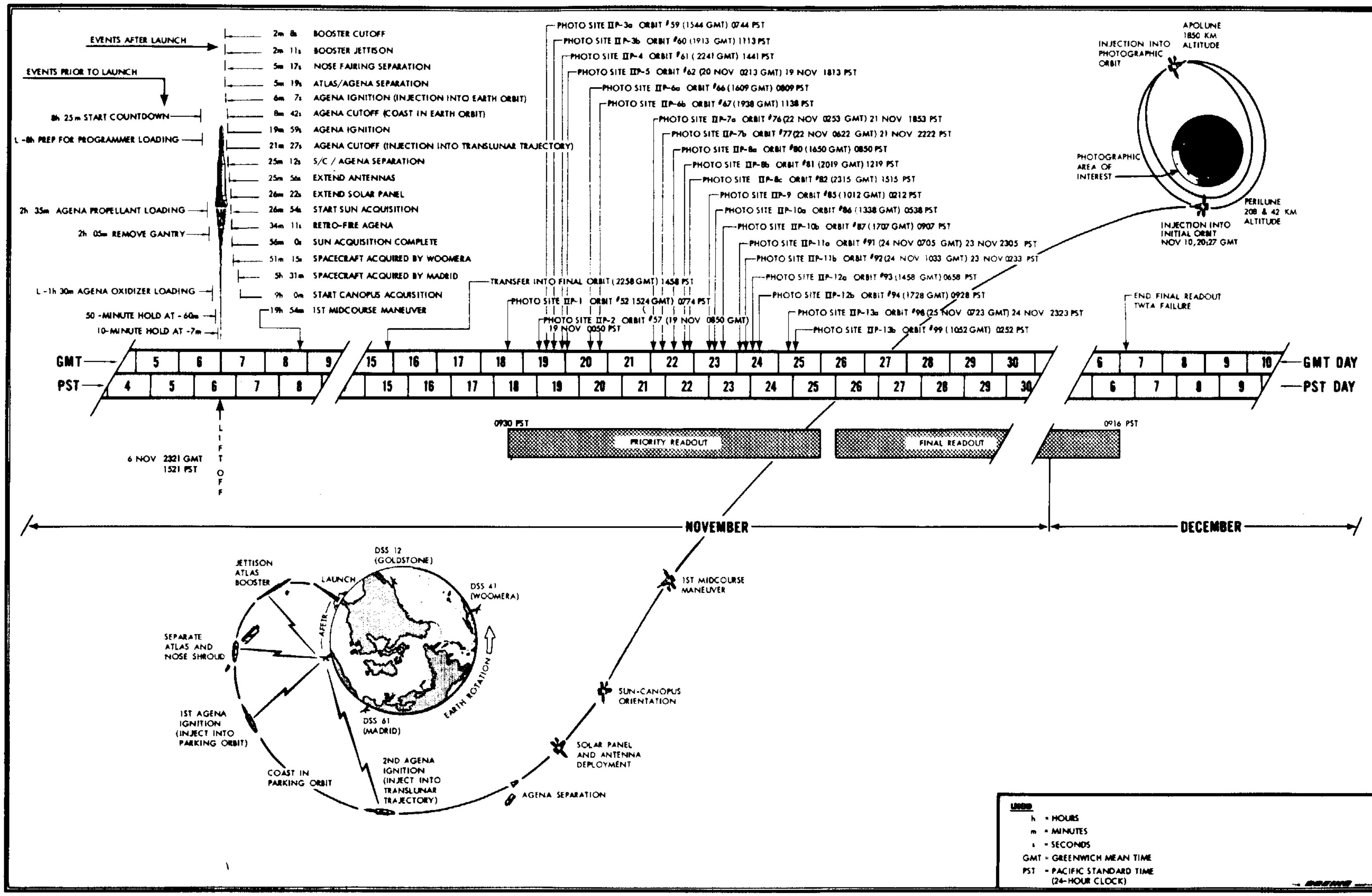

Figure 1.3-1: Lunar Orbiter II Flight Profile

Transfer to the final ellipse was accomplished during Orbit 33, 9 days after launch, by reducing the spacecraft velocity by 28.1 meters per second. A series of 16 exposures was taken of Primary Site IIP-1 on Orbit 52, which was immediately followed by a series of four additional exposures (Site IIS-1) in the same orbit. The initial readout of lunar photographs was accomplished during Orbit 53 and was simultaneously recorded at the Deep Space Stations at Woomera, Australia and Madrid, Spain. (Early evaluation of these photos showed that both cameras were operating properly and that the telemetered indication of multiple shutter operations was not valid.)

Photography progressed normally for the next 50 orbits and each of the 13 primary and 17 secondary sites was photographed as planned (except for Secondary Site IIS-10.2). During Orbit 62 an eight-frame sequence was taken of the Ranger VIII impact area. A crater, believed to be from the Ranger VIII impact, was identified in Telephoto Frame 70. As in Mission I, photos were taken of areas of scientific interest on both the near- and farsides of the Moon. Most of the telephoto photographs read out during the mission were of very good quality. The wide-angle (80-mm) lens was of good quality except where varying degrees of overexposure were expected. (Where possible, shutter speeds were selected to increase the telephoto exposure to compensate for the difference in lens transmission characteristics.)

The "Bimat cut" command was transmitted and executed during Orbit 105 and the first lunar photo of the final readout period was transmitted during Orbit 107. An average of 2.8 frames (approximately 33 inches) per orbit of the spacecraft film was read out during each final readout period. During Orbit 179 on December 7, the traveling-wave-tube amplifier (TWTA) failed to turn on when commanded and the final readout phase was terminated after having read out 98.5% of all photography. At this time approximately eight of the 211 exposed frames remained to be read out. (Frames read out in priority readout were sufficient to obtain complete wide-angle coverage of the site and selected portions of all the telephoto exposures, except the first and eighth exposure of Site IIP-1.)

Micrometeoroid hits were recorded November 15, November 29, and December 4, with no detectable effect or damage to other systems. The total radiation dosage detected was 1.75 rads near the film cassette and 1.0 rad in the vicinity of the camera looper. These levels had no effect on the spacecraft film. (Note: 0.75 rad detected near the film cassette was accumulated while passing through the Van Allen belt, during which time the looper detector was turned off.)

The spacecraft was operated at a commanded pitch angle off the sunline for approximately one half of the mission to maintain spacecraft temperatures within design operating limits.

1.3.2 SPACECRAFT PERFORMANCE

Lunar Orbiter II performance is best evaluated in the light of program and specific mission objectives. Accordingly, individual subsystem performance as it relates to these objectives is discussed in the following paragraphs.

To place the photo subsystem in the proper location and attitude at the right time to obtain the desired photographs, the Lunar Orbiter must:

- Be injected into a selected orbit about the Moon whose size, shape, and center of gravity and mass are not precisely known;
- Perform a critical attitude maneuver and a precise velocity reduction to transfer into a specified lower photographic orbit;
- Continue to operate in an unknown radiation environment and in an unknown density of micrometeoroids over an extended time;
- Accomplish a precise attitude maneuver prior to photographing each specified site and actuate the cameras at precisely the commanded time;
- Respond to tracking interrogations to provide the tracking data required to determine the orbit parameters and compute photographic mission maneuver requirements.

Failure to satisfy any of these conditions could jeopardize successful accomplishment of the Lunar Orbiter mission. How well Lunar Orbiter II accomplished these critical tasks is shown in Table 1.3-1, which is indicative of the control accuracy accomplished by the attitude and velocity control subsystems.

Table 1.3-1: Trajectory Change Summary							
	Desired Trajectory		Velocity Change (Meters Per Second)		Actual Trajectory	
			Desired	Actual		
Cislunar Midcourse	Aim Point	6023 km	21.1	21.1	Aim Point	6056 km
Lunar Orbit Injection	H_p H_a INCL	202 km 1850 km 11.94 deg	829.7	829.7	H_p H_a INCL	196 km 1867 km 11.97 deg$\pm$0.05
Orbit Transfer	H_p H_a INCL	50.2 km 1858 km 11.91 deg	28.09	28.1	H_p H_a INCL	49.7 km 1853 km 11.89 deg$\pm$0.10

From the orbits established about the Moon, the spacecraft proceeded to accomplish the many sequences of events and maneuvers required to complete the mission. Each of the 13 primary photo sites and 16 of the 17 secondary sites were photographed as planned. With the exception of the first eight photographic frames taken, all readout requirements were completed. The failure of the TWTA on the 32nd day after launch precluded the transmission of these photos.

Spacecraft performance telemetry data indicated a few subsystem irregularities (such as camera shutter counts, spacecraft equipment mounting deck temperatures, occasional loss of Canopus track, and TWTA data) were of interest to, and required real-time diagnosis by, the subsystem analysts. Only one failure (the TWTA) caused a reduction in the amount of photographic data obtained.

The performance of each spacecraft subsystem discussed in the following paragraphs also includes a brief functional description.

1.3.2.1 Photo Subsystem Performance

Photo subsystem performance was satisfactory through all phases of the mission. Each of the 13 primary and 17 secondary sites was photographed as planned except for Secondary Site IIS-10.2, which was redefined during the mission because the planned site would require operating the spacecraft on batteries and thus violate a design restriction.

———— • ————

The Lunar Orbiter photo subsystem simultaneously exposes two pictures at a time, processes film, and converts the information contained on the film to an electrical signal for transmission to Earth. The complete system, shown schematically in Figure 1.3-2, is contained in a pressurized temperature-controlled container.

The camera system features a dual-lens (telephoto and wide-angle) optical system that simultaneously produces two images on the 70-mm SO-243 film. Both lenses operate at a fixed aperture of f/5.6 with controllable shutter speeds of 0.04, 0.02, and 0.01 second.

A double-curtained focal-plane shutter is used with the telephoto lens and a between-the-lens shutter is used with the wide-angle lens. Volume limitations within the photo system container necessitated the use of a mirror in the optical path of the 610-mm lens. This mirror results in the reversal of all telephoto images on the spacecraft film (from left to right across the flight path) with respect to the wide-angle system.

An auxiliary optical system, which operates through the high-resolution-lens system, samples the image of the lunar terrain and determines a velocity-to-height (V/H) ratio. This output is converted to image motion compensation (IMC), which moves each camera platen to compensate for image motion at the film plane. The V/H ratio also controls the spacing of shutter operations to provide the commanded overlap. Camera exposure time for each frame is exposed on the film in digital code by 20 timing lights.

The latent image (exposed) film is developed, fixed, and dried by the processor-dryer. Processing is accomplished by temporarily laminating the emulsion side of the Bimat film against the SO-243 film emulsion as it travels around the processor drum.

The photographic data are converted by the readout system into an electrical form that can be transmitted to the ground receiving station. Scanning the film with a 6.5-micron-diameter high-intensity beam of light produces variations in light intensity proportional to the changes in film density. A photomultiplier tube converts these variations to an analog electrical voltage, and the readout system electronics adds timing and synchronization pulses, forming the composite video signal shown in Figure 1.3-3.

Thus, it is possible to transmit continuous variations in film tone or density rather than the discrete steps associated with a digital system. The electrical signals are fed to a video amplifier and passed to the modulation selector; transmission is via a traveling-wave-tube amplifier (TWTA) and high-gain antenna.

As a result of Mission I performance, some changes were made in the photo subsystem prior to Mission II. These included:

- The addition of an integrating circuit in the focal-plane-shutter control circuits to ensure that an output signal represents a valid command pulse (containing amplitude and duration) and not the result of an electrical transient.
- The addition of a filter on the 28-volt line to minimize electromagnetic interference and possible triggering of photo subsystem circuits.
- The platen clamping spring tension was increased to ensure immobility of the film during exposure, improve the film flatness, and maintain focus.
- Reseau marks were pre-exposed on the spacecraft film in a specific pattern to assist in compensating for any nonlinearities in the optical-mechanical scanner.

Evaluation of the Mission II photos indicated that these design changes eliminated the undesirable results identified in Mission I and that the reseau marks were of considerable value

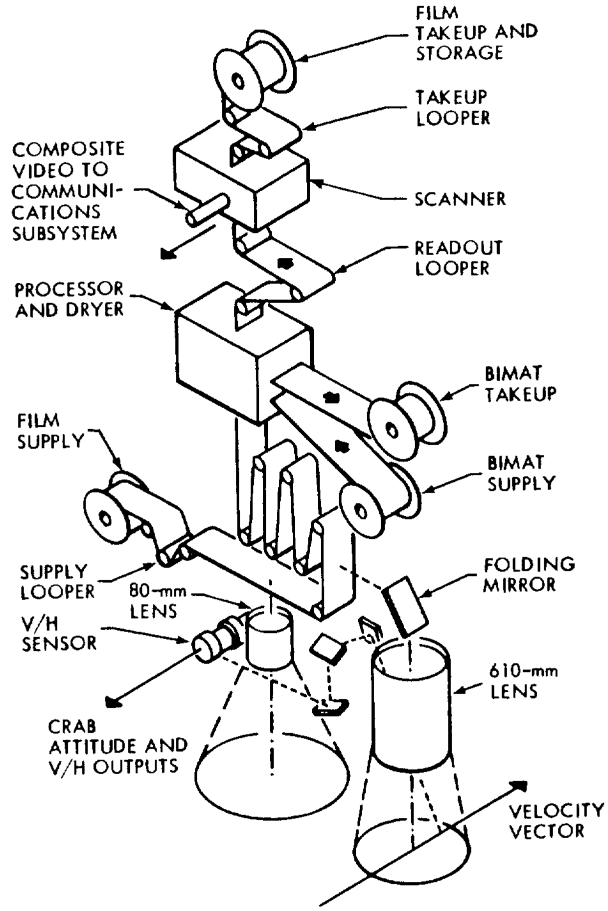

Figure 1.3-2: Photo Subsystem

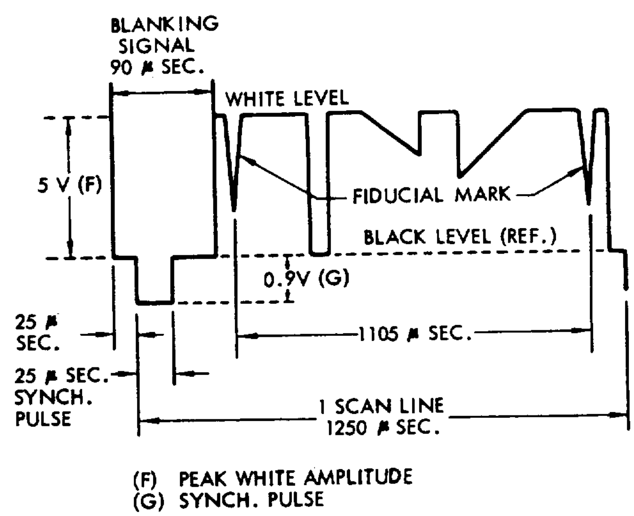

Figure 1.3-3: Video Signal Waveform

in reassembly and interpretation of photo data. Analysis of the average density data indicated that the exposures were generally satisfactory and within the limits imposed by the difference in light transmission characteristics of the two lenses. In addition, an operational decision was made to select the shutter speeds to provide more nearly optimum telephoto exposure and to accept the resulting overexposure degradation in wide-angle photography. The 53 processing periods required during the mission generated a corresponding number of stoplines and local degradation of film processing. A combination of increasing spacecraft temperatures and the Bimat dryout temperature limitations resulted in decreasing the priority readout period from 43 to 27 minutes after Orbit 82. During final readout the maximum readout period was controlled by Sun and Earth occultation periods and the TWTA temperatures. An average of 2.8 frames (approximately 33 inches) of spacecraft film was read out during each final readout period.

The shutter count telemetry data showed improper outputs varying from less than half count to more than double counts while the photos confirmed single operation of the shutters. An intermittent connection or failure of one or more components or connections in the first counter flip-flop could produce the results recorded. This telemetry monitoring circuit could not interfere with or affect the operation of the photo subsystem. Although data from this channel was highly desirable to support the real-time assessment of photo subsystem operation, the required information was recovered by computations, based upon the telemetry channels monitoring film movement, to support the operational control functions.

Evaluation of the telephoto and wide-angle photos showed density inequalities of approximately 0.3, which is being evaluated. A neutral-density filter has been incorporated in the wide-angle lens of the photo subsystem for subsequent flights.

Both telephoto and wide-angle photos indicated that photo subsystem operation was satisfactory during the exposure, processing, and readout phases of the mission.

1.3.2.2 Power Subsystem Performance

The power subsystem performed without a problem throughout Mission II. Solar array current was higher than Mission I, primarily due to a significant increase in solar intensity.

•

All electrical power required and used by the spacecraft is generated by the solar cells mounted on the four solar panels. Solar energy is converted into electrical energy to supply spacecraft loads, power subsystem losses, and charge the hermetically sealed nickel-cadmium battery. The subsystem is shown schematically in Figure 1.3-4. Excess electrical energy is dissipated through heat dissipation elements. The shunt regulator also limits the output of the solar array to a maximum of 31 volts. Auxiliary regulators provide closely regulated 20-volt d.c. outputs for the temperature sensors and the telemetry converter. Charge controller electronics protect the battery from overvoltage and overtemperature conditions by regulating the charging current. The 12-ampere-hour battery (packaged in two 10-cell modules) provides electrical power at all times when there is insufficient output from the solar array.

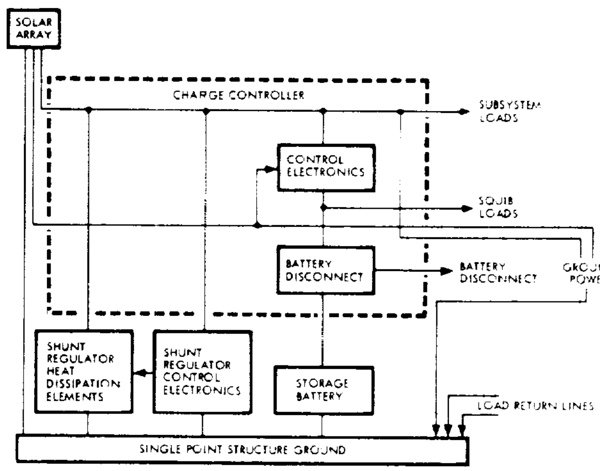

Figure 1.3-4: Power Subsystem Block Diagram

Each of the four solar panels has 2,714 individual solar cells mounted in a 12.25-square-foot area. The N-on-P silicon solar cells on each solar panel are connected into five diode-isolated circuits. Individual circuits are connected in series-parallel combinations.

•

Table 1.3-2 shows minimum, maximum, and nominal load currents experienced during the mission. The results are grouped by spacecraft operating modes as well as daytime and nighttime operation.

Spacecraft electrical loads were near the expected nominals throughout the mission. Figure 1.3-5 shows battery characteristics for a typical orbit during the final readout period.

Table 1.3-2: Spacecraft Electrical Loads

S/C Base Load	"Inhibit Htrs" on	Photo Heaters / "Inhibit Heaters" off / "Solar Eclipse" on	Photo Heaters / "Inhibit Heaters" off / "Solar Eclipse" off	Canopus Tracker	Propellant Heaters	TWTA	R/O Electronics	R/O Drive	Processor	S/C Mode	Spacecraft Electrical Load EE07 (amps) Min.	Nom.	Max.
Daytime													
X	X									Cruise (2)	3.37	3.49	3.74
		X								(2)	0	0.51	0.63
			X							(2)	0	1.40	2.20
				X								0.12	
X		X								Cruise Daytime Standby	3.37	4.00	4.38
X			X							Cruise Daytime Standby	3.37	4.89	5.95
					X							1.85	
X		X			X						5.22	5.85	6.23
X			X		X						5.22	6.74	7.80
						X						1.60	
X			X			X				TWTA on	4.97	6.49	7.45
X	X					X				TWTA on	4.97	5.09	5.35
X	X					X	X			R/O Elect. on	5.38	6.50	6.76
X	X					X	X	X		Readout	6.62	6.74	7.00
X									X	Process	4.68	5.35	6.00
Nighttime													
X	X									Cruise Nighttime Standby	3.52	3.56	3.88
X		X								Cruise Nighttime Standby	3.91	3.96	4.14
				X								0.15	
X		X		X						Acquire Canopus	4.05	4.11	4.29
					X						1.36	1.50	1.55
X		X			X						5.27	5.46	5.69

(1) Heaters Inhibited (2) Function of S/C Temp. (3) Function of Bus Voltage

During the photographic mission the depth of battery discharge, at the end of Sun occultation, varied from 25 to 28%. Sunrise was occulted from the tracking stations during much of the latter portion of the mission, making it necessary to estimate the battery conditions at sunrise. It was estimated the pre-sunrise battery voltage decreased slowly from 24.9 volts in the initial orbit to approximately 24.25 volts at the end of the photo mission.

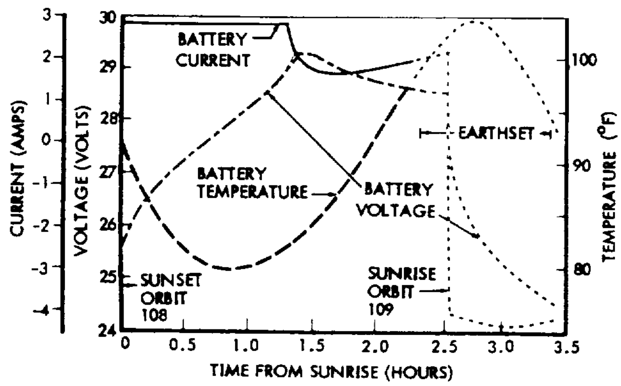

Figure 1.3-5: Battery Characteristics – Orbit 108-109

1.3.2.3 Communications Subsystem Performance

Communications subsystem performance was satisfactory through all phases of the mission until the TWTA would not turn on (within 12 hours of the planned end of the photographic mission). This failure did not affect the performance of the low-gain-antenna transmissions.

The Lunar Orbiter communications system is an S-band system capable of transmitting telemetry and video data, doppler and ranging information, and receiving and decoding command messages and interrogations. Major components of the communications subsystem as shown in Figure 1.3-6 are the transponder, command decoder, multiplexer encoder, modulation selector, telemetry sensors, traveling-wave-tube amplifier, and two antennas.

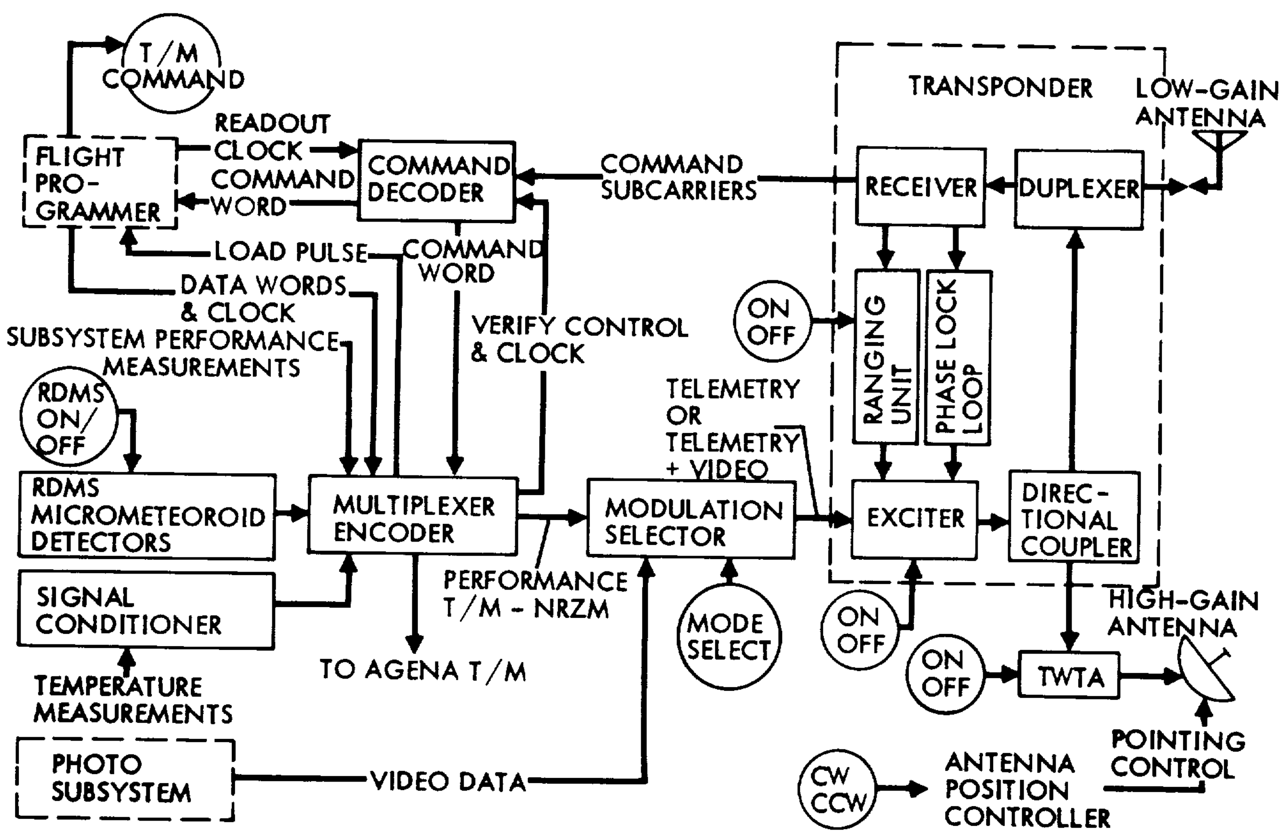

Figure 1.3-6: Communications Subsystem Block Diagram

The transponder consists of an automatic phase tracking receiver with a nominal receiving frequency of 2116.38 MHz, narrow- and wide-band phase detectors, a phase modulator, and a 0.5-watt transmitter with a nominal frequency of 2298.33 MHz. In the two-way phase lock mode the transmitted frequency is coherently locked to the received frequency in the ratio of 240 to 221.

The command decoder is the command data interface between the transponder receiver and the flight programmer. To verify that the digital commands have been properly decoded, the decoded command is temporarily stored in a shift register, and retransmitted to the DSIF by the telemetry system. After validating the proper decoding of the command, appropriate signals are transmitted to the spacecraft to shift the stored command into the flight programmer for execution at the proper time. The command decoder also contains the unique binary address of the spacecraft.

The PCM multiplexer encoder is the central device that outputs performance telemetry data into the desired format for transmission. Seventy-seven inputs are sequentially sampled at one sample per frame, and one channel is sampled at eight times per frame in the analog section. The output of these 85 data samples is converted from analog to digital form. The multiplexer also combines the 20-bit flight programmer words, the 133 one-bit discretes, and the four-bit spacecraft identification code into nine-bit parallel output words.

The modulation selector mixes the photo video information and the 50-bit-per-second performance telemetry information for input to the transponder for transmission. The selector receives control signals from the flight programmer to operate in one of the following modes:

MODE	DATA TYPE	ANTENNA EMPLOYED
1	Ranging and Performance Telemetry	Low Gain
2	Photo Video and Performance Telemetry	High Gain
3	Performance Telemetry	Low Gain

(A Mode 4 exists which is implemented by selecting the normal Mode 2 modulation but exercising the Mode 3 transmission method when no video input data are available. The selection of this particular mode increases the available power in the downlink carrier.)

The telemetry system samples the output of sensors within the various spacecraft subsystems. The normal telemetry data channels include such information as temperatures, pressures, voltages, currents, and error signals. Special instrumentation includes 20 micrometeoroid detectors located on the tank deck periphery. Radiation dosage measurement, in the form of two scintillation counter dosimeters and the associated logic, are mounted in the photo subsystem area.

The traveling-wave-tube amplifier (TWTA) consists of a traveling-wave tube, a bandpass filter, and the required power supplies. The equipment is used only to transmit the wideband video data and telemetry (Mode 2) during photo readout. It has a minimum power output of 10 watts. All of the necessary controls and sequencing for warmup of the traveling-wave tube are self-contained.

The spacecraft employs two antennas, a high-gain antenna which provides a strongly directional pattern and a low-gain antenna which is as nearly omnidirectional as practical. The low-gain antenna is a biconical-discone slot-fed antenna mounted at the end of an 82-inch boom. The high-gain antenna is a 36-inch parabolic reflector that provides at least 20.5 db of gain within ± 5 degrees of the antenna axis. The radiated output is right-hand circularly polarized. The antenna dish is mounted on a boom and is rotatable in 1-degree increments about the boom axis, to permit adjustments for the varying relative positions of the Sun, Moon, and Earth.

The spacecraft was initially acquired by the DSN station at Ascension 21.6 minutes after launch immediately after separation from the Agena and prior to antenna deployment. In the early portion of the mission it was found that the 30-kHz oscillator in the modulation selector was approximately 110 Hz above nominal center frequency. Tuning of the ground demodulators eliminated any problem in data recovery.

There were no errors in any of the verified command words executed by the flight programmer. The threshold command operation was approximately -123 dbm carrier signal at the spacecraft.

Transponder performance was satisfactory throughout the mission. As the mission progressed, telemetry data showed that rf output power varied inversely with the transponder temperature as expected. Changes in ground transmitter power levels were evident in the transponder AGC performance data (one tone command modulation produced a 2-db decrease in power level while a 3- to 4-db decrease was evident during two-tone command modulation. Range modulation produced an 8.5-db decrease in power level).

Minor problems requiring increases in ground transmitter power and frequency were evident until good orbit determination and doppler predictions were established.

Both the high- and low-gain antennas performed successfully and were properly deployed when the spacecraft was initially acquired by the Woomera Deep Space Station. Data analysis indicates that the directional-antenna gain was approximately 24.5 db and the omnidirectional antenna pattern was normal.

The TWTA operated satisfactorily for 129 on-off cycles and 198 operating hours before it failed to turn on during Orbit 179. Priority readout was initiated on Orbit 53 and completed during Orbit 104. The average operating time during this period was 39.4 minutes per orbit. Final readout was initiated on Orbit 106 and terminated when the TWTA failed to turn on. Readout time per orbit averaged 135.5 minutes during the final readout period.

The TWTA collector temperature and equipment mounting deck temperature showed the following:

	Priority Readout	Final Readout
Maximum TWTA Collector Temperature	158 - 189°F	174 - 199°F
Equipment Mounting Deck Temperature at Turn-On	38 - 76°F	36.6 - 53.3°F
Maximum Equipment Deck Temperature with TWTA On	77 - 95°F	87 - 100°F

Some increases in the TWTA helix current were noted at turn-on beginning in Orbit 74 and continuing through the priority readout period. Beginning with final readout an additional increase in helix current was evident at each turn-on. Although these turn-on indications were not normal, the TWTA output continued to be normal.

Postmission testing at both Hughes and Boeing has not duplicated the failure characteristics or isolated the cause of failure. This testing is continuing in an effort to isolate the cause. Subsequent Lunar Orbiter missions will also be closely monitored for any data that will assist in resolving the failure.

1.3.2.4 Attitude Control Subsystem Performance

Operational performance of the attitude control subsystem was entirely adequate to satisfy all mission objectives. All problems encountered were resolved by minor changes to operational procedures, enabling the spacecraft to meet all performance requirements.

Execution of all spacecraft events and maneuvers is controlled by or through the attitude control subsystem (ACS), Figure 1.3.7, to precisely position the spacecraft for picture taking, velocity changes, or orbit transfers.

The basic operating modes are:

Celestial Hold – The basic references in this mode are the Sun and Canopus; the gyro systems operate as rate sensors. This mode was planned for use during normal cruise operations and as the initial conditions for all commanded attitude changes. (In practice the spacecraft was locked to the Canopus reference during lunar night.)

Inertial Hold – The basic reference in this mode are the three gyros operating as attitude-angle sensors. This mode is used during all attitude and velocity change maneuvers, and whenever the celestial reference system is occulted.

Maneuver Mode – In this mode the spacecraft acquires the commanded angular rate about a single axis. The remaining two gyros may be held in the "inertial hold" mode.

Engine On, Inertial Hold – This mode is similar to the previously defined "inertial hold" mode except that the attitude of the spacecraft during

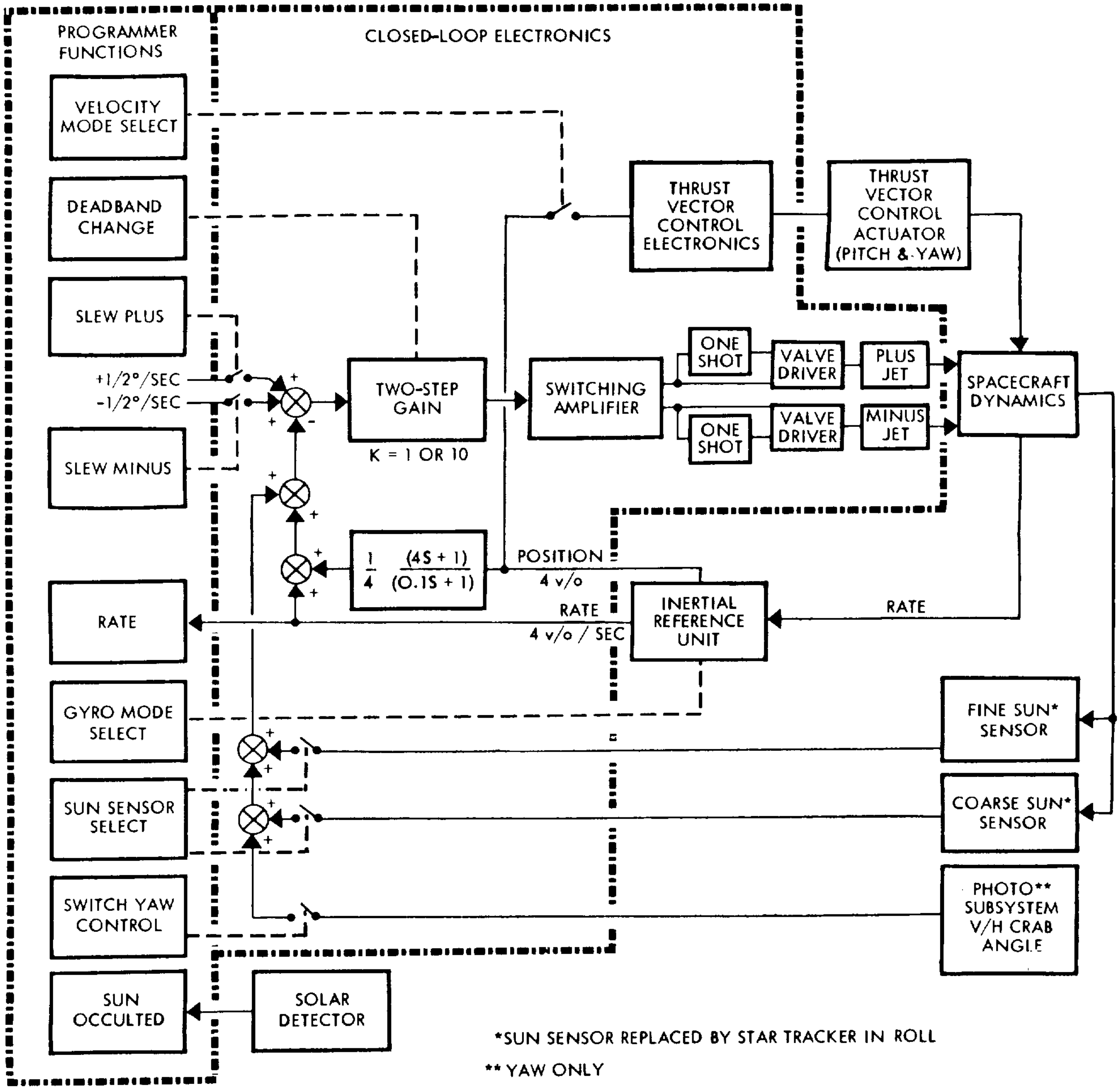

Figure 1.3-7: Attitude Control System Functional Block Diagram

the velocity change is accomplished by feedback control to the engine actuators.

Limit Cycling – The spacecraft is commanded to maintain a position within ±0.2 degree for all photographic and velocity control maneuvers or whenever commanded. (The normal deadband is ±2 degrees.)

The on-board digital programmer directs the spacecraft activities by either stored-program command or real-time command. The unit provides spacecraft time, performs computations and comparisons, and controls 120 spacecraft functions through real-time, stored, and automatic program modes. The information stored in the 128-word memory is completely accessible at all times through appropriate programming instructions. A capability of providing up to 16 hours of stored information and instructions for the spacecraft is inherent in the flight programmer design. This feature provides a high degree of reliability of executing commands without redundant equipment.

The inertial reference unit (IRU) maintains the spacecraft attitude. Three gyros provide appropriate rate or angular deviation information to maintain proper attitude and position control. A linear accelerometer provides velocity change information in increments of 0.011 foot per second to the flight programmer during any firing of the velocity control engine.

Sun sensors are located in five positions about the spacecraft to provide spherical coverage and ensure Sun acquisition and lockon and the resulting alignment of the solar panels. Error signals are generated whenever angular deviation from the spacecraft-sunline exists. A celestial reference line for the spacecraft roll axis is established by identifying the celestial body that the star tracker acquires, locks on, and tracks. Under normal conditions the star, Canopus, is used for this purpose; however, any known celestial body of suitable brightness and within the tracker's field of view as the spacecraft is rotated about the roll axis can be used to satisfy this function.

The closed-loop electronics (CLE) provides the switching and electronic controls for the reaction control thrusters and positioning of the velocity control engine actuators. Attitude maneuver and control is maintained by the controlled ejection of nitrogen gas through the cold gas thrusters mounted on the periphery of the engine deck. During a velocity control maneuver, gimbaling of the velocity control engine is used to maintain stable orientation of the spacecraft.

●

The attitude control subsystem maintained stable operation through the velocity change maneuvers, normal limit cycle operation, and all photographic maneuvers. A total of 284 single-axis maneuvers was required to support all operational functions during the 31-day mission. The maneuver accuracies about each axis were:

Roll	-0.05%
Pitch	-0.02%
Yaw	-0.11%

Spacecraft termperature control required the spacecraft to be pitched (26 to 38 degrees) away from the Sun for approximately 56% of the mission. There were no control problems associated with these maneuvers. Table 1.3-3 identifies the maneuvers performed for each requirement.

The flight programmer properly acted upon all commands received from the command decoder. These included 1289 real-time commands and 2282 stored-program commands. In addition the repetitive execution of stored-program commands increased the total commands executed to a value of approximately 12,000 individual commands.

Midcourse correction, orbit injection, and orbit transfer maneuvers were performed based on a normal Sun reference in an automatic control mode. Roll axis control was based upon Canopus acquisition in the "open loop" mode and employing ground calculations by the subsystem analyst to determine the roll commands required.

To maintain the spacecraft temperatures within allowable limits, it was necessary to pitch the spacecraft off the sunline at prescribed intervals. No control problems were encountered during these maneuvers. As the pitch angles increased, the output from the yaw Sun sensor fell off faster than the expected cosine of the pitch angle relationship and at 30 degrees pitch the output was 0.77 rather than the expected 0.866. At present there is no conclusive explanation for this additional falloff.

Canopus track was lost immediately after firing the propellant squib valve in preparation for the midcourse correction, and the velocity change maneuver was postponed. An additional star map was made and the maneuver was rescheduled and precisely executed employing the Canopus tracker in the open-loop mode.

The change of paint on the low-gain antenna, its boom, and the solar panels made a significant improvement in the performance of the star tracker system. In spite of this, reflected light from the lunar surface affected the operation of the tracker as the field of view approached the design operating limit of 30 degrees from the illuminated surface. Therefore it was necessary to employ the following sequence of roll control during the photographic and readout periods.

- Turn tracker on after sunset.
- Acquire Canopus in closed-loop mode.
- Update roll attitude.
- Turn tracker off before sunrise.

Operation of the reaction control subsystem thrusters was satisfactory throughout the flight.

Table 1.3-3: Maneuver Summary

Function	Planned	Actual Roll	Actual Pitch	Actual Yaw	Total
Velocity change	12	6	6	0	12
Photography	216	80	66	70	216
Star map	3	3	0	0	3
Thermal pitch-off	6	0	9	0	9
Attitude update	25	14	3	13	30
Others	4	8	6	0	14
Total	266	111	90	83	284
Narrow deadband maneuvers		98	82	78	258
Wide deadband maneuvers		13	8	5	26
Total		111	90	83	284

Table 1.3-4: Sun-Canopus Acquisition Summary

	Narrow Deadband	Wide Deadband	Total
Canopus acquisition	139	7	146
Sun acquisition	99	21	120
Total	238	28	266

The Sun and Canopus were acquired a total of 266 times during the mission with the control mode breakdown as shown in Table 1.3-4.

Telemetry data indicate that there were thruster firings when the star tracker was turned on. Although these transient firings caused minute spacecraft movement within the normal dead band control zone and no corrective thruster operations were required, they did not significantly affect the operational performance of the mission. The number of thruster operations during the mission was estimated from the performance data as shown in Table 1.3-5. The random phasing of thruster operation and long telemetry sampling interval was such that there was insufficient data obtained to determine the actual thrust produced by the pitch thrusters. The actual thrust developed by the thrusters appears to be slightly higher than predicted from ground test data. Data obtained during the photo mission, as well as during the extended mission, indicate no degradation in thruster performance due to the numerous operating cycles.

The inertial reference unit (IRU) performed satisfactorily during 746 hours of "on" time during the photo mission. Gyro rate integrate mode drift rates were within the specified +0.5 degree per hour. The average drift rates about each axis were measured to be:

- Pitch rate +0.2 degree per hour
- Roll rate +0.2 degree per hour
- Yaw rate +0.3 degree per hour

The maximum rate measured was 0.45 degree per hour.

Table 1.3-5: Thruster Performance				
Function	Roll	Pitch	Yaw	Total
Limit Cycle	3840	4800	5280	13,920
Maneuvers	514	420	406	1,340
Totals	4354	5220	5686	15,260
Actual Thrust (lb)	0.069	No data	0.064	

1.3.2.5 Velocity Control Subsystem Performance

Operation and performance of the velocity control subsystem was excellent during the three propulsion maneuvers performed.

The velocity control subsystem provides the velocity change capability required for midcourse correction, lunar orbit injection, and orbit adjustment as required. The spacecraft includes a 100-pound-thrust, gimbaled liquid-fuel rocket engine. The propulsion system uses a radiation-cooled bipropellant liquid rocket engine that employs nitrogen tetroxide (N_2O_4) as the oxidizer and Aerozine-50 (a 50-50 mixture by weight of hydrazine and unsymmetrical dimethylhydrazine, UDMH) as the fuel. The propellants are expelled from the tanks by pressurized nitrogen acting against teflon expulsion bladders. The propellants are hypergolic and no ignition system is required.

The engine is mounted on two-axis gimbals with electrical-mechanical actuators providing thrust directional control during engine operations. A central nitrogen storage tank provides (through separate regulators) the gas required to expel: (1) the propellants in the velocity control system, and (2) the gas for the attitude control thrusters. Figure 1.3-8 identifies subsystem components and shows how they are connected. The specified propellant load provides a nominal velocity change capability of 1017 meters per second at an oxidizer-to-fuel ratio of 2.0.

Analysis of flight data provided the following velocity control engine performance data summarized in Table 1.3-6.

During these maneuvers stable attitude control was maintained. The pitch actuator maintained the engine between +0.1 and -0.2 degree of the commanded angle. Correspoondingly the yaw actuator maintained the engine between +0.1 and +0.3 degree.

The propellant tank heaters were activated 25 times for a total of 1545 minutes to maintain the

Table 1.3-6: Velocity Control Engine Performance Summary

	Velocity Change (mps)	Burn Time (sec)	Thrust (lb)	Specific Impulse (lb-sec/lb)
Midcourse				
Predict	21.1	18.4 ± 0.6	100	276
Actual	21.1	18.1	100.5	276.5
Lunar Injection				
Predict	829.7	617.7 ± 10	100	276
Actual	829.7	611.6	101	276
Orbit Transfer				
Predict	28.09	17.5±0.9	101.5	276
Actual	28.1	17.4	102.25	276

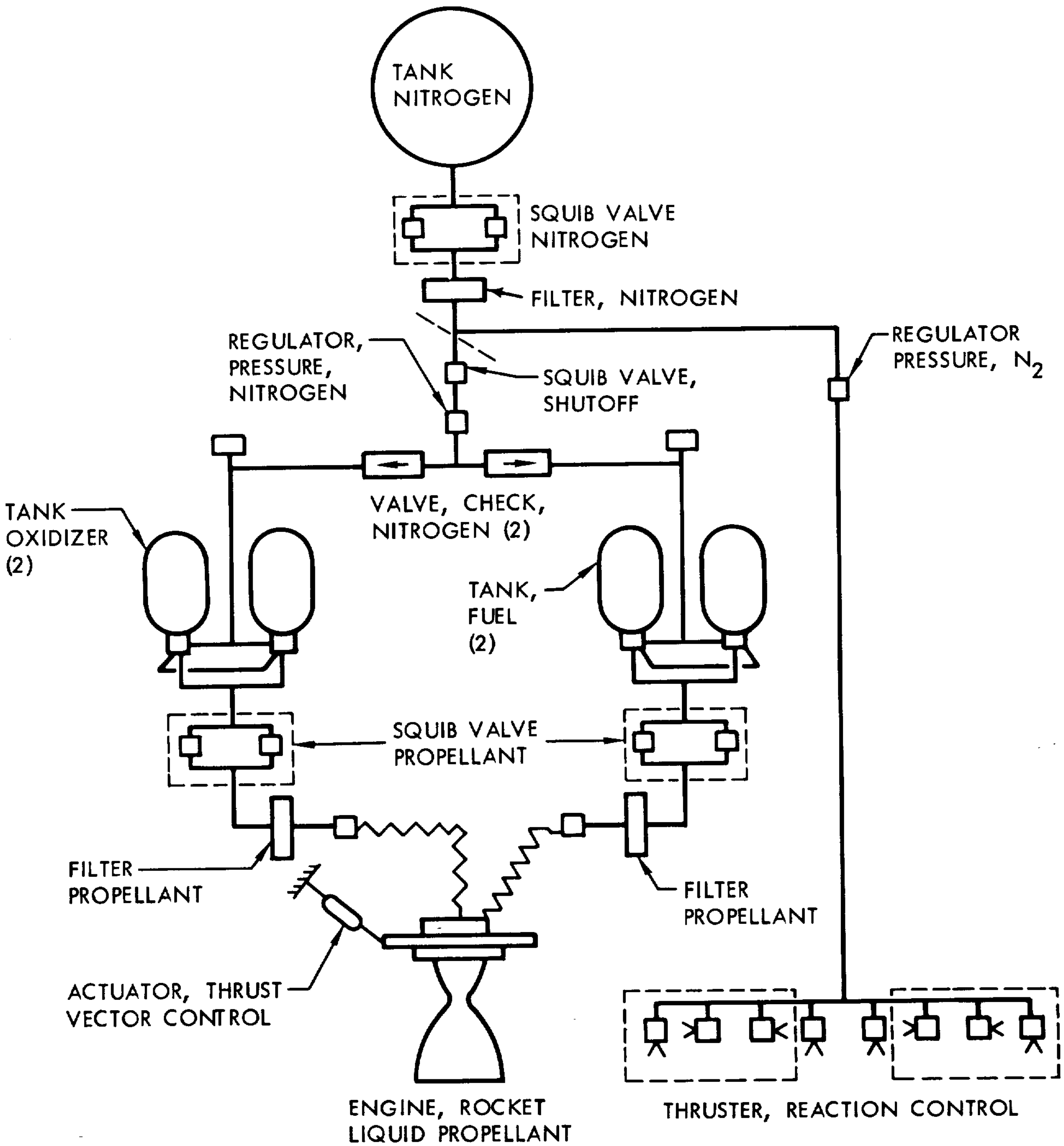

Figure 1.3-8: Velocity and Reaction Control Subsystem

propellant temperature above 40°F. Operation of the propellant squib valve and the shutoff valve was satisfactory. The shutoff squib valve was fired on December 8 (after termination of the photo mission) and sealed off the propellant tanks at the nominal regulated pressure levels for use as desired during the extended mission.

1.3.2.6 Structures, Mechanism, and Integration Elements Performance

All components comprising the structure, thermal control, wiring, and mechanisms operated properly and there were no adverse effects observed from the three recorded micrometeoroid hits. Some of the temperature data indicated the possibility of a fourth micrometeoroid impact on the spacecraft structure. As in Mission I the spacecraft had to be oriented 26 to 38 degrees off the sunline to maintain the spacecraft temperatures within acceptable operating limits.

•

The Lunar Orbiter spacecraft structure includes three decks and their supporting structure. The equipment mounting deck includes a structural ring around the perimeter of a stiffened plate. Mounted on this deck are the photo subsystem and the majority of the spacecraft electrical components. The tank deck is a machined ring, v-shaped in cross section, closed out with a flat sheet. Fuel, oxidizer, and nitrogen tanks are mounted on this deck. The 20 micrometeoroid detectors are located on the periphery of the ring. The engine deck is a beam-stiffened plate that supports the velocity control engine, its control actuators, the reaction control thrusters, and the heat shield that protects the propellant tanks during engine operation.

Prior to deployment, the low- and high-gain antennas are positioned and locked along the edges of these three decks. The four solar panels are mounted directly under the equipment mounting deck and in the stowed position are compactly folded into the space below it. Electrically fired squibs unlock the antennas and the solar panels at the appropriate time to permit them to be deployed into the flight attitude.

Thermal control of the spacecraft is passively maintained. An isolating thermal barrier, highly reflective on both the interior and exterior surfaces, encloses the spacecraft structure, except for the Sun-oriented equipment mounting deck and the insulated heat shield on the engine deck. The objective is to maintain spacecraft temperature within the thermal barrier within a nominal range of 35 to 85°F. The equipment mounting deck exterior surface is painted with a silicone-based paint that has a zinc-oxide pigment selected to achieve the desired heat balance. This paint has the properties of high emissivity in the infrared region (for dissipation of the spacecraft heat) and low absorption at the wavelengths that contain most of the Sun's emitted heat.

A camera thermal door protects the photo subsystem lenses from heat loss and direct sunlight except during photographic periods. Immediately prior to each photographic sequence, the door is opened to permit photography.

•

The antenna and solar panel deployment sequences were satisfactorily completed as planned approximately 26 minutes after launch, according to telemetry data.

Temperatures of the equipment mounting deck increased more rapidly than predicted when the solar panels were oriented perpendicular to the sunline. The additional coating of S-13G material over the original coating of B-1056 temporarily improved the performance over that experienced during Mission I. The temperatures achieved did not impair accomplishment of photo mission objectives. (It does not appear that the TWTA failure was caused by excessive EMD temperatures.)

Figure 1.3-9 shows a comparison of the thermal absorptivity data for Lunar Orbiter I and II missions and the samples which had been solar vacuum tested by the Hughes Aircraft Company. Degradation of the thermal coating and resultant transfer of additional heat to the equipment mounting deck is believed to be produced by ultraviolet radiation and low-energy protons. Some slight degradation could be attributed to micrometeoroid impacts.

Three paint sample coupons and one silver second-surface mirror were attached to the exterior of the equipment deck to evaluate their possible use on future spacecraft. The data received from the paint samples indicated that they operated at a higher temperature than the equipment deck, whereas the mirror coupon temperature was considerably lower. These data are being evaluated.

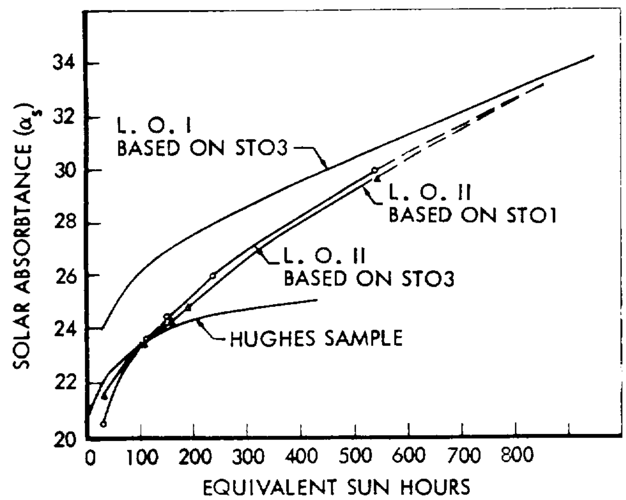

Figure 1.3-9: Thermal Coating Solar Absorptance Degradation

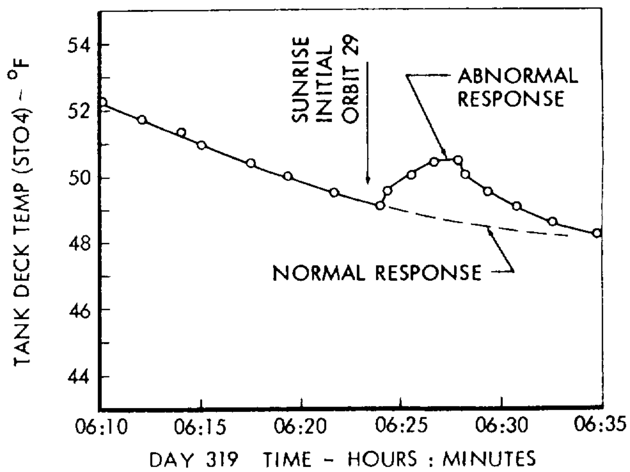

Figure 1.3-10: Thermistor Anomaly

The tank deck temperature data during Orbit 29 showed an unexpected deviation from the normal trace, as shown in Figure 1.3-10. These data may indicate that a micrometeoroid penetrated the spacecraft and impacted near the thermistor. The temperature rise could have resulted from the conversion of the micrometeoroid's kinetic energy to thermal energy.

1.3.3 OPERATIONAL PERFORMANCE

Operation and control of the Lunar Orbiter II spacecraft required the integrated services of a large number of specialists stationed at the SFOF in Pasadena, California, as well as at the worldwide Deep Space Stations. Mission advisors and other specialists were assigned from the Lunar Orbiter Project Office, supporting government agencies, Jet Propulsion Laboratory, the Deep Space Stations, and The Boeing Company.

The Langley Research Center exercised management control of the mission through the mission director. Two primary deputies were employed: the first, the launch operations director located at Cape Kennedy; the second, the space flight operations director located at the SFOF. Once the countdown started, the launch operations director directed the progress of the countdown on the launch pad, while the space flight operations director directed the countdown of the Deep Space Network. From the time that these countdowns were synchronized, all decisions (other than Eastern Test Range safety factors) regarding the countdown were made by the mission director, based on recommendations from the launch operations director and/or the space flight operations director.

After liftoff, the performance of the launch vehicle and spacecraft was monitored in the launch mission control center at ETR by the mission director. Telemetry data were used by the launch team and were relayed in real time to the SFOF through the Cape Kennedy DSS. The dissemination of spacecraft performance and tracking data to the launch and operations teams enabled efficient and orderly transfer of control from Cape Kennedy to the SFOF.

After the spacecraft had been acquired by the Deep Space Network, flight control of the spacecraft was assumed by the space flight operations director. Thereafter, the mission director moved to the SFOF and continued control of the mission. Spacecraft operations control was delegated to the space flight operations director.

Control of the mission was centralized at the SFOF for the remainder of the mission. All commands to the spacecraft were coordinated by the SPAC and FPAC teams of subsystem specialists and submitted to the space flight operations director for approval prior to being transmitted to the DSIF site for retransmission to the spacecraft. As a backup capability, each prime DSIF was supplied with a contingency capability (including predetermined commands and process tapes) to permit local assumption of the basic mission control functions in the event of communications failures.

Although Mission II was more complex than

Mission I, detailed premission planning provided the required control and look-ahead visibility with less strain on the operating team. Two major changes in mission operational planning and control procedures were implemented for Mission II:

- All requirements for secondary-site photography were included in the mission plan;
- An off-line planning group was established at the SFOF to review and implement changes to the mission plan.

Spacecraft performance was so nearly normal that the preplanned sequences were followed with only minor exceptions.

1.3.3.1 Spacecraft Control

The flight operations team was divided into three groups (designated red, white, and blue) to provide 24-hour coverage of mission operations at the Space Flight Operations Facility. Overlap was scheduled to allow detailed coordination between the on-coming and off-going system analysts. Approximately 95% of the operations team had been members of the Mission I team.

Spacecraft control was maintained throughout the mission by the generation, verification, and transmission of execute commands from the Earth-based facilities. A total of 3,571 commands (1,289 real-time and 2,282 stored-program) were generated and executed without incident. Approximately 50 additional backup commands were transmitted to the spacecraft, but did not require execution.

Command preparation activity was divided into two parts, namely:

- Off-line planning;
- On-line command preparations.

During peak activity periods there was one off-line and one on-line command programmer specialist on each team.

The off-line programmer specialist accomplished the following, based on the film budget and core map schedule of the mission plan:

- Planned the layout of each core map;
- Defined the contents of each command sequence;
- Prepared a planning command matrix map;
- Prepared an event flow chart for the on-line programmer;
- Prepared a spacecraft event sequence in GMT for review and approval.

The on-line programmer specialist accomplished the following, based on the off-line programmer specialist's planning as approved by the mission advisors and mission control:

- Prepared commands to be transmitted to the spacecraft;
- Incorporated data (magnitude, time, camera mode, etc.) contained in the command preparation directive.

Preparation of each core map was started approximately 14 to 16 hours before the scheduled transmission and ended by the preliminary command conference approximately 7 hours before transmission. In some instances it required two transmission windows to transmit the complete core map.

The flight programmer breadboard equipment – installed in the mission support area of the Space Flight Operations Facility – was operated continuously (as if in flight) to follow the mission in real time from the launch countdown through the end of the photo readout. At the same time that the command sequence was transmitted to the spacecraft by the DSS, a paper tape (produced when the commands were sent to the DSS) inserted the same data in the programmer breadboard. During Earth occultation periods the operation of the spacecraft flight programmer was followed by monitoring the operation of the breadboard programmer.

As a result of Mission I experience, changes were implemented in the output of the spacecraft time/Greenwich Mean Time correlation (TIML) program that increased its usefulness.

- For Mission I, the sum of the equipment and transmission time delays was rounded off to the nearest tenth of a second. As the spacecraft orbited the Moon, the variable transmission delay introduced excessive errors in the subsequent spacecraft clock predict outputs of the TIML program. The TIML program now carries out the total delay value to the nearest hundredth second. This substantially decreased the errors in the clock predicts.
- The calculations required to convert spacecraft clock time recorded on the film to GMT values were performed manually during Mission I. An additional

capability was added to the TIML program to calculate the GMT value corresponding to a recorded time.

Mission II required that the spacecraft be pitched off the sunline for approximately 56% of the mission. Improved procedures, developed from Mission I experience, produced a large reduction (from 221 to 39) in the spacecraft maneuvers required for thermal pitch-off and attitude update. During these maneuvers the spacecraft was pitched from 26 to 38 degrees away from the sunline to control spacecraft temperatures and reduce thermal coating degradation.

During these thermal control maneuvers it was found that, for a given solar array voltage and temperature, the array current is very nearly proportional to the cosine of the angle between the Sun vector and a line normal to the array panels. This angle is also the vector sum of the pitch and yaw angles. Since the shunt regulator maintains a constant voltage output and the array temperature was telemetered, a separate method of verifying the execution of the pitch and yaw commands was established as a mission control tool.

During the November launch period the star Canopus approaches the limb of the Moon when viewed from the spacecraft as it approaches the Apollo zone of interest. Under these conditions the reflections from the illuminated limb, by direct or reflected paths, can interfere with or prevent the retention of reacquisition of Canopus. Since this condition was expected to occur prior to the execution of the photo maneuvers for Mission II, a backup roll control method was included in the premission operational planning. This method was implemented for the photo maneuvers as follows. The star tracker was used in the closed-loop mode (tracker error signal fed to the flight programmer) to accurately position the spacecraft in roll. The roll position change from the initiation of inertial hold until the camera-on time was determined based on the inflight roll drift rate. This roll position change was included in the photo maneuver computation so that the spacecraft was properly oriented over the site.

1.3.3.2 Flight Path Control

The Lunar Orbiter trajectory was controlled during the boost phase and injection into cislunar orbit by a combination of the Atlas guidance and control system at AFETR and the onboard Agena computers. After acquisition by the Deep Space Station at Woomera, Australia, trajectory control was assumed and maintained by the Space Flight Operations Facility in Pasadena, California. During the first 6 hours of the mission following injection, the Deep Space Network performed orbit determination calculations to ensure DSS acquisition. Guidance and trajectory control calculations for controlling mission trajectories were performed by the Lunar Orbiter Operations group.

Lunar Orbiter flight path control is the responsibility of the flight path analysis and command (FPAC) team located at the Space Flight Operations Facility (SFOF) in Pasadena, California. Flight path control by the FPAC team entails execution of the following functions:

- Tracking Data Analysis – assessment of tracking data (doppler and range) and preparation of DSS tracking predictions;
- Orbit Determination – editing of raw tracking data and determination of the trajectory that best fits the tracking data;
- Flight Path Control – determination of corrective or planned maneuvers based on orbit determination results and nominal flight plan requirements.

FPAC activities during the mission were divided into the following phases:

- Injection through midcourse;
- Midcourse through deboost;
- Initial ellipse;
- Photo ellipse.

Each of the phases is discussed in the following sections.

Injection Through Midcourse

The purposes of this phase were to:

- Calculate the optimal orbit-injection point;
- Select the cislunar trajectory that satisfies the injection constraints;
- Determine the required midcourse maneuver.

DSS-51, Johannesburg, South Africa, acquired the spacecraft shortly after separation from the Agena. A tracking data sample rate of 10 seconds was employed for the first 31 minutes of tracking. Thereafter, except during the midcourse maneuver execution, the sampling interval was increased to 60 seconds. The predicted lunar encounter parameters ($\bar{B} \cdot \bar{T}$, $\bar{B} \cdot \bar{R}$, and encounter time) indicated that the Agena performance resulted in a trajectory well within the midcourse capability of the spacecraft, and that even though a midcourse maneuver was required, the execution time of the midcourse maneuver was not critical. The midcourse maneuver was planned to be executed approximately 37 hours after cislunar injection so that both Madrid (DSS-61) and Goldstone (DSS-12) would view the spacecraft during the engine burn period. Because Canopus tracker lock was lost when the velocity control squib valves were activated, the maneuver was rescheduled for the next two-station (DSS-12 and DSS-41) view period, approximately 43.5 hours after injection.

The midcourse maneuver consisted of a 41.90-degree roll, a 30.16-degree pitch, and a 21.1-meter-per-second velocity change. This attitude maneuver was selected from 12 possible attitude maneuvers based on the following criteria:

- DSS line-of-sight vector not passing through an antenna null;
- Minimum total maneuver angular rotation;
- Achieve longest time of Sun lock.

Engine ignition occurred at 19:30:00 GMT on November 8 and lasted 18.1 seconds.

Midcourse through Deboost

Approximately 5 hours of tracking data were used for the first orbit determination after the midcourse maneuver. These initial computations were within 8 km for apolune and 12 seconds for the time of closest approach of the corresponding best-estimate orbit determination solution based on 25 hours of tracking data. Table 1.3-7 summarizes the encounter parameters.

The deboost maneuver command was based on 21.5 hours of tracking data. The selected initial ellipse orbital elements, chosen from several orbit injection solutions, are compared to the prelaunch nominal values in Table 1.3-8.

The attitude maneuver and required ΔV to deboost into the selected initial ellipse were determined to be:

Roll	-8.96 degrees
Pitch	-101.38 degrees
ΔV	829.7 meters per second

Engine ignition occurred at 20:26:37.3 GMT on November 10 and lasted 611.6 seconds. The maneuver was observed by the Goldstone and Woomera tracking stations.

Initial Ellipse

Immediately after the deboost maneuver, a quick orbit determination was made to ensure rapid reacquisition of the spacecraft by the Deep Space Network when it emerged from behind the Moon. Figure 1.3-11 shows the deboost geometry and timing of significant events in establishing the initial lunar orbit. A comparison of the orbit elements of the orbit design, the first orbit determination (using 15 minutes of two-station-view tracking data), and the best estimate are shown in Table 1.3-9, where the best estimate of orbital elements was based on an orbit determination using 7.5 hours of two-way tracking data.

Table 1.3.7: Summary of Encounter Parameters

Element	Midcourse Designed	First Orbit Determination	Best Estimate
Altitude at Closest Approach (km)	2724.7	2724	2732
Time of Closest Approach (Seconds after 20:39GMT, Nov. 10)	0.0	24.4	12.5
$\bar{B} \cdot \bar{T}$ (km)	6010.1	6032	6043.6
$\bar{B} \cdot \bar{R}$ (km)	-390.5	-393.0	-373.3
$\bar{B}$ (km)	6022.8	6055.0	6055.1

Table 1.3-8: Initial-Ellipse Orbit Element Comparison		
	Selected In Flight	Prelaunch
Apolune Altitude (km)	1850.0	1850.0
Perilune Altitude (km)	202.1	200.0
Orbit Inclination (deg)*	11.94	11.95
Ascending-Node Longitude (deg)*	341.8	340.8
Argument of Perilune (deg)*	162.1	156.8

*Selenographic-of-date coordinates.

Table 1.3-9: Initial-Ellipse Orbital Elements			
Orbital Elements	Deboost Design	First Orbit Determination	Best Estimate
Perilune Altitude (km)	202.1	192.5	196.3
Apolune Altitude (km)	1850.0	1850.9	1871.3
Orbit Inclination (deg)*	11.94	11.75	11.97
Ascending Node Longitude (deg)*	341.8	347.01	341.7
Argument of Perilune (deg)*	162.1	157.16	161.6

*Selenographic-of-date coordinates.

The data scatter in orbital elements for Mission II was considerably less than during Mission I. This was the result of improved orbit determination procedures that reflected Mission I experience and the improvement in lunar gravitational field estimates developed by Langley Research Center from Mission I selenodetic data. Thus, it was possible to perform the orbit transfer maneuver 13 orbits earlier than planned and allow additional time for accurate establishment of the photo orbits.

The orbit transfer maneuver design was based on the following ground rules:

- Minimum perilune altitude of 45.3 km;
- Minimum photo sidelap of 5%;
- Illumination band of 60 to 80 degrees for primary sites;
- Transfer at least 24 hours prior to first photo;
- Minimum of 30 minutes between Earth occultation and engine ignition.

Optimizing these requirements for an orbit transfer maneuver resulted in an engine ignition time of 22:58:24.53 GMT on November 15 with a burn time of 17.4 seconds. The required spacecraft maneuver was:

Roll	33.01 degrees
Pitch	23.47 degrees
ΔV	28.1 meters per second

The orbital elements before and after the orbit transfer maneuver are shown in Table 1.3-10.

Photo Ellipse

The principal FPAC tasks during this period included:

- High-quality orbit determination prior to each primary photo event;
- Determination of attitude maneuvers and camera-on times for primary-site photography;

- Design of secondary photo site attitude maneuvers and camera-on times on a noninterference basis with primary photo activity;

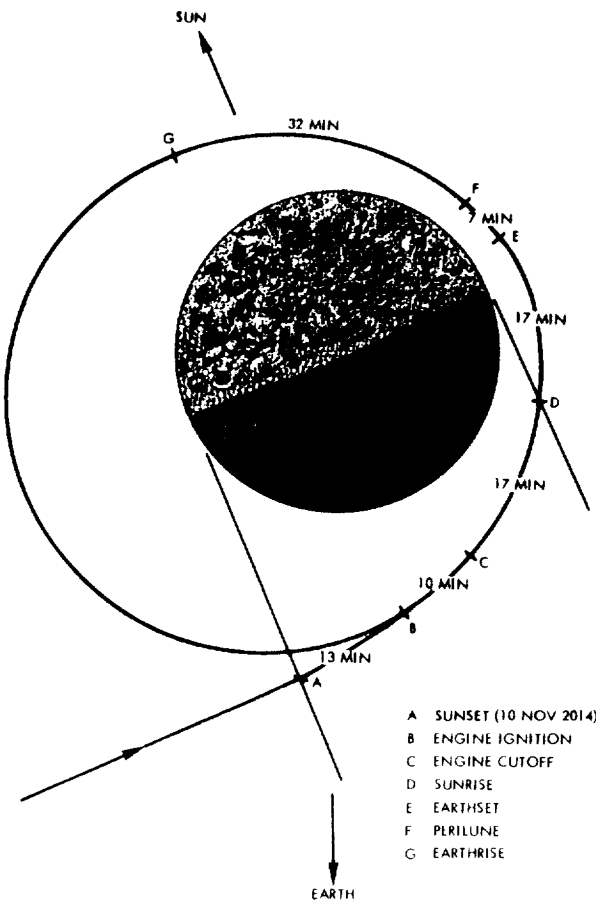

Figure 1.3-11: Lunar Orbit Injection Geometry

- Trajectory predictions, including occultation periods and sunrise and sunset times.

A total of 23 orbit determinations was made during the phototaking period, of which 17 were used to directly support command conferences for photography. A preliminary command conference was held about 10 hours before the photo sequences and a final conference about 7 hours before the first photo of the sequence. This required the prediction of spacecraft position and velocity for maneuver calculations as much as 16 to 18 hours in advance. The determination of camera-on time was set during the final conference.

Subsequent to Mission I, a DSIF procedure change provided for tracking data acquisition during photo readout. Thus, it was possible to delete the requirement to omit readout every ninth orbit to obtain tracking data. Although the data were more noisy (2 to 10 times) caused by video data interference, it was usable. Careful processing of the data and an increase of about 20% in the computer time were required to support this function. The procedure allowed the photo readout phase to progress at a more rapid rate than planned.

Orbit Phase Kepler Elements

The characteristics of the lunar orbits of Lunar Orbiter II are presented in Figures 1.3-12 through 1.3-16. These illustrations are histories of perilune radius, apolune radius, orbit inclination, argument of perilune, and longitude of the ascending node. To clearly show the complete mission, these figures cover the 30-day period from lunar injection (Days 314 to 341) and include both ellipses.

Table 1.3-10: Orbit Transfer Elements

Element	Pretransfer	Posttransfer
Apolune Radius (km)	3582.5	3590.3
Perilune Radius (km)	1951.3	1788.3
Orbit Inclination (deg)*	12.03	11.94
Ascending-Node Longitude (deg)*	164.9	163.3
Argument of Perilune (deg)*	272.5	272.8

*Selenographic of date coordinates.

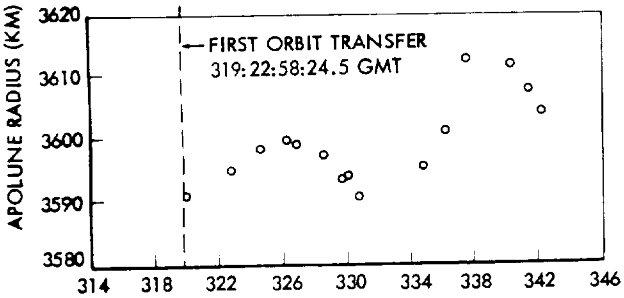

Figure 1.3-12: Apolune Radius History

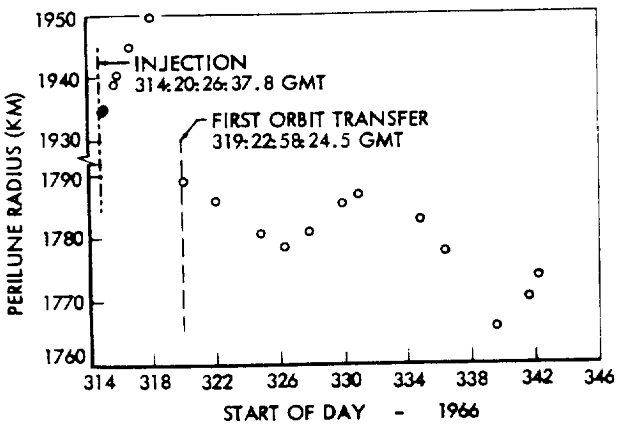

Figure 1.3-13: Perilune Radius History

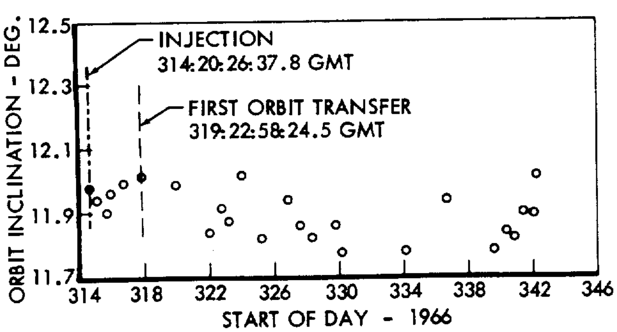

Figure 1.3-14: Orbit Inclination History

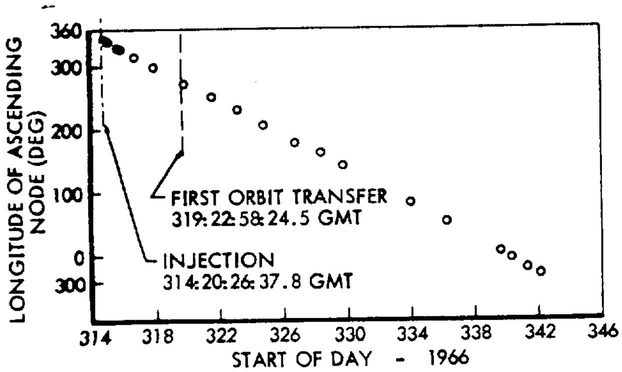

Figure 1.3-15: Longitude of Ascending-Node History

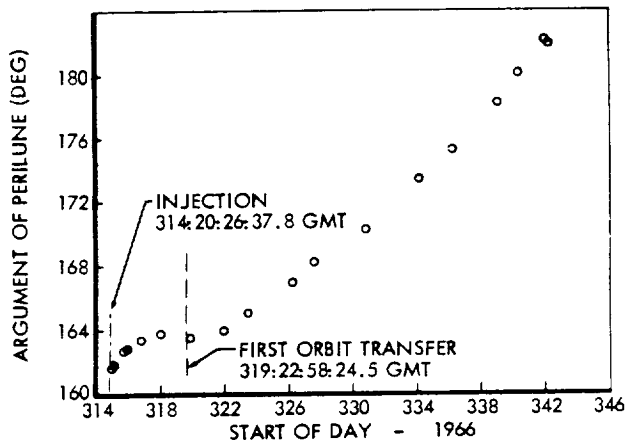

Figure 1.3-16: Argument of Perilune History

1.3.4 GROUND SYSTEM PERFORMANCE

The Lunar Orbiter ground system provides the facilities and equipment required to receive, record, and transmit data and commands between the Space Flight Operations Facility and the spacecraft. In addition, all facilities necessary to sustain mission operations were provided. This was accomplished through a complex consisting of three primary Deep Space Stations (DSS), the Space Flight Operations Facility (SFOF), and the ground communications system (GCS) which provided voice and data communication between all locations. Separate facilities were provided at Eastman Kodak, Rochester, New York, and at Langley Research Center, Hampton, Virginia, to process and evaluate the photo data obtained.

All of these facilities provided the required support during the mission and only minor irregularities were encountered. Each area is separately discussed in the following sections.

1.3.4.1 Space Flight Operations Facility (SFOF)

The Space Flight Operations Facility provided the mission control center as well as the facilities to process and display data to support operational mission control. The entire system performed satisfactorily.

Three computer strings were used to support Mission II for the periods indicated. A dual Mode 2 configuration was used to support all critical phases of the mission.

Computer String	Total Hours	Dual Mode 2
X	514	149
Y	377	131
W	96	32
Total	987	312

Subsequent to Mission I a set of ground reconstruction equipment (GRE) was installed at the SFOF and connected by microwave link to the Lunar Orbiter equipment at Goldstone DSS. This installation enabled the recording of real-time video data on film at the SFOF to assist in operational control and mission analysis. During photo readout no significant problems were encountered and no readout time was lost. Minor problems were encountered in processing the film but they were easily corrected and no data were lost.

The Lunar Orbiter software system for Mission II contained some changes which resulted from Mission I experience. These changes were incorporated and demonstrated prior to the Mission II training exercise. Performance of the entire software system was exceptional during the mission. The additional capability added to the FPAC and SPAC programs based upon Mission I shortcomings improved and simplified operational control during Mission II.

The 14 SPAC programs were executed a total of 3,536 times. Of these 3,314 were completed, 160 had input errors, 51 contained system errors, and 11 contained software errors. The 11 software errors were in the thermal control program (COOL). The error was diagnosed and compensation applied in real time during the mission. Corrections were made and verified prior to Mission III.

Telemetry processing system (TPS) and central computing complex (CCC) sections of the data processing system provided telemetry data processing, tracking data processing, command generation transmission and verification, and prediction generation and transmission to support the Lunar Orbiter mission. Hardware performance of associated computers and the data processing system was outstanding.

During the first 6 hours, the DSN was responsible for both orbit determination and data quality determination, as well as the history of data quality and analysis throughout the remainder of the mission. Jet Propulsion Laboratory personnel performed the first orbit determination after cislunar injection. The orbits were determined within the allowable time and showed a nominal injection that was subsequently verified by later orbit-determination computations.

Excellent tracking data were obtained after orbit injection and during the initial orbit. The data-quality determination was consistent among all three stations.

1.3.4.2 Deep Space Stations (DSS)

The Deep Space Stations (Goldstone, California; Woomera, Australia; and Madrid, Spain) supported the Lunar Orbiter mission by:

- Obtaining and processing telemetry and video data from the spacecraft;
- Transmitting commands to the spacecraft;
- Communicating and transmitting both processed and raw data to higher user facilities.

Real-time tracking and telemetry data were transmitted through the ground communications system. The video data were recorded on video magnetic tapes and, by mission-dependent equipment, on 35-mm film. All physical material, such as processed films, video tapes, logs, and other reports, were sent to the appropriate destinations via air transportation. All commitments were met and the incidence of error was low.

An overheating problem in the traveling-wave maser low-noise amplifier in the antenna microwave system necessitated that all sites use the alternate parametric amplifier in lieu of the maser for varying times. At one time during this outage DSS-11 successfully tracked and commanded the spacecraft while the Goldstone DSS-12 maser was being repaired. Telemetry data and commands were successfully transmitted by microwave link between the two sites.

Performance of the ground reconstruction equipment (GRE) was satisfactory and the film processing and evaluation functions were properly accomplished to support all readout periods. In many instances during priority and final readouts, readout data were simultaneously recorded at two sites.

1.3.4.3 Ground Communication System (GCS)

Ground communications between the DSS and the SFOF consist of one high-speed data line (HSDL), three full duplex teletype (TTY) lines, and one voice line. Communication lines to overseas sites are routed through the Goddard Space Flight Center at Greenbelt, Maryland.

Overall performance of the system was excellent in the Goldstone area and good for the overseas stations. High-speed data lines were reported out on several occasions at each site; however, in all but four cases the teletype backup was operable and supplied a selected 87% of the telemetry data to the SFOF. The outages for each site for 31 days of operation are summarized in Table 1.3-11.

Table 1.3-11: Data Transmission Outages

Station	Outages	Total Time (minutes)
Goldstone	3	21
Woomera	16	225
Madrid	13	238

Communications from Madrid via both the HSDL and TTY were out four times; approximately 30 minutes of data were lost. These data communication outages occurred during mission noncritical periods.

1.3.4.4 Photo Processing

Photo processing at Eastman Kodak included the making of negative transparencies and positive transparencies by successive-generation contact printing from the original GRE 35-mm positive transparencies. The GRE film was also optically reassembled into 9.5-by 14.5-inch subframes containing 14 framelets. This reassembled negative was used to produce positive and negative transparencies by successive-generation contact printing.

GRE 35-mm film was printed on Type 5234 Eastman Fine-Grain Duplicating Film. Processing goals were to have a density of 0.50 to reproduce on the copy at a value of 2.00 and a density of 2.00 to reproduce at a value of 0.50 (where a density of 0.50 corresponds to white and 2.00 corresponds to black). The inverse of densities is the normal result of the film transparency copy process, in which white areas on the original produce black areas on the copy. These densities were within 0.10 density of the received D-maximum and within 0.05 density of the received D-minimum.

Copying results for the 9.5-inch film in terms of density reproduction were as follows:

GRE Film Density	Reassembly Printer Average Density	
	Actual Value	Desired Value
2.00	0.41	0.40
0.50	1.87	1.90

The 0.1 change in desired value was made to provide an improvement in tone reproduction.

A processing and priority schedule was developed for the 35-mm film to satisfy the urgent requirement for film copies within the daily output capacity (30,000 feet per day) of the assigned facilities.

1.3.4.5 Langley Photo Data Assessment Facility

The primary functions accomplished at the Photo Data Assessment Facility at Langley Research Center were to make:

- A duplicate copy of the original video tape;
- An analog tape copy containing only the video data;
- One GRE film for each analog tape;
- Two additional GRE films as priority permitted.

A total of 308 video tapes was received during the mission. These tapes were used to produce:

- 1,299 rolls of 35-mm GRE film;
- 15 video tape (10-MHz signal) duplicate copies;
- 280 analog tape duplicates.

A limited number of the GRE film produced were made to improve the photo quality. This was accomplished by playing the video tape through an amplifier and then into the GRE set. This gain change improved the detail contained in overexposed areas, by shifting the gray scales, at the expense of losing detail in the original dark or shadow areas of the selected photos. Comparing the original and the enhanced photos provided the analyst with additional visibility of the areas being evaluated.

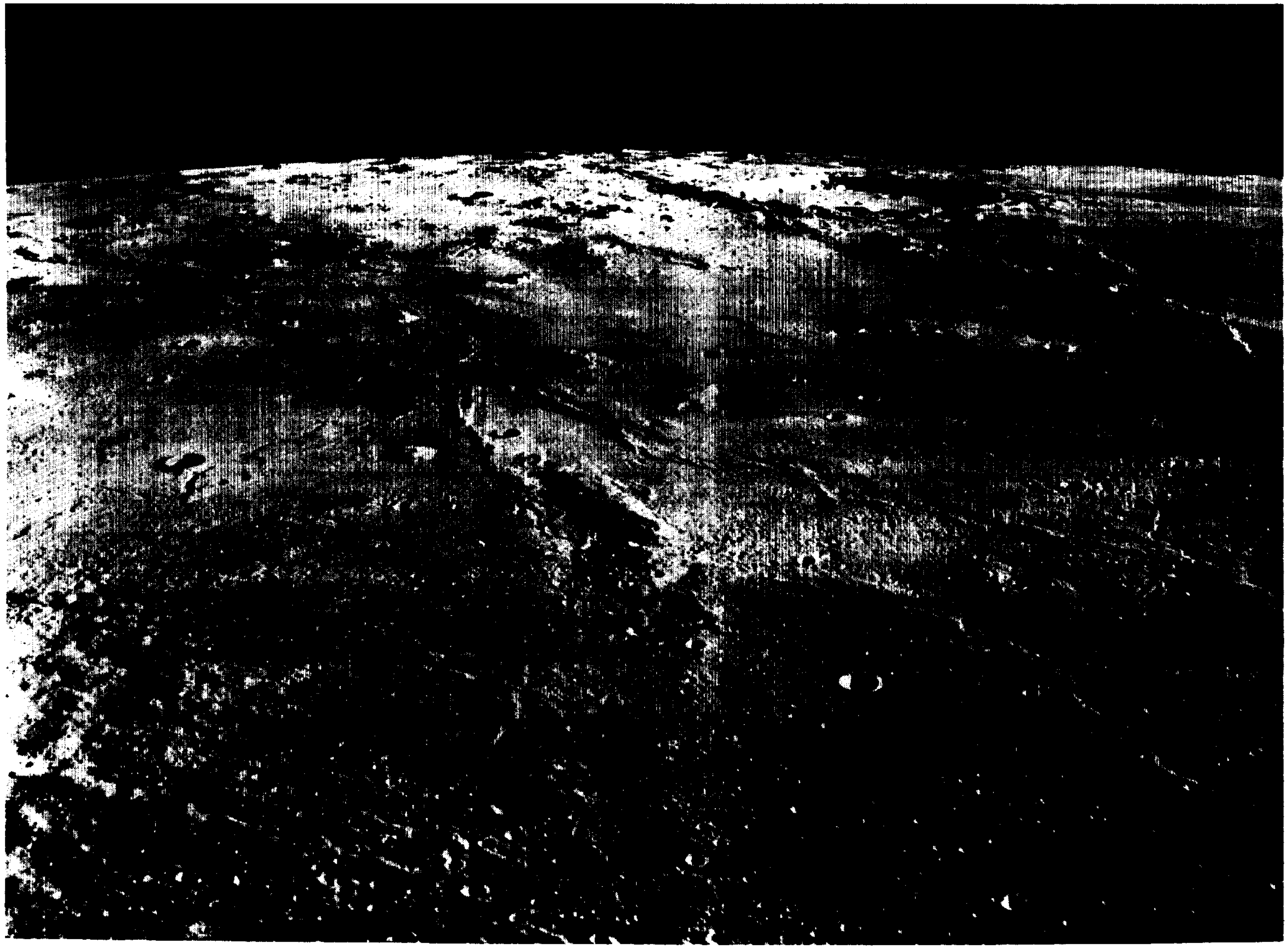

Wide-Angle Frame 213 — Site IIS-15
Looking north toward the crater Marius

1.4 MISSION DATA

Each Lunar Orbiter mission has an objective to provide four types of data—photographic, lunar environmental, tracking, and performance. All of these objectives were satisfactorily accomplished, as verified by the data obtained and separately discussed in the following sections.

Wide-angle and telephoto photographic data was obtained from all of the designated targets. The telephoto coverage provided – for the first time – photos with a resolution capability of approximately 1 meter at the primary sites.

The spacecraft detected three known micrometeoroid impacts with no noticeable effect on subsystem performance or mission data.

1.4.1 PHOTOGRAPHIC DATA

During the Lunar Orbiter II photographic mission, 422 telephoto and wide-angle photographs (211 dual exposures) were taken of the 13 planned primary and 17 secondary sites. All of the photographs of the nearside were taken from spacecraft altitudes of 41 to 57 kilometers. The eight photographs of the farside were taken from altitudes between 1450 and 1517 kilometers. Secondary Site IIS-14, centered near the eastern limb, produced both near- and farside coverage. These photos provided approximately 48,000 and 200,000 square kilometers of nearside coverage from the vertical and oblique photography, respectively. Nearly 12,000 square kilometers of this area was vertical photography at resolutions approaching 1 meter with the telephoto camera. Nearly 2,000,000 square kilometers of newly photographed areas on the farside were also obtained with the wide-angle camera with a resolution of about 325 meters. Of this area, about 325,000 square kilometers were also photographed with the telephoto lens having a resolution of about 40 meters.

Overall photographic coverage of the mission is shown in Table 1.4-1. In addition to normal vertical photography of the primary sites, vertical and oblique photos were taken of the secondary sites to enhance the interpretation of topographic features, provide converging stereo coverage of specific areas, and extend the photographic area beyond the orbit limitations. Primary-site photography was accomplished according to the prepared plan, except that Primary Sites IIP-11, and -12 were delayed one orbit to provide better site coverage. This also delayed Secondary Site IIS-13 photography by one orbit. Secondary Site IIS-10 was redefined during the mission because the planned oblique would have required a spacecraft maneuver resulting in the loss of solar panel illumination and spacecraft operation on batteries. (This condition would have violated a basic design requirement that all photography be accomplished during solar illumination periods.) A vertical photo of the crater Gambert C (an identified thermal anomaly crater) was then substituted and successfully obtained.

The failure of the traveling-wave-tube amplifier to turn on prevented final readout of approximately 16 of the 422 photos taken. During priority readout, however, 11 of these photos were read out in whole or in part. The combination of priority and final readout of the wide-angle photos and the forward overlap of successive photos provided 100% of the photo coverage of primary Site IIP-1 even though three of the wide-angle photos were not read out. Figure 1.4-1 shows the coverage of Site IIP-1 photographed by the telephoto camera. The shaded areas show the section reconstruction from both the priority and final readout periods.

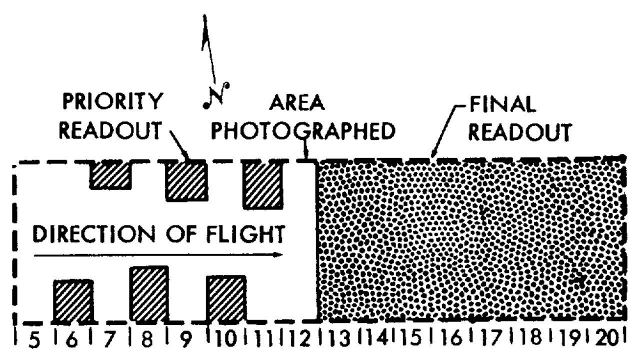

Figure 1.4-1: Readout Coverage of Primary Site IIP-I Telephoto Coverage

Mission Photography

The analysis and assessment of mission photography was based upon second-generation GRE positive transparencies, third-generation 9.5-inch reassembled negative transparencies, and

Table 1.4-1: Photographic Coverage Summary

Photo Site	Number of Frames	Approximate Area Photographed			
		Wide Angle		Telephoto	
		Size (km)	Area $km^2 x10^{-3}$	Size (km)	Area $km^2 x10^{-3}$
Primary Sites					
IIP-1	16	93 x 38	3.53	65 x 17	1.11
IIP-2	8	57 x 36	2.05	31 x 16	0.50
IIP-3	16	60 x 47	2.82	32 x 26	0.83
IIP-4	8	63 x 40	2.52	34 x 17	0.58
IIP-5	8	55 x 35	1.93	29 x 15	0.44
IIP-6	16	62 x 49	3.04	33 x 27	0.89
IIP-7	16	53 x 44	2.33	28 x 24	0.67
IIP-8	24	64 x 71	4.54	34 x 45	1.53
IIP-9	8	58 x 36	2.09	31 x 16	0.50
IIP-10	16	56 x 46	2.58	30 x 25	0.75
IIP-11	16	69 x 55	3.80	37 x 31	1.15
IIP-12	16	57 x 45	2.57	31 x 26	0.81
IIP-13	16	59 x 48	2.83	31 x 26	0.81
Secondary Sites					
IIS-1	4	43 x 37	1.59	16 x 16	0.26
IIS-2	8	47 x 40	1.88	17 x 19	0.32
IIS-3	1	1175 x 1390	1633	133 x 530	70.49
IIS-4*	1	1275 x 1405	1791	150 x 705	105.75
IIS-5*	1	1002 x 1185	1187	142 x 622	88.32
IIS-6	1	31 x 38	1.18	4 x 17	0.07
IIS-7*	1		48		28
IIS-8	1	33 x 39	1.29	4 x 17	0.07
IIS-9	1	28 x 34	0.95	4 x 15	0.06
IIS-10.2	1	29 x 34	0.99	4 x 15	0.06
IIS-11	1	35 x 42	1.47	5 x 18	0.08
IIS-12*	1		44		25
IIS-13	1	33 x 39	1.29	4 x 17	0.07
IIS-14	1	1229 x 1447	1778	137 x 545	74.67
IIP-15*	1		61		35
IIP-16	1	33 x 39	1.29	4 x 17	0.07
IIP-17*	1		49		28

Farside Photos: Sites IIS-3, 4, 5, 14
*Oblique photos containing lunar horizon.

paper prints made from manually reassembled GRE film. Primary photo site photography was examined by selecting frames from the start, middle, and end of a photo sequence.

Lunar orbital photography was made particularly difficult by uncertainties in knowledge of the Moon's surface characteristics and its photometric function, both of which are critical to photography. The Moon has unique reflectance characteristics unlike any encountered in terrestrial photography. The wide range of reflectance can and did produce photographic images in adjacent areas having a density range that exceeded the capability of the spacecraft readout system (thus obliterating detail in areas of density extremes) while exhibiting excellent detail in the surrounding areas. Experience gained during Mission I was used to refine the selection of photographic parameters required to determine the required exposure settings.

To aid in the evaluation of Mission II photos, reseau marks illustrated in Figure 1.4-2 were pre-exposed on the spacecraft film at the same time as the edge data. The fixed orientation can assist the photo analyst in the detection and compensation for distortions introduced after imaging by the camera lens.

Overall quality of the wide-angle (80-mm lens) photographs was very good except where degradation was expected by selecting the shutter speed to more nearly optimize the telephoto exposure. This caused about 40% of the wide-angle photographs to be overexposed by varying degrees and a proportionate loss of data detail. Examination of these photos by microdensitometer measurements, and visual examination with a 10 to 30X zoom macroscope, showed that the resolution requirement (8 meters plus a correction for the altitude difference from 46 kilometers) was met at all primary sites. Exposure levels were generally good; however, photos of some local areas were overexposed by the unknown and uncertain local surface characteristics. In some instances, where side overlap was obtained, different shutter settings were used on the later pass to more nearly optimize the photos obtained. Forward stereo coverage was obtained at all primary sites. Side overlap provided additional stereo coverage on eight of the primary sites. The near- and farside oblique photos of secondary sites provided high-quality photos over wide areas. These photos provided significant data to assist in interpreting topographic features and establishing the criteria for navigational-aid selection.

The telephoto (610-mm lens) photo quality was generally good, although there were some exceptions. The 24% difference in light transmission characteristics of the two lenses resulted in a nominally underexposed photo during the early site photography, except for those sites where the wide-angle photos were overexposed. (This reduction in light transmission produced increased detail in those local areas where the corresponding wide-angle coverage was severely overexposed.) The operational decision to select shutter speeds based on the telephoto lens characteristics produced corresponding improvements, commensurate with the limited shutter speeds available. Examination of photos showed that the resolution requirement (1 meter with a proportional correction for the altitude difference from 46 kilometers) was met at all primary sites. There was no evidence of any irregularities in the performance of the focal-plane shutter. The desired nominal 5% forward overlap in telephoto coverage was attained on all multiframe sequences. A limited amount of stereo coverage was obtained in the telephoto exposures on successive orbits covering eight of the primary sites.

The impact point of Ranger VIII has been identified as one of two small bright craters (see Figure 1.4-10) in Telephoto Frame 70. These (7- and 15-meter-diameter) craters lie close to the estimated impact point derived from extending the trajectory established from the Ranger photo formats and are approximately the expected size.

A comparison of the coordinates of the primary-site locations shown in Table 1.1-1 and the results shown in Table 1.4-2 show that the photographic coverage was not always centered on the specified location because of operational limitations, which included such items as: the photo orbit did not always pass directly over the site; camera-on time was determined for the first frame of the sequence only; subsequent exposures were controlled by the spacecraft velocity-to-height determination; varia-

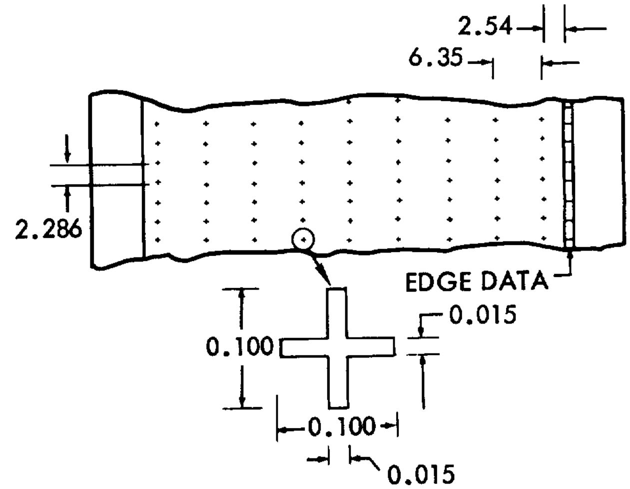

(dimensions in millimeters on spacecraft film)

Figure 1.4-2: Pre-exposed Reseau Mark Characteristics tions of spacecraft attitude during the photo sequence, variations in lunar surface elevations, uncertainties in the mathematical model of the Moon, and errors in the lunar charts all contribute to the apparent displacements. A similar comparison can be made for the near-vertical secondary sites. All of the oblique photos contained the lunar surface features specified for each secondary site.

The matching of individual photos with the most recent lunar charts indicate varying degrees of agreement. Contributing factors to this problem are discussed as follows. A secondary objective of the Lunar Orbiter program is to obtain tracking data from which to refine the mathematical model of the Moon. To compute the photo supporting data and predicted photo locations, the best available estimates for these parameters must be used in the orbit determination routines. Therefore, some discrepancies can be expected in the coordination of the computed photo location with the maps made from Earth-based observations.

Other errors in locating the photos stem from spacecraft attitude variations within the ± 0.2-degree control deadband and the lunar surface elevation changes. It must also be remembered that considerable effort is required to transfer the data from the unrectified, non-orthographic projection photographs to the Mercator projection maps. In general, the lunar feature matching between the photos and lunar charts indicate that the predicted photo locations are generally consistent with the chart "reliability diagram." Continued analysis and comparison of photos obtained from each photo mission will result in more accurately defining the lunar surface, and reducing the positioning error in subsequent lunar charts.

Secondary-site telephoto coverage of the near- and farside with vertical and oblique orientation produced high-quality results. Exceptional photographs of the craters Copernicus and Marius were obtained and are shown on pages vi and 54.

The converging telephoto stereo experiment to determine the feasibility of photographing a single area from two successive orbits produced excellent results. Figure 1.4-3 shows the coverage obtained on each pass. Approximately 75% of the telephoto coverage of the site provided stereo visibility. Stereo analysis techniques must compensate for the scale change caused by the camera axis tilting.

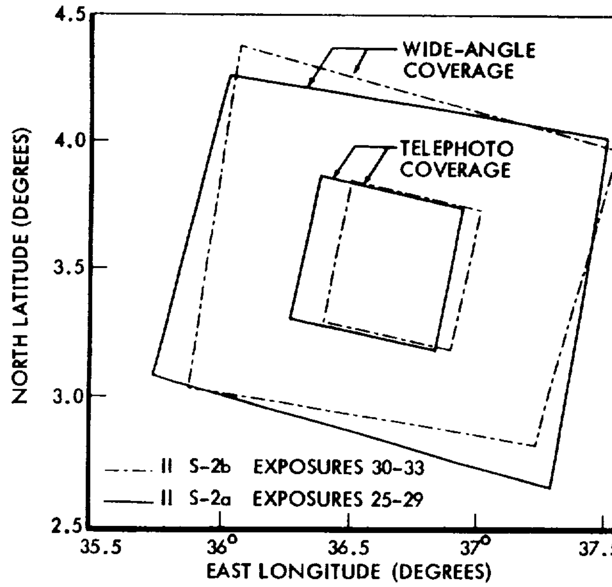

Figure 1.4-3: Converging Stereo Coverage (Site IIS-2)

The following conclusions were drawn from an analysis by the Aeronautical Chart and Information Center working in conjunction with the Lunar Orbiter Photo Data Screening group. The results were based on a stereo model scale of 1:21,800.

- A spot-heighting test achieved a standard deviation (vertical) of 0.7 meter at random reseau intersections. A standard deviation of 0.46 meter was achieved at well defined, high-contract feature points.
- Two-meter relative contours were drawn over a small area of the model. A repeatability test was made by drawing contours over the same area a number of times.
- As a result of the test, it is estimated that relative elevations of control points could be computed with a standard deviation of about 1 meter on high-resolution convergent exposures of this type.

Photo Coverage

Table 1.4-2 summarizes the photographic coverage of the primary sites for Mission II and provides significant supporting data for each site. The angle of incidence is defined as the angle between the Sun's rays and the normal to the lunar surface. The phase angle is the angle between the camera axis and the Sun's rays. The angle and altitude ranges are for the first and last frame of the sequence, respectively.

Table 1.4-2

Primary-Site Supporting Data

Photo Site	Spacecraft Exposure No. /Orbit	Shutter Speed (sec)	Location of Photo Center		Spacecraft Altitude (km)	Approximate Framelet Width		Phase Angle (deg)	Angle of Incidence (deg)
			Longitude	Latitude		Wide Angle (km)	Telephoto (km)		
IIP-1	5-20/52	0.04	36.9°E	4.4°N	48 - 47	1.5	0.20	72.9	74.5 - 72.6
IIP-2	35-42/57	0.02	34.0°E	2.7°N	45 - 46	1.5	0.19	67.8	68.0 - 67.2
IIP-3a	43-50/59	0.04	21.3°E	4.5°N	48 - 47	1.5	0.20	75.6	77.3 - 76.3
IIP-3b	51-58/60	0.04	21.1°E	4.1°N	46 - 45	1.5	0.19	74.4	75.7 - 74.8
IIP-4	59-66/61	0.04	15.7°E	4.8°N	50 - 49	1.6	0.21	77.7	79.4 - 78.5
IIP-5	67-74/62	0.04	24.8°E	2.8°N	43	1.4	0.18	69.1	68.4 - 67.6
IIP-6a	76-83/66	0.02	24.2°E	1.1°N	47 - 48	1.5	0.20	62.6	62.0 - 61.1
IIP-6b	84-91/67	0.02	24.0°E	0.7°N	49 - 50	1.6	0.21	61.1	60.4 - 59.4
IIP-7a	96-103/76	0.02	1.7°W	2.5°N	41	1.3	0.17	70.2	70.2 - 69.4
IIP-7b	104-111/77	0.02	1.9°W	2.1°N	41 - 42	1.3	0.17	68.7	68.6 - 67.8
IIP-8a	113-120/80	0.02	0.8°W	0.7°N	47 - 48	1.5	0.20	63.1	62.3 - 61.4
IIP-8b	121-128/81	0.02	1.0°W	0.3°N	49 - 50	1.6	0.21	61.7	60.7 - 59.8
IIP-8c	129-136/82	0.02	1.2°W	0.1°S	52 - 54	1.7	0.22	60.2	59.2 - 58.2
IIP-9	138-145/85	0.02	12.9°W	1.1°N	44 - 45	1.4	0.19	66.1	65.6 - 64.7
IIP-10a	146-153/86	0.04	27.1°W	3.6°N	45 - 44	1.4	0.19	76.9	78.1 - 77.2
IIP-10b	154-161/87	0.04	27.1°W	3.2°N	44 - 43	1.4	0.18	75.5	76.3 - 75.5
IIP-11a	163-170/91	0.02	19.7°W	0.1°N	51 - 53	1.7	0.22	62.9	61.8 - 60.9
IIP-11b	171-178/92	0.02	19.7°W	0.3°S	55 - 57	1.8	0.23	61.5	60.1 - 59.0
IIP-12a	179-186/93	0.04	34.1°W	2.3°N	44	1.4	0.19	72.8	72.7 - 71.9
IIP-12b	187-194/94	0.02	34.0°W	1.9°N	45	1.4	0.19	71.4	70.9 - 70.0
IIP-13a	197-204/98	0.04	41.7°W	1.9°N	45	1.4	0.19	71.8	71.6 - 70.7
IIP-13b	205-212/99	0.02	41.7°W	1.5°N	46 - 47	1.5	0.19	70.4	69.8 - 68.9

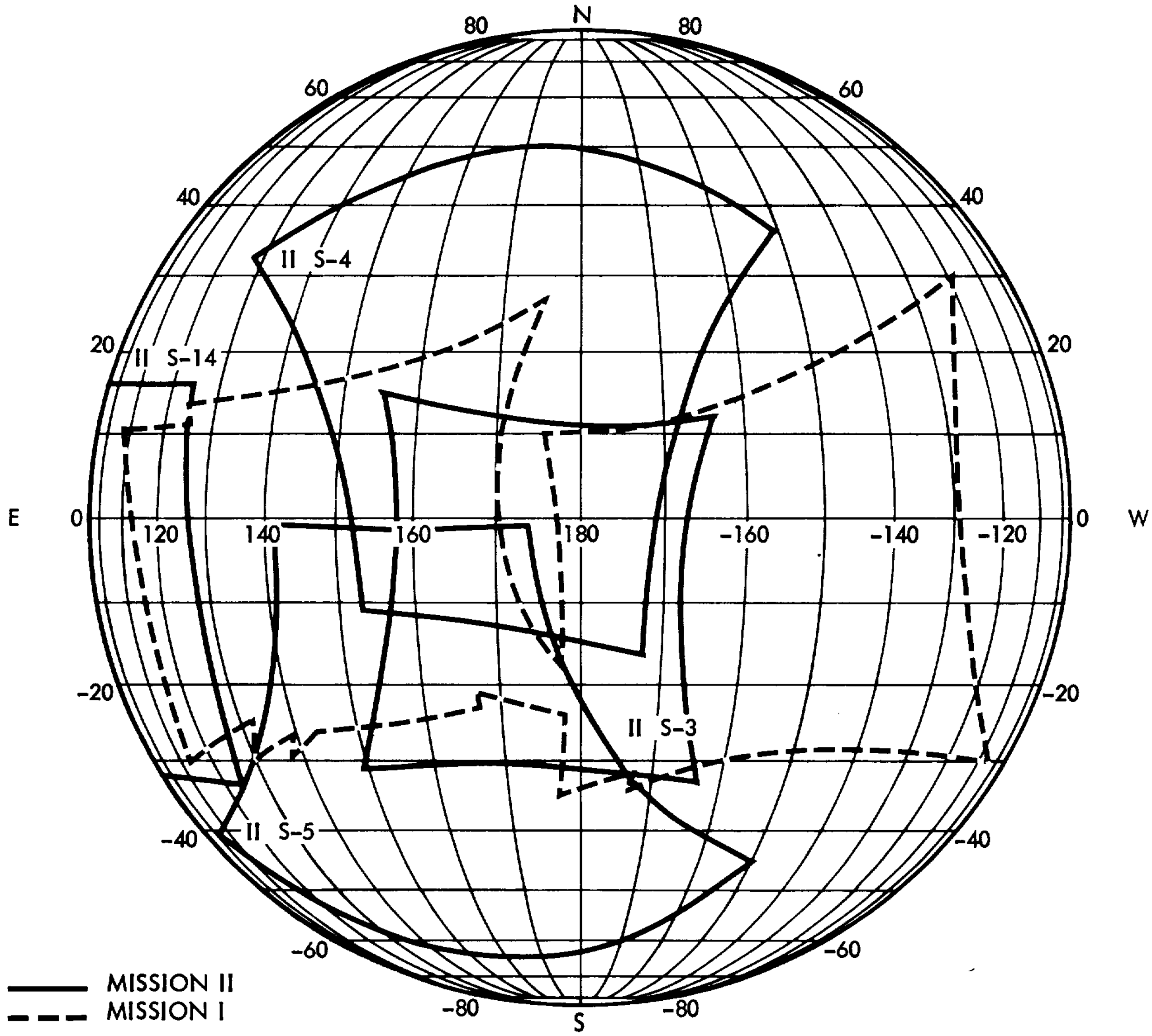

Figure 1.4-4: Lunar Orbiter Farside Photographic Coverage

Photo coverage of the farside is presented in two forms. Table 1.4-4 provides significant supporting data for the four photos taken on Mission II. Figure 1.4-4 shows the actual areas covered by each photo which is superimposed on the envelope of coverage from Mission I. Secondary Sites IIS-4 and -5 were oblique photos, therefore the scale factor changes throughout the photo. The following photographs, Figures 1.4-5 through 1.4-22, are representative of portions of the primary photo sites identified for this mission. Also included are representative farside photography, frontside areas of interest, and examples of moderate resolution and accompanying high resolution. Each photo contains a descriptive caption.

Corresponding data for the secondary sites on the nearside are given in Table 1.4-3. The slant distance is defined as the distance between the camera and the principal ground point (the intersection of the projected camera axis and the lunar surface). Tilt angle is defined as the true angle between the camera axis and the local vertical through the spacecraft. Tilt azimuth is the clockwise angle from lunar north to principal ground point measured from the vertical projection of the spacecraft on the lunar surface. Secondary Sites IIS-7, -12, -15, and -17 were oblique photos, therefore the scale factor changes throughout the photo. The framelet width numbers given apply at the center of the photo format only.

Table 1.4-3
Nearside Secondary-Site Supporting Data

Photo Site	Spacecraft Exposure No. /Orbit	Shutter Speed (sec)	Location of Photo Center		Spacecraft Altitude (km)	Slant Distance (km)	Framelet Width		Phase Angle (deg)	Angle of Incidence (deg)	Tilt Angle (deg)	Tilt Azimuth (deg)
			Longitude	Latitude			Wide Angle (km)	Telephoto (km)				
IIS-1	21-24/52	0.04	41.1°E	3.2°N	46	46	1.5	0.19	72.9	69.4	3.5	102
IIS-2a	25-28/53	0.04	36.6°E	3.5°N	46	48	1.5	0.19	81.1	72.0	12.1	136
IIS-2b	29-32/54	0.02	36.6°E	3.5°N	46	47	1.5	0.19	62.1	70.2	11.8	318
IIS-6	92/69	0.02	4.4°E	4.3°N	44	45	1.4	0.18	78.6	76.1	12.8	11
IIS-7	93/71	0.02	1.1°W	0.3°N	44	129	4.2*	0.54*	76.1	78.0	68.0	191
IIS-8	94/73	0.01	12.2°E	0.8°N	48	48	1.6	0.20	61.8	61.1	0.7	96
IIS-9	95/75	0.02	0.8°W	2.6°N	41	41	1.3	0.17	69.6	70.6	1.0	284
IIS-10.2	112/79	0.02	12.1°W	3.4°N	42	42	1.3	0.17	74.3	75.0	0.7	284
IIS-11	137/83	0.04	27.6°W	4.9°N	51	51	1.6	0.21	81.5	83.5	1.9	283
IIS-12	162/89	0.01	20.0°W	5.6°N	46	147	4.7*	0.62*	80.8	65.4	69.6	0
IIS-13	195/96	0.04	46.3°W	3.6°N	48	48	1.6	0.20	76.3	79.2	2.9	282
IIS-15	213/100	0.04	52.9°W	8.1°N	49	151	4.8*	0.63*	96.1	7.9	68.8	12
IIS-16	214/101	0.04	53.8°W	3.2°N	48	48	1.6	0.20	77.8	78.0	0.2	291
IIS-17	215/102	0.04	58.3°W	7.2°N	51	119	3.8*	0.50*	95.5	80.8	62.9	12

*Oblique photo, applies at center of photo format only

Table 1.4-4:
Farside Secondary-Site Supporting Data

Photo Site	Spacecraft Exposure No. /Orbit	Shutter Speed (sec)	Location of Photo Center		Spacecraft Altitude (km)	Slant Distance (km)	Framelet Width		Phase Angle (deg)	Angle of Incidence (deg)	Tilt Angle (deg)	Tilt Azimuth (deg)
			Longitude	Latitude			Wide Angle (km)	Telephoto (km)				
IIS-3	33 / 55	0.02	174.3°E	10.1°S	1453	1453	46.7	6.1	69.9	70.1	0.2	162
IIS-4	34/56	0.02	173.8°E	5.0°N	1450	1576	46.1 so. edge 50.6 center	6.0 so. edge 6.6 center	69.9	71.1	16.6	6
IIS-5	75 /64	0.02	158.2°E	20.7°S	1466	1533	47.1 no. edge 49.3 center	6.2 no. edge 6.4 center	69.9	70.8	12.4	181
IIS-14	196 /97	0.02	101.0°E	8.8°S	1517	1517	48.8	6.3	69.9	70.6	0.4	99

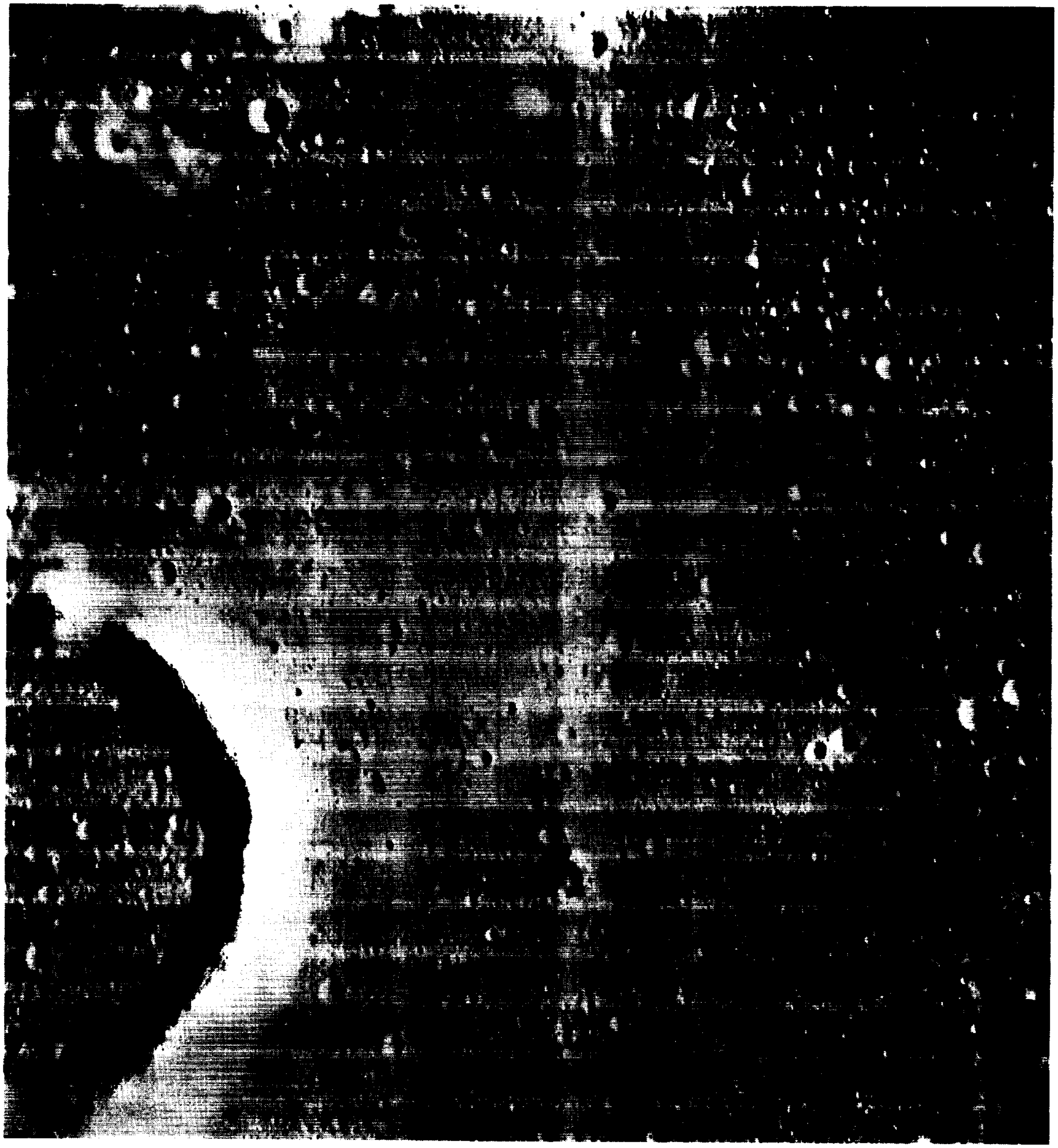

Figure 1.4-5: **Wide-Angle Frame 5 – Site IIP-1**

Framelet Width: 1.56 km

Large rim at left is crater Maskelyne F.

Figure 1.4-6: **Wide-Angle Frame 40 – Site IIP-2** Framelet Width: 1.43 km

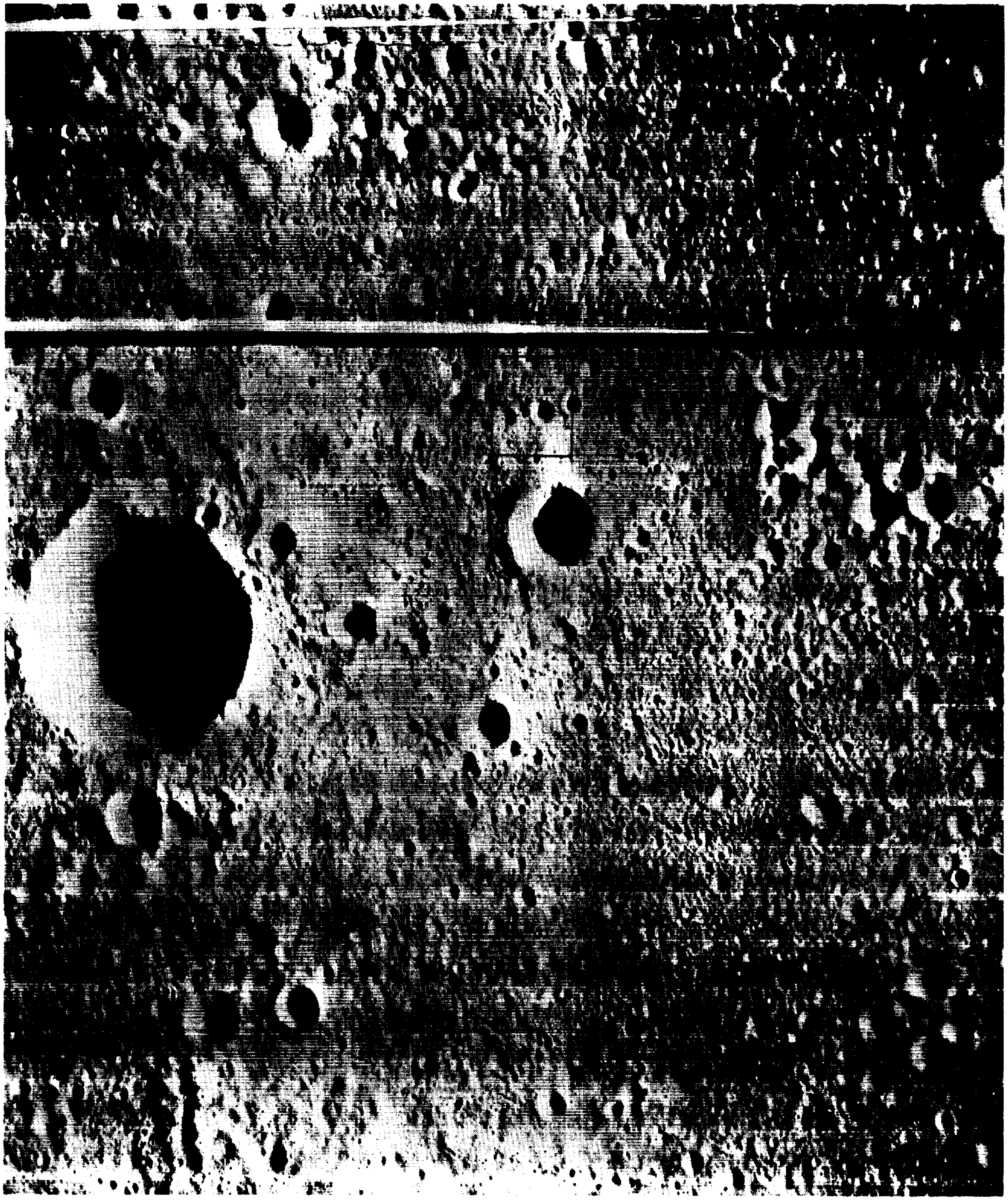

Figure 1.4-7: **Wide-Angle Frame 61 — Site IIP-4** Framelet Width: 1.61 km

Large crater is Ariadaeus B.

Outlined area covered by Figure 1.4-9.

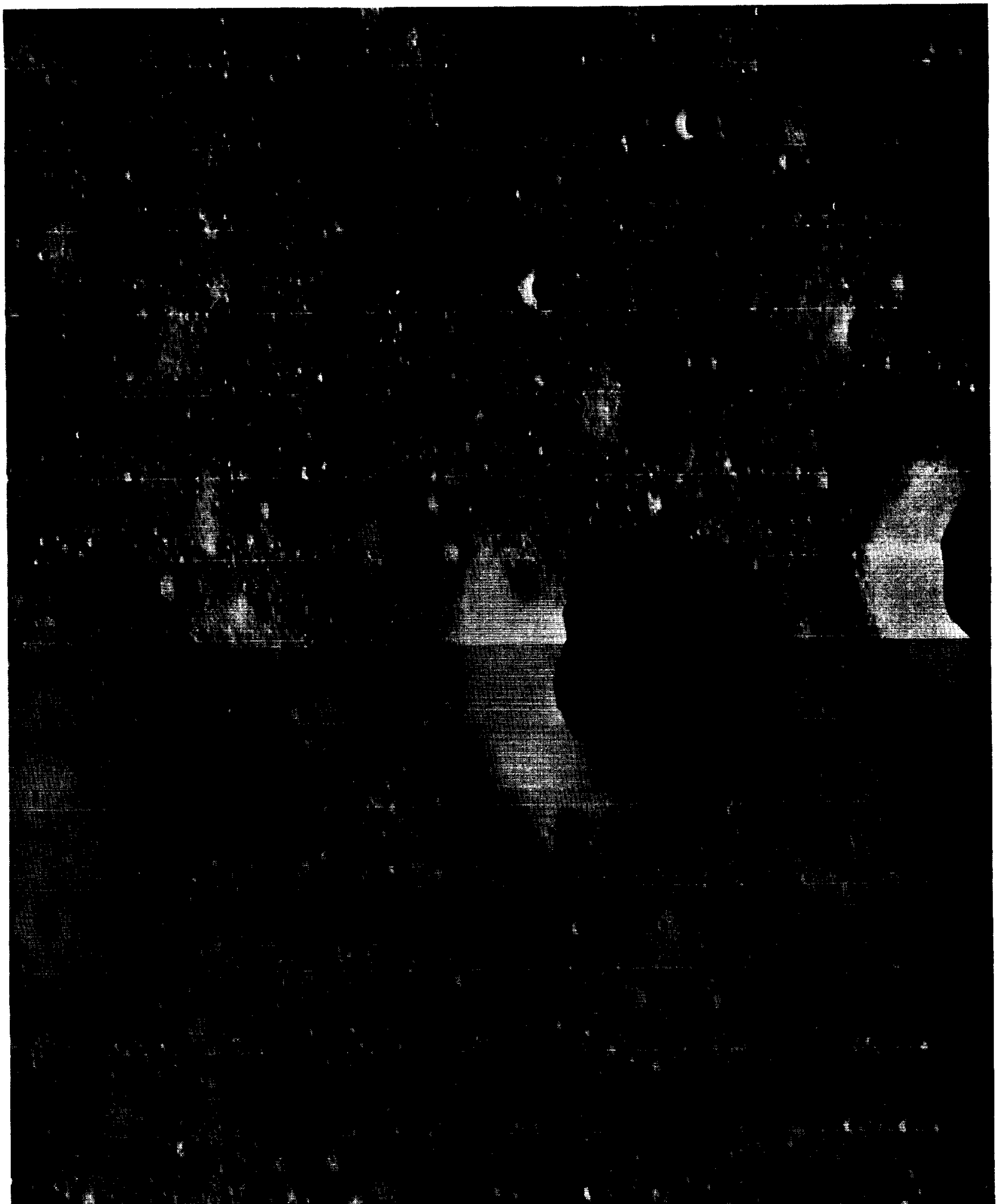

Figure 1.4-8: **Section of Telephoto Frame 61 — Site IIP-4** Framelet Width: 0.208 km
General surface characteristics where spires were observed between and below two larger craters

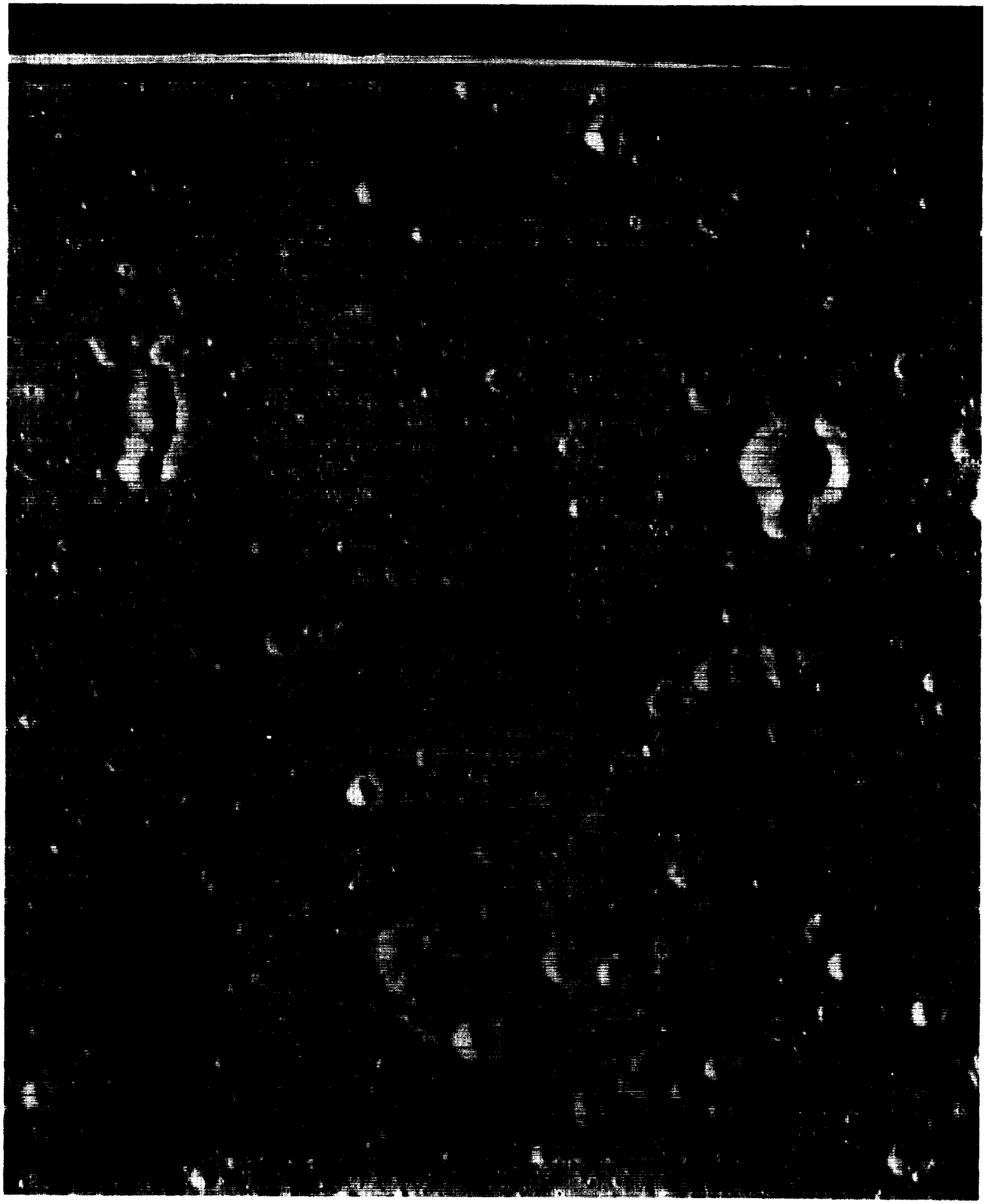

Figure 1.4-9: **Wide-Angle Frame 69 – Site IIP-5** Framelet Width: 1.40 km
Outlined area indicates Ranger VIII impact area.
Wide line near top is a processor stop line.

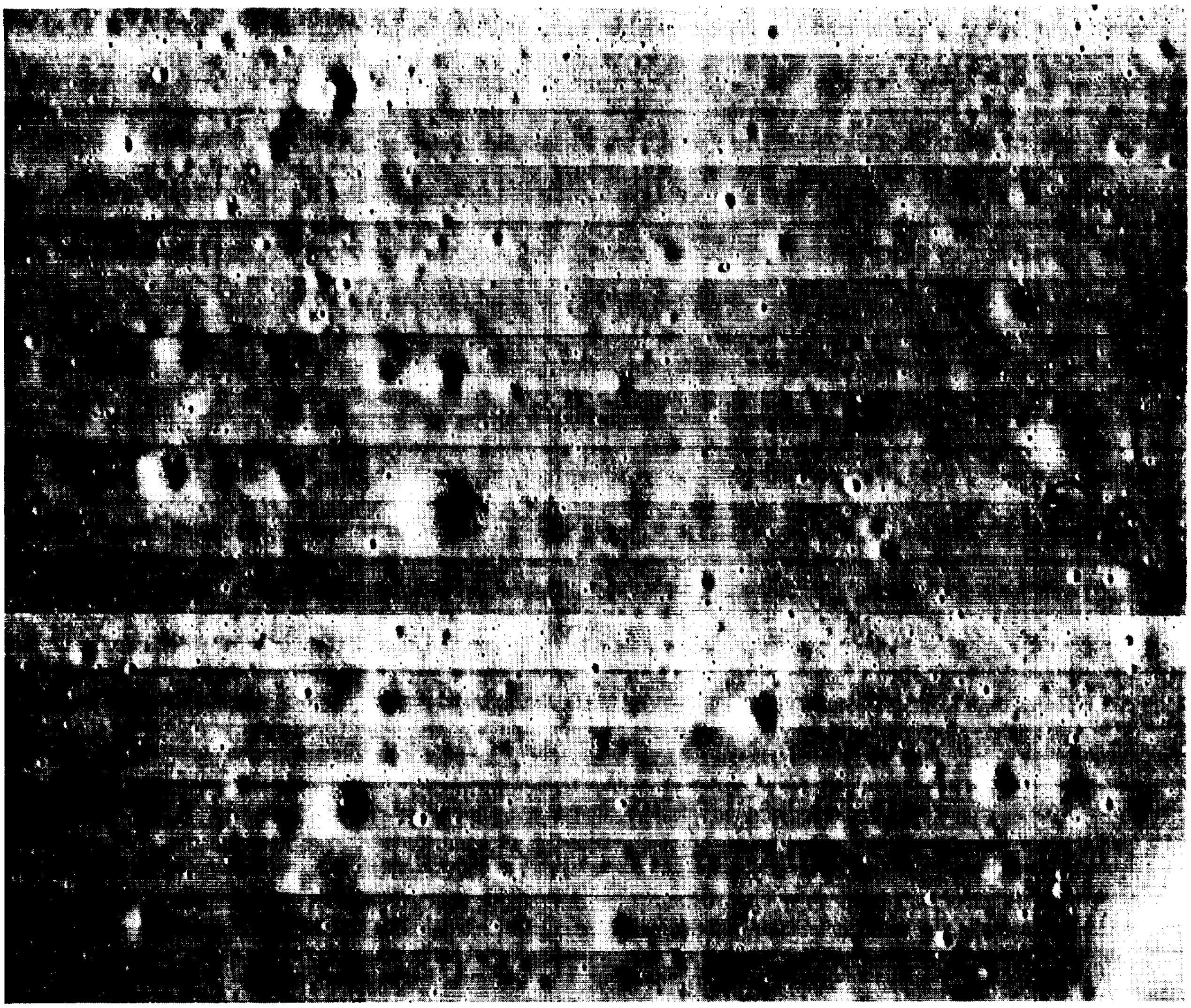

Figure 1.4-10: **Section of Telephoto Frame 70 – Site IIP-5** Framelet Width: 0.181 km
Outlined area shows Ranger VIII impact area.

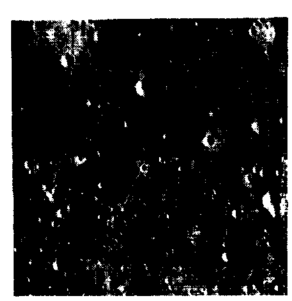

Figure 1.4-11:
Section of Telephoto Frame 70 – Site IIP-5
Blowup of probable Ranger VIII impact craters.

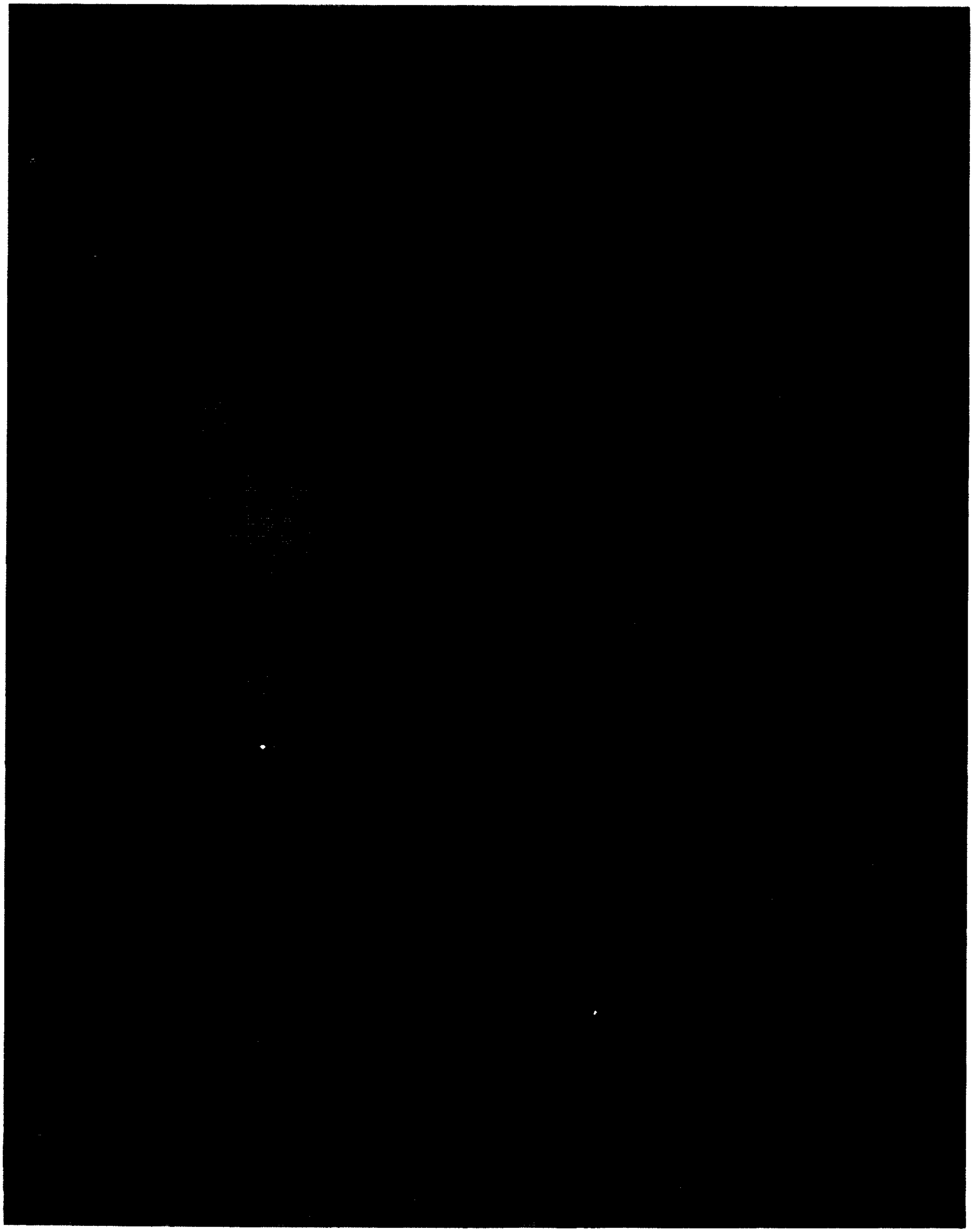

Figure 1.4-12: **Section of Telephoto Frame 73 – Site IIP-5** Framelet Width: 0.182 km

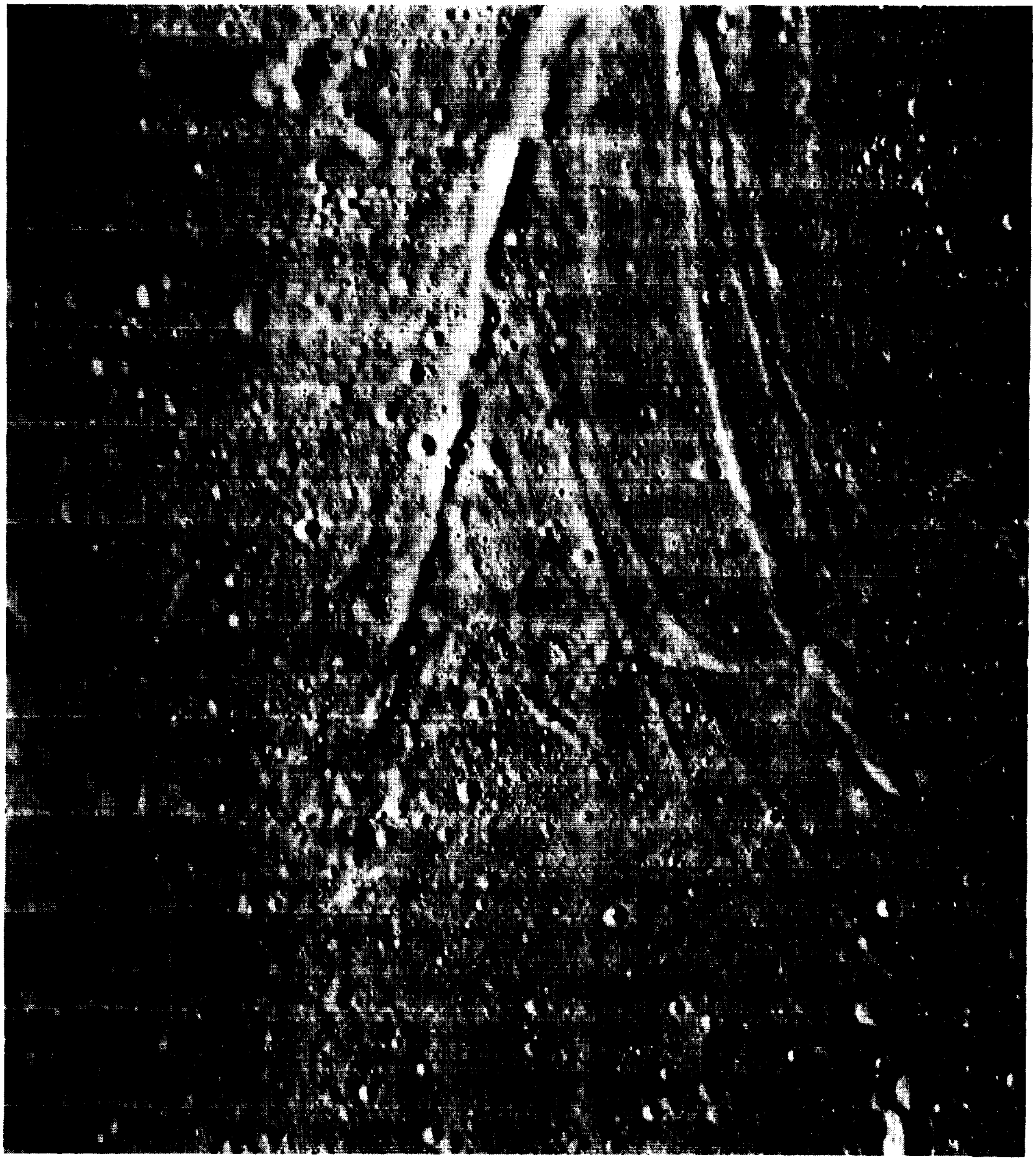

Figure 1.4-13: **Wide-Angle Frame 43 – Site IIP-3**

Framelet Width: 1.55 km

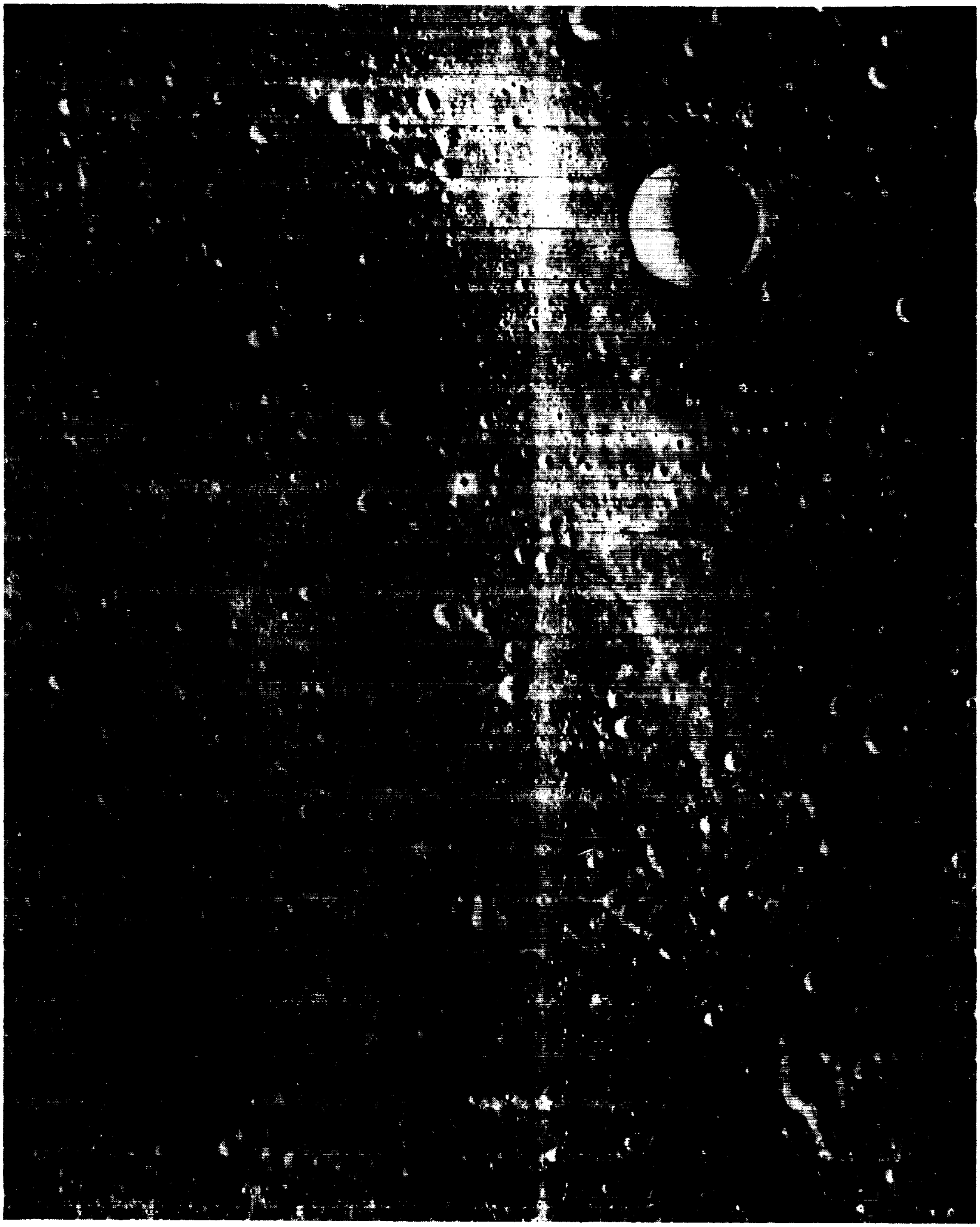

Figure 1.4-14: **Wide-Angle Frame 83 – Site IIP-6** Framelet Width: 1.54 km
Large crater is Sabine E.

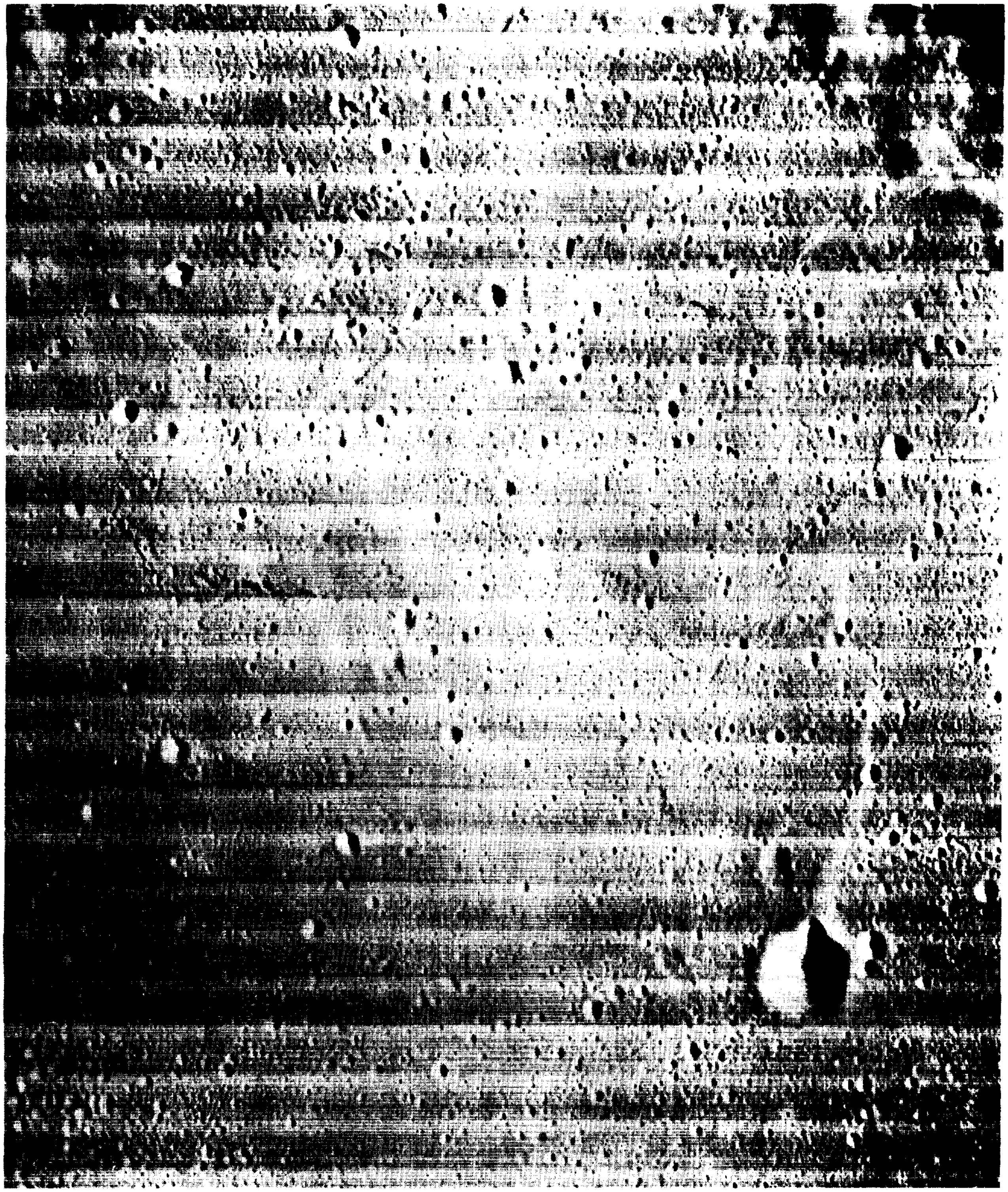

Figure 1.4-15: **Wide-Angle Frame 108 – Site IIP-7** Framelet Width: 1.32 km

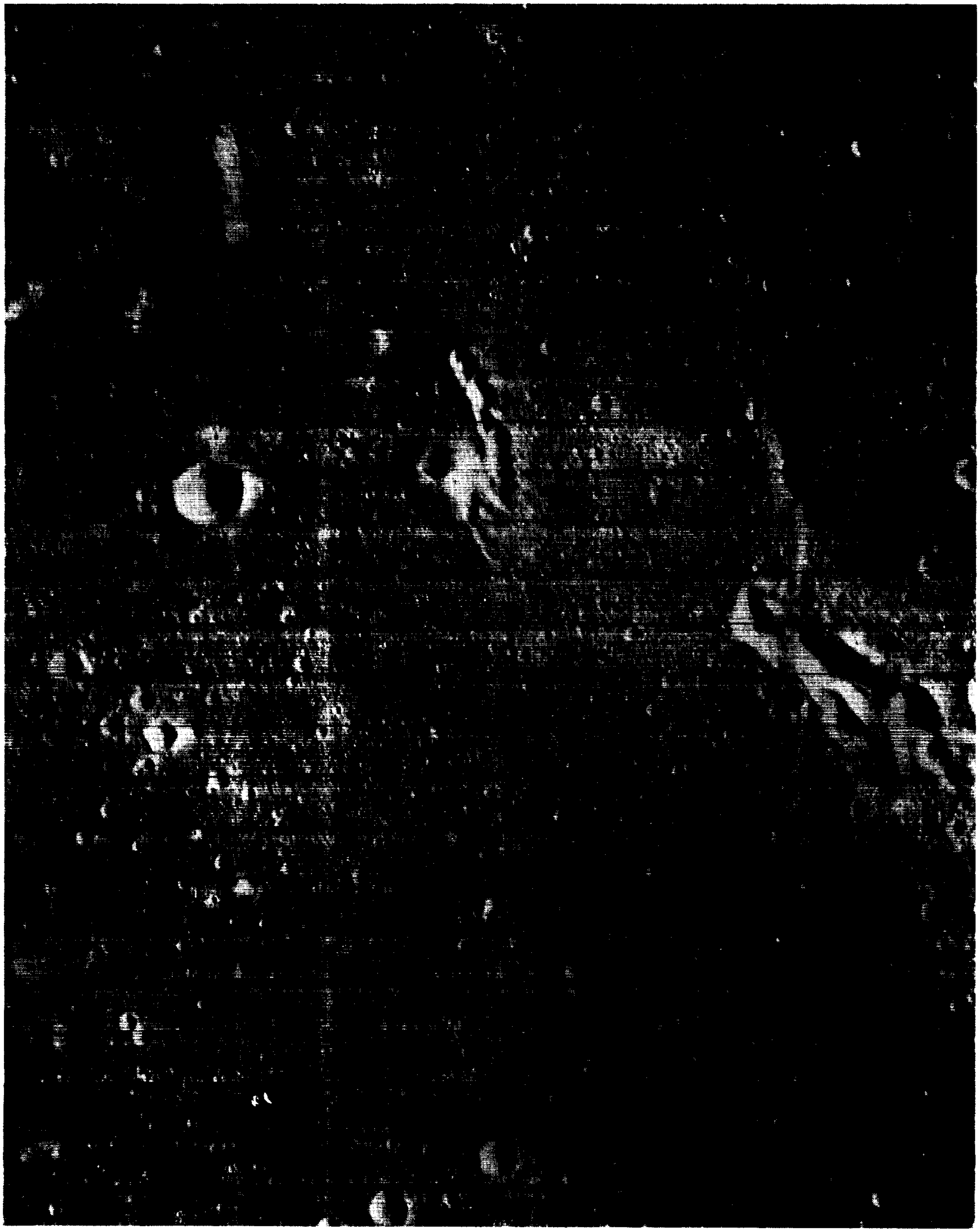

Figure 1.4-16: **Wide-Angle Frame 140 — Site IIP-9** Framelet Width: 1.43 km

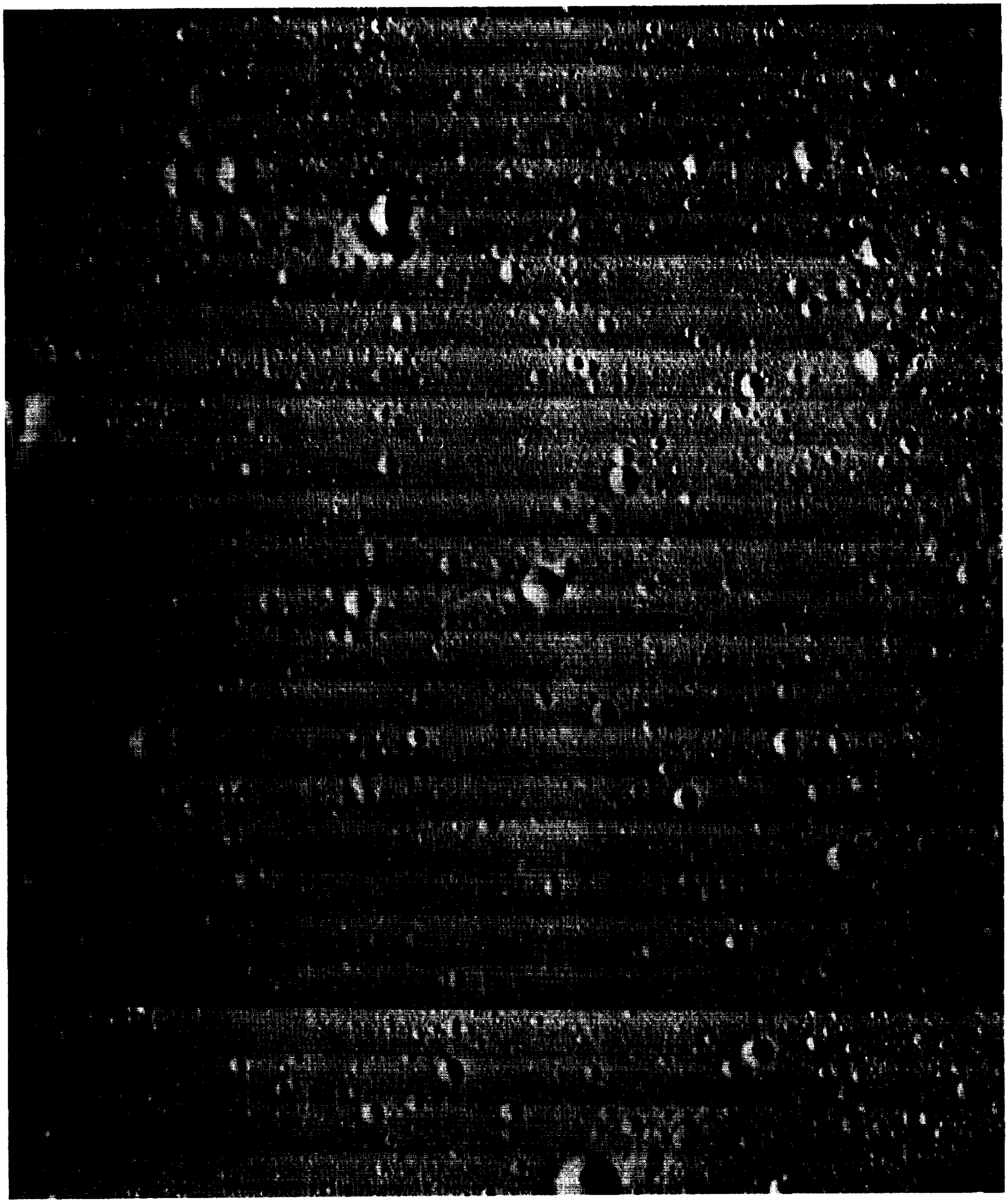

Figure 1.4-17: **Wide-Angle Frame 154 – Site IIP-10** Framelet Width: 1.39 km

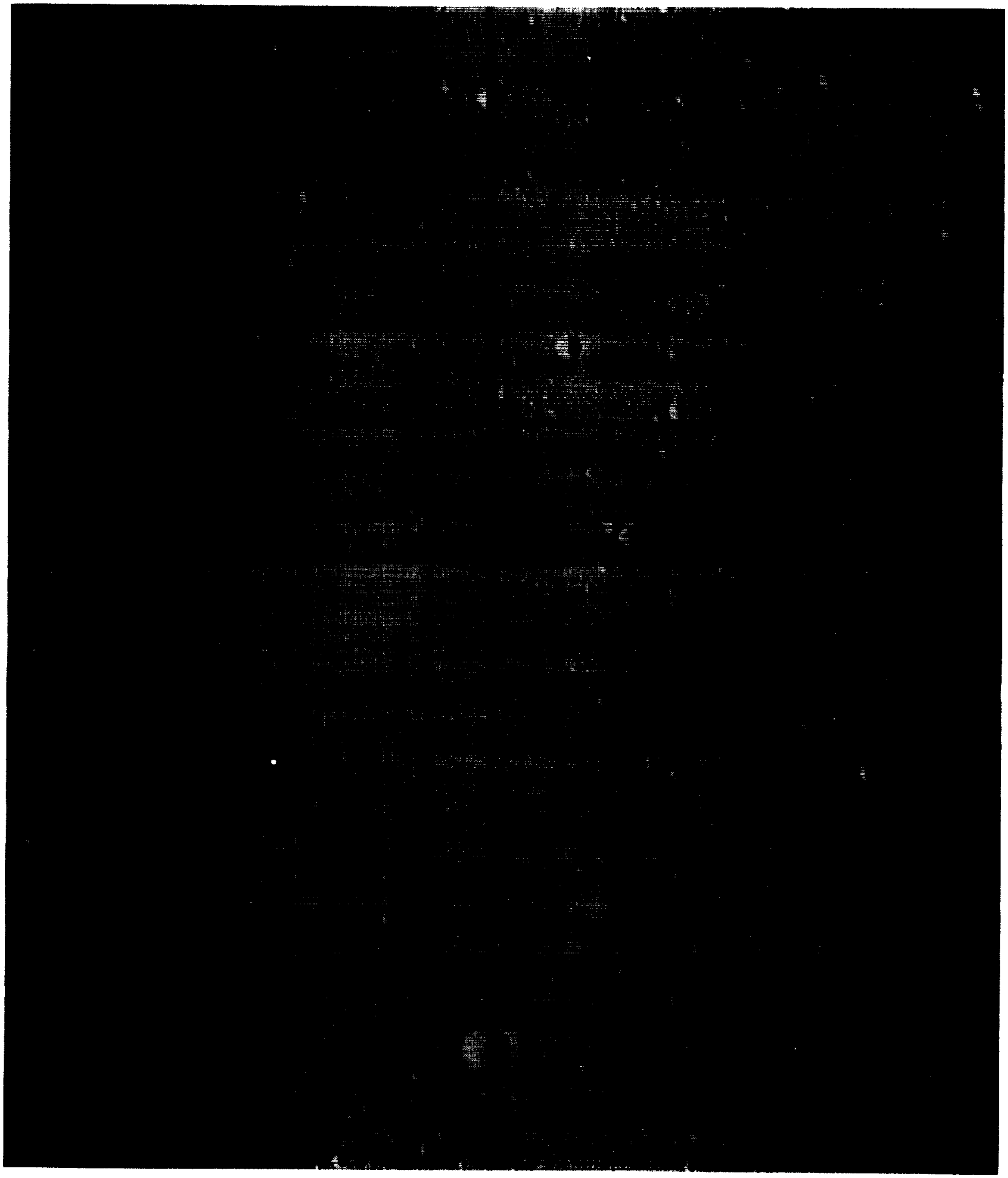

Figure 1.4-18: **Wide-Angle Frame 193 — Site IIP-12** Framelet Width: 1.43 km

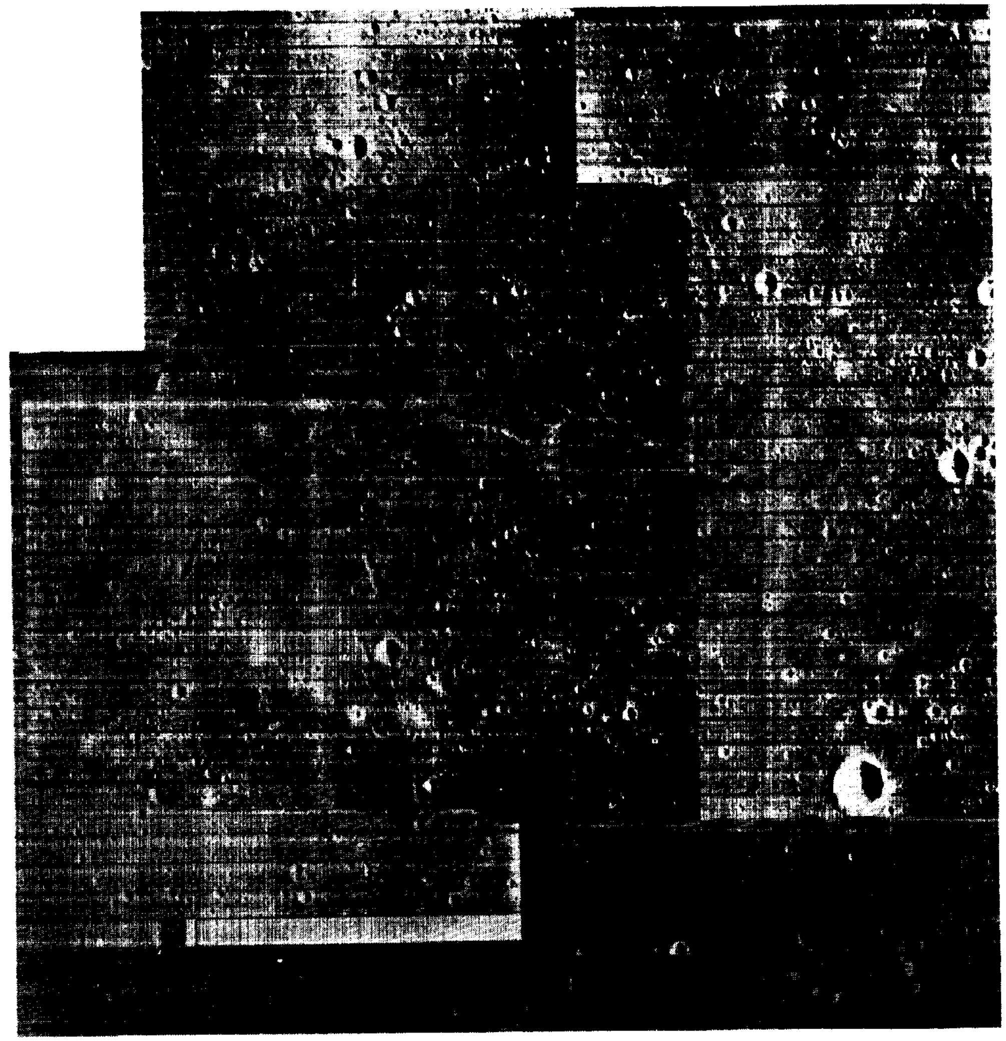

Figure 1.4-19: **Wide-Angle Coverage – Site IIP-8** Framelet Width: ≈ 1.6 km
Mosaic made by NASA to support screening evaluations

Figure 1.4-20: **Wide-Angle Coverage – Site IIP-11** Framelet Width: ≈ 1.7 km
Outlined area covered by Figure 1.4-21
Mosaic made by NASA to support screening evaluations

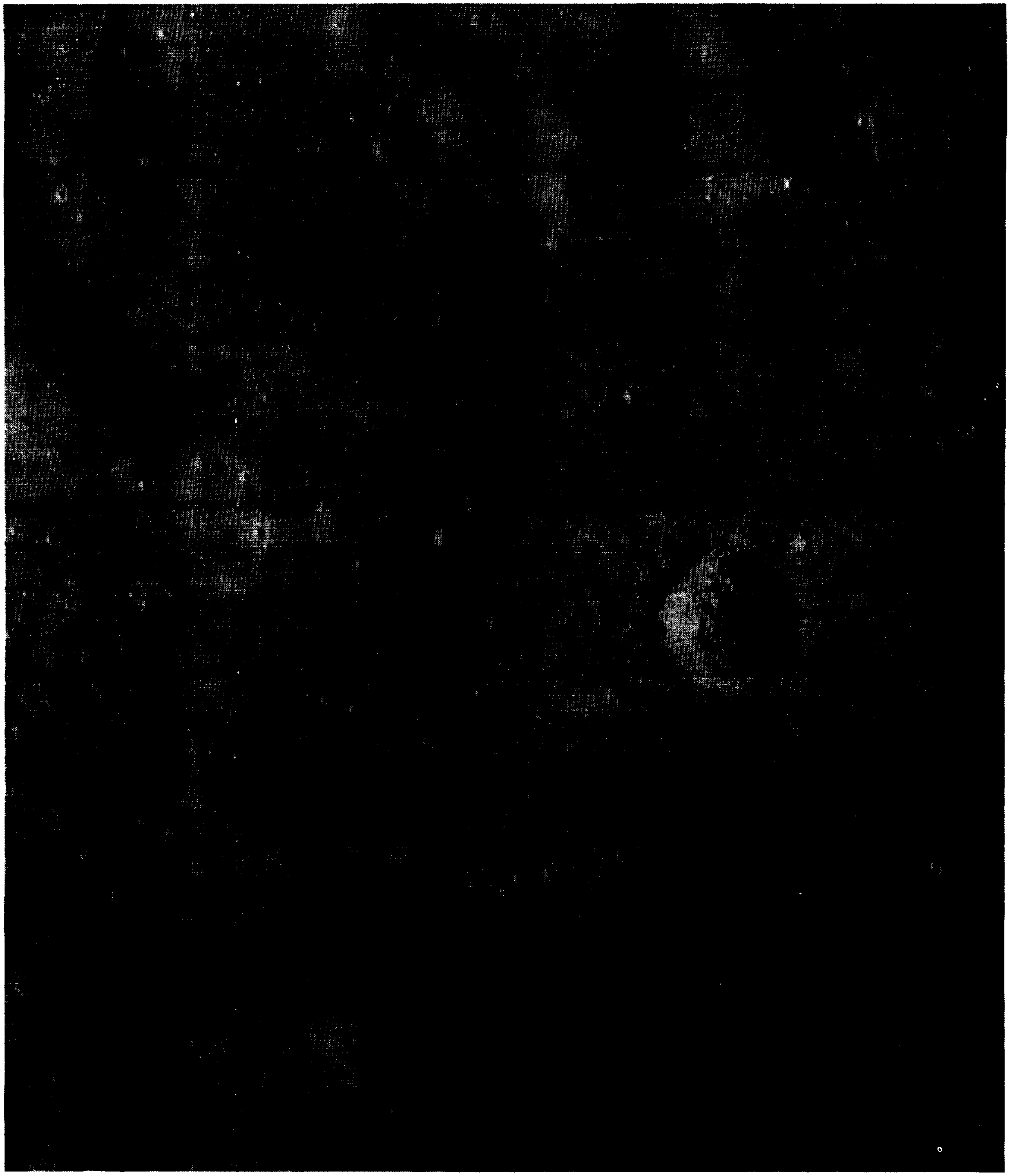

Figure 1.4-21: **Section of Telephoto Frame 177 — Site IIP-11** Framelet Width: 0.229 km
Shows small surface objects and detail

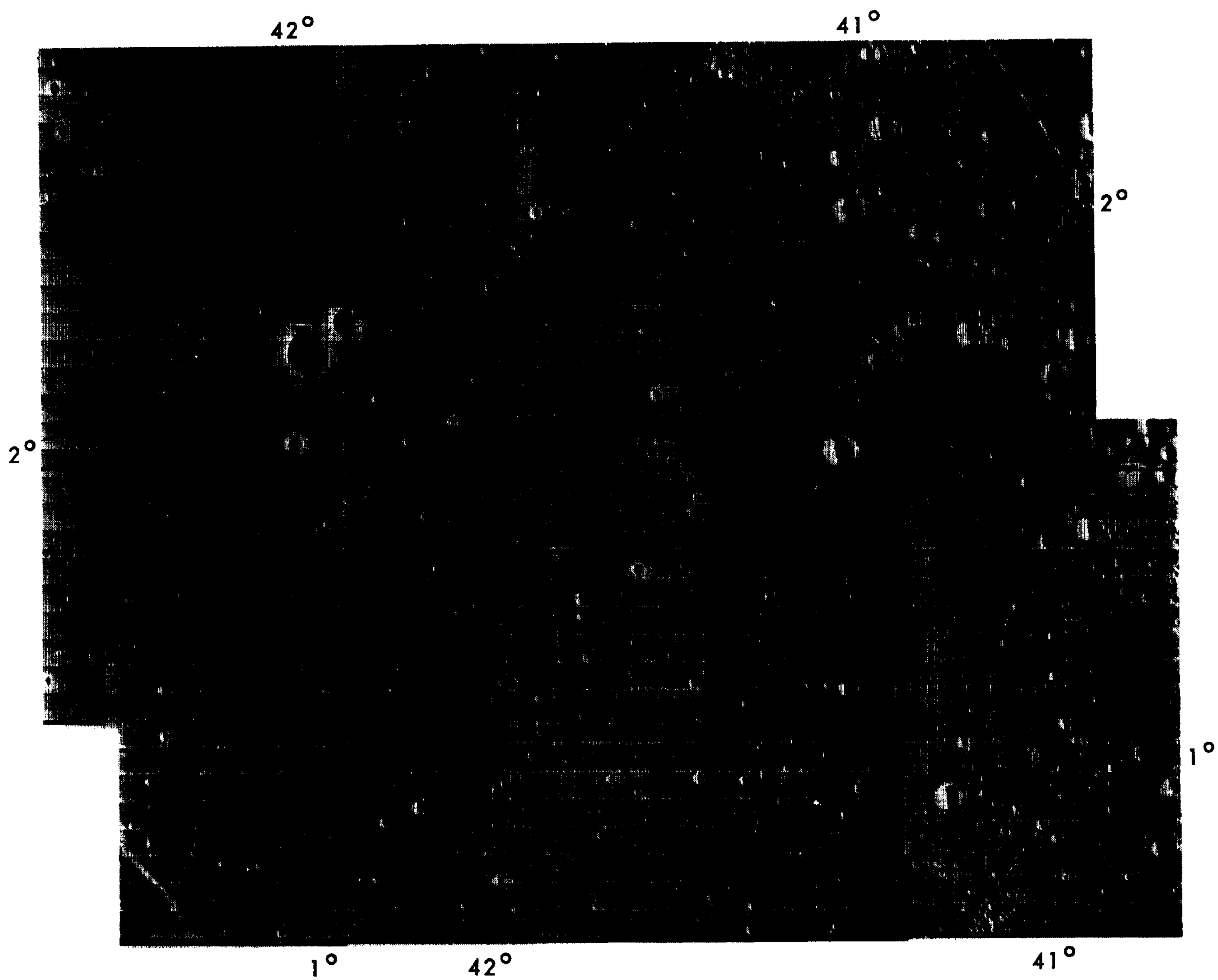

Figure 1.4-22: **Wide-Angle Coverage – Site IIP-13** Framelet Width: ≈ 1.5 km
Mosaic made by NASA to support screening evaluations

1.4.2 ENVIRONMENTAL DATA

Two types of telemetry instrumentation were installed on Lunar Orbiter II to monitor lunar environmental conditions. Two radiation dosimeters were mounted adjacent to the photo subsystem. Twenty individual micrometeoroid detectors were circumferentially mounted on the tank deck.

Radiation Data

Dosimeter 1 (DFO4), located near the film cassette, had a sensitivity of 0.25 rad per count, with a capacity of 0 to 255 counts. Dosimeter 2 (DF05), located near the camera looper, had a sensitivity of 0.5 rad per count and a similar capacity of 0 to 255 counts. Due to the inherent shielding of the spacecraft, the photo subsystem structure, and the 2-grams-per-square-centimeter aluminum shielding provided the film supply cassette, it was estimated that solar flares of magnitude 2 or less would have a negligible effect on the undeveloped film. Flares of magnitude 3 or greater would produce considerable fog on the film.

Radiation encountered during the Lunar Orbiter mission came from two sources: Van Allen belts and galactic-cosmic radiation. It was expected that the amounts of radiation received from the Van Allen belts and from galactic-cosmic sources would have little or no effect on the photographic mission.

During Lunar Orbiter II's mission, the radiation dosimetry measurement system (RDMS) functioned normally and provided data on the Earth's trapped radiation belts and the radiation environment encountered by the spacecraft during cislunar and lunar orbiting mission phases.

Dosimeter 1 (DF04) verified that the spacecraft penetrated the Van Allen belts and recorded a total radiation dose of 0.75 rad at the film cassette.

Dosimeter 2 (DF05) was not turned on until the spacecraft had emerged from the Van Allen belts. At the end of the photo mission, Dosimeter 1 recorded a total dosage of 1.75 rads while Dosimeter 2 indicated a total of 1.0 rad. The individual state changes of these detectors is shown in Table 1.4-5.

Micrometeoroid Data

During the photographic portion of Mission II, three micrometeoroid hits were recorded by the detectors mounted on the periphery of the tank deck. The hits were recorded as follows by discrete channel state change recorded at:

Detector 4 during Day 319 - 12:45:40 GMT
Detector 5 during Day 329 - 17:22:56 GMT (at Earthrise)
Detector 13 during Day 338 - 02:04:47 GMT

No detectable effect on the operation of the spacecraft was observed.

The actual time of impact on Detector 5 is not known because the event occurred during an Earth occultation period. Figure 1.4-23 shows the position of the spacecraft with respect to the Moon and the roll position of the detector at the time of the recorded impact. The location of the detectors about the tank deck is also shown.

The telemetered tank deck temperature data indicated a possible additional hit near the instrumentation thermistor. This temperature anomaly began about 30 seconds after sunrise of Orbit 29 and produced a deck temperature rise of 1.5°F over a period of 4 minutes as shown in Figure 1.3-10. The temperature rise could be attributed to conversion of the kinetic energy of the micrometeoroid into thermal energy at impact.

The increased micrometeoroid activity detected during Mission II may be related to the annual meteoric shower attributed to the shooting star Leonid. This star activity occurs in mid-November of each year.

1.4.3 TRACKING DATA

Improved orbit determination procedures, based

Table 1.4-5: Radiation Data Summary					
GMT Time of Change				Radiation Counter	New Reading (rad)
Days	Hours	Min	Sec		
311	00	25	40.8	DF04	0.50
311	00	44	29.8	DF04	0.75
318	04	15	43.2	DF04	1.00
325	20	11	7.2	DF05	0.5
325	21	05	15.9	DF04	1.25
332	16	11	07	DF04	1.50
340	13	48	16	DF04	1.75
340*	16	(03-13)		DF05	1.0

*This state change occurred during an Earth occultation period.

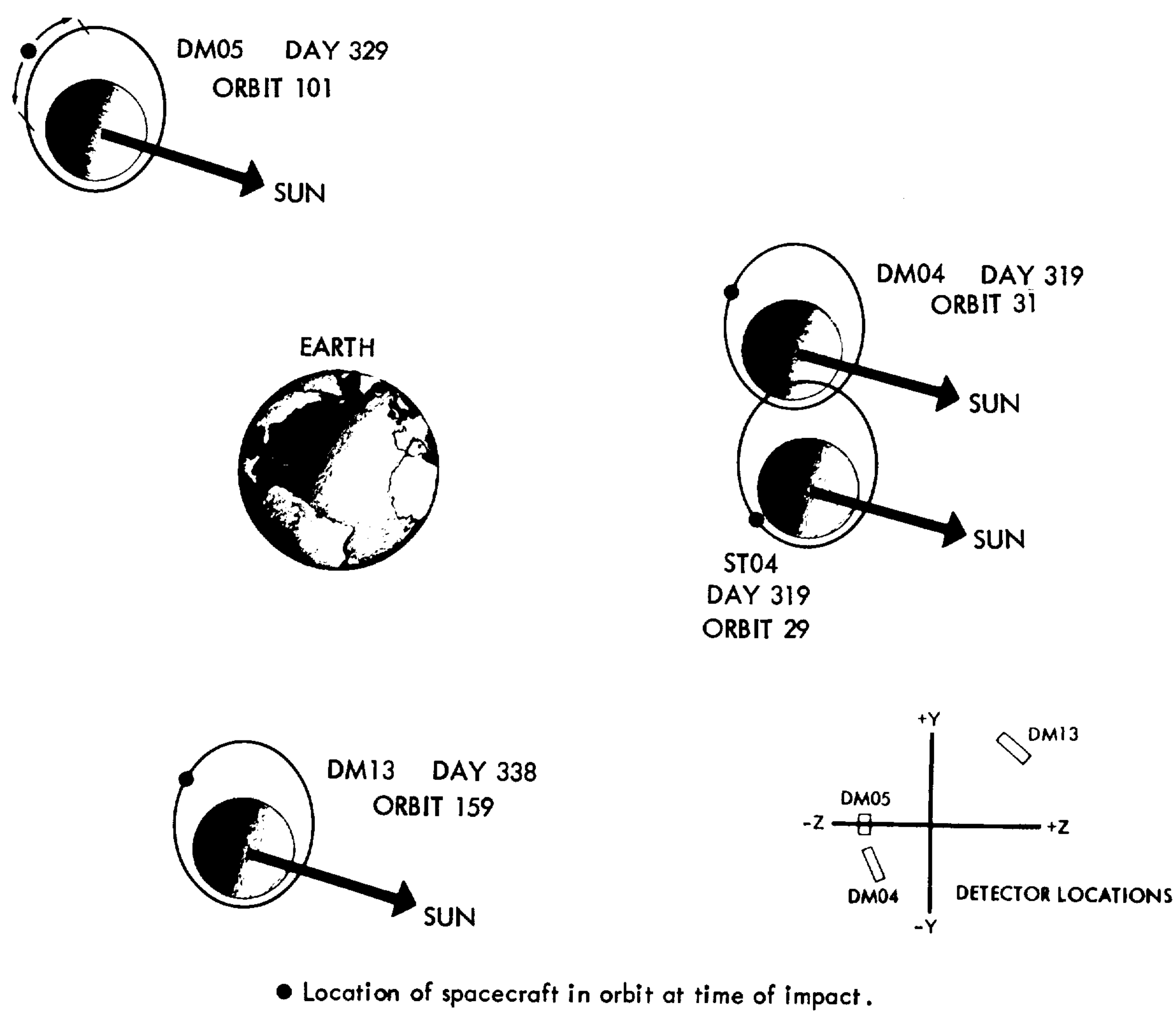

Figure 1.4-23: Geometry of Micrometeoroid Hits

upon Mission I experience and the improvement in the lunar gravitational field estimates developed by Langley Research Center from Mission I selenodetic data, resulted in a larger percentage of good data available at the SFOF. Prior to the TWTA failure a total of 819 station hours of tracking data was obtained by the Deep Space Network. Over 200 hours of spacecraft ranging was performed. The 36 time correlation checks completed enable the synchronization of the station clocks to within 50 microseconds or better. All of this data has been furnished to NASA and will be further elevated to refine the mathematical model of the Moon. The following discussions are pertinent to the quality of the tracking data obtained and the performance accuracy of the tracking system.

DSIF Tracking Data System

The overall performance of the DSIF Tracking Data System was very good with no loss of data during the entire photographic mission. There were some areas of improved data acquisition as the result of procedural changes and the addition of new software at the sites. Significant changes were:

- Ranging data was taken earlier in the mission and more frequently than in Lunar Orbiter I, providing the Orbit Determination Program (ODP) with another data type.
- Time correlation experiments were carried out more frequently.
- Doppler data was obtained during the photo readout phase by using Receiver 2 in an AGC mode, resulting in usable doppler data during a time period that was essentially wasted on Lunar Orbiter I from an orbit determination point of view.
- The antenna positioning system was used at all the stations for most of the lunar orbit phase.
- The Interim Monitor Program was used at all the sites to allow them to evaluate their own performance and alert the SFOF to any indication of malfunction.

The orbit determination computations were generated at various times in the mission, depending on the availability of improved state vectors from the ODP, and in general were far better than previous missions due to the better lunar harmonic coefficients and to corrected occultation time computation. All errors were within $\pm$ 300 Hz in doppler and about 30 seconds in occultation times during the lunar orbit phase.

Lunar Orbiter Mission II provided an opportunity to fully analyze ranging as a data type throughout the mission. Data was obtained in nearly a continuous manner during nonoccultation periods and thus significantly aided the re-establishment of the orbit after engine burn periods.

Transmission of the ranging code was reversed in phase from the received code apparently due to a wiring error in the transponder. This Lunar Orbiter II spacecraft transponder phase reversal made the ranging data indicate the range was a half module number greater than the actual range. One-half module number is about the distance to the Moon, or exactly 392,881,104 range units (one range unit is about 1.04 meters). This was easily compensated for by adding this amount to the internal spacecraft and ground station delay values which are removed from the data in the Orbit Data Generator Program. The 1σ noise on the data seemed slightly less on this mission. It ranged from a low of 2 meters to a high of 10 meters. Since the noise increased as the spacecraft went into lunar orbit, the estimated 10-meter figure is the sum of orbit uncertainty, program numerical significance problems, and ranging system noise.

Tracking Data Validation

The tracking data validation function was accomplished with the aid of the Tracking Data Monitor Program (TDM) at Goldstone. Two-way doppler data was backfed to the computer facility at DSS-12 and processed in the tracking data monitor (TDM). The program computes observed minus predicted values for the two-way doppler and the angles. It also computes a running standard deviation on the last five points. In addition the program removes any large biases or trends and computes pseudo-residuals and standard deviation from the detrended data. In this manner any inaccuracies due to the predicts will not affect the data quality estimates. The output was transmitted to the SFOF by teletype and printed in tabular form. It was also plotted on the Milgo 30 by 30 printer through the 7044 plot routine. Overall program performance was greatly improved over Lunar Orbiter I.

In the cislunar phase the TDM generated its own predicted quantities by means of an internal trajectory subprogram. In this phase the predicts were very accurate and the residuals remain less than 1 Hz. The noise computed by the detrended method was less than 0.1 Hz, confirming that the data was of high quality. The internal trajectory routine was unable to compute predicts in lunar orbit; therefore, the regular JPL predicts were transmitted to the program during this phase as a base for the residual computation.

Tracking Data Quality

After injection into the initial lunar ellipse, ranging data again showed its usefulness. The first orbit estimates obtained showed biases in range of several kilometers and skewed residuals, indicating a poor estimate. These estimates gave parameter values slightly off the planned values (i.e., orbit after motor burn). However, when more data was added to the fit, the ranging residuals dropped to 100 meters and were no longer skewed and the estimates also were much closer to the predicted values. Approximately 12 hours of data is required to re-establish a good orbit in the lunar orbit phase. The ranging data shows good agreement with Dr. Eckert's corrections to the lunar ephemeris as shown in Figure 1.4-24. There was only about a 100-meter departure from his correction and the range residual obtained from our uncorrected lunar ephemeris.

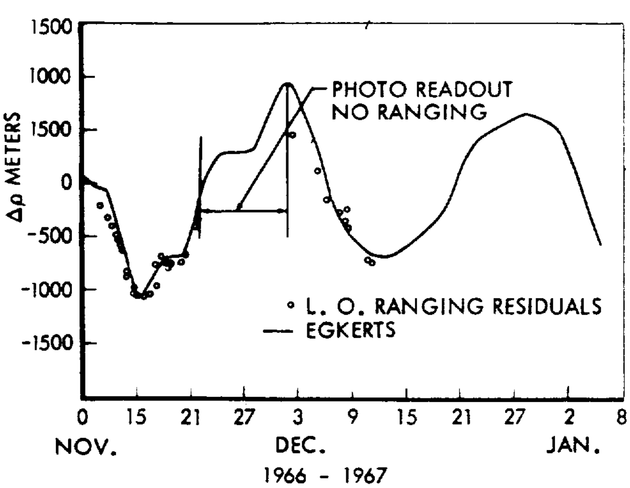

Figure 1.4-24: Ranging Data Residuals

Usable tracking data was obtained during photo readout by using a second receiver to enable recording of the data. The noise level was increased by approximately a factor of 5 higher than normal, but there was no detectable bias and good orbit estimates were obtained. Toward the end of the photo readout phase there was some difficulty encountered in obtaining good convergence. This is not believed to be attributable to the data quality; once convergence was obtained, the data residuals were normal and consistent. Areas of investigation along this line of convergence were: (1) the low altitude and strong potential effect (i.e., 27-km altitude compared to 50 otherwise); (2) possible poor partials near pericenter causing a singularity; and (3) the choice of epoch for initial conditions. (This is related with item 2 above). Since data near pericenter still cannot be fit to a random noise level and its use introduces unknown biases, the policy of omitting pericenter data (20 minutes each side of pericenter) was used throughout the mission. Investigation of orbit estimates and predictions based on orbits determined without pericenter data were a factor of approximately two better than those using pericenter data. This does not mean that pericenter data is not desirable. It is important data for selenodesy reduction and the determination techniques of data handling for future missions.

Tracking data quality reports were made consistently throughout the active mission. The data quality was excellent, surpassing DSN's performance on Lunar Orbiter I. There were fewer anomalies and TTY data received at JPL was cleaner and much more usable, not only due to DSN obtaining two-way and three-way doppler and ranging throughout, but also due to good spacecraft performance.

DSN Data Recordings

Tracking data were recorded at the Deep Space Stations and the Space Flight Operations Facility to satisfy requirements for the selenographic data. The Deep Space Station recording was a five-level teletype paper tape. During the mission, the tracking data were transmitted to the SFOF via normal teletype messages. At the Space Flight Operations Facility teletype data were received by communications terminal equipment and passed to the raw data table on the 1301 disk by the IBM 7044 I/O processor. These data were processed by the TTYX program to separate the telemetry data and tracking data in the messages received, and stored on the tracking raw data file on dish. The tracking data processor (TDP) program generated the master tracking data table on the 1301 disk by smoothing and sorting the data from the tracking raw data file by Deep Space Station identification.

The output of this program was also recorded on magnetic tape and identified as the tracking data deliverable to NASA. An orbit data generator routine extracted selected master data file tracking data, smoothed it, sorted it according to time, and inserted it in the orbit determination program input file. Upon command from the FPAC area, orbit parameters were computed or predicted, based upon the selected data from the orbit determination program input file and the orbit determination program, and inserted into the data display files for subsequent display by the user.

The raw tracking data paper tapes recorded at each Deep Space Station and the output of the tracking data processor at the Space Flight Operations Facility, recorded on Magnetic tape, were collected and delivered to NASA for follow-on selenodeteic analysis purposes.

1.4.4 PERFORMANCE TELEMETRY

Spacecraft performance telemetry data was obtained via three different methods.

Prior to spacecraft separation the data was transmitted via assigned subcarriers of the VHF Agena telemetry link. This data was recorded at AFETR and, after real-time demodulation, transferred to DDS-71 (Cape Kennedy) for retransmission to the SFOF computers. In addition, the AFETR stations recorded the S-band signal directly from the spacecraft. After separation the performance data was received directly from the spacecraft by the Deep Space Stations and reformatted for transmission to the SFOF. In all cases, the data was available for the subsystem analyst to continuously monitor the operational status of all spacecraft subsystems and environmental conditions.

The performance telemetry data obtained via "S" band transmissions, as recorded by the AFETR instrumentation stations and ships, is summarized in Figure 1.4-25.

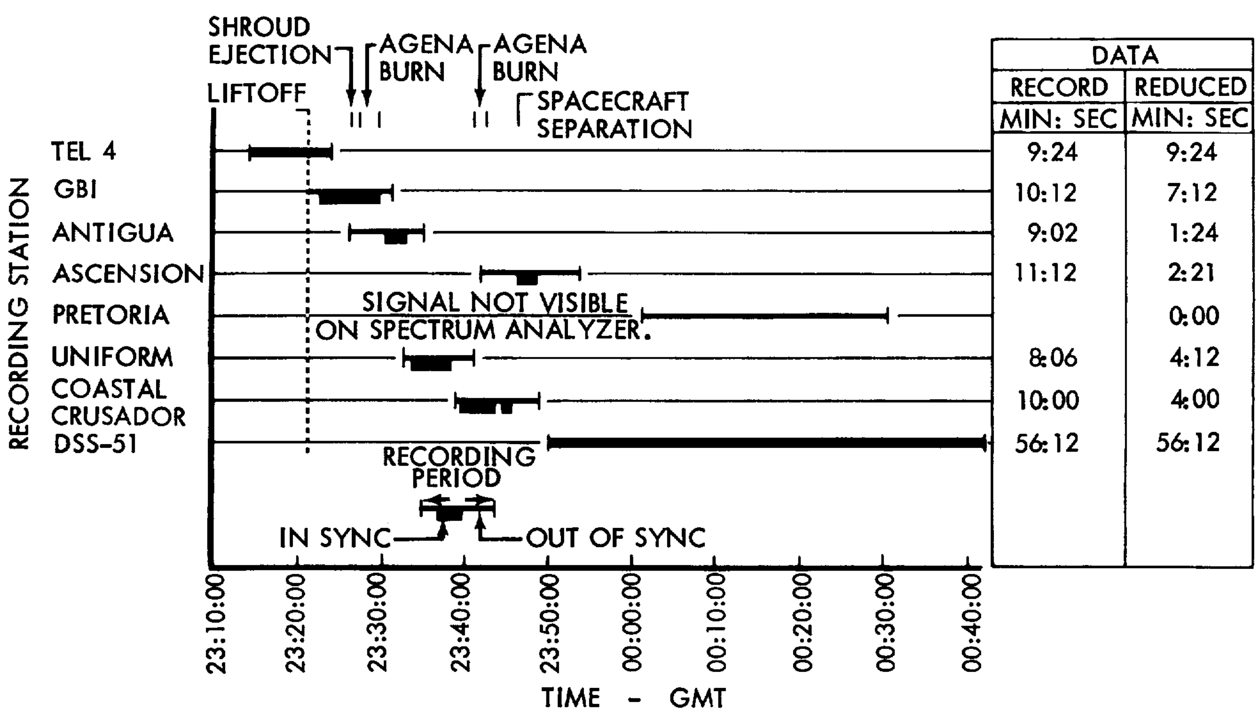

Figure 1.4-25: AFETR Telemetry Summary (S-Band)

Mission Support by the DSN began 6 hours prior to liftoff on November 6, 1966, on a 24-hour coverage basis, and terminated with the conclusion of photo readout on December 7, 1966. Table 1.4-6 summarizes the data recorded by the DSN during this period.

Table 1.4-6: DSN Telemetry Summary

Deep Space Station	Total Passes	Telemetered Frames		Percent Recovered
		Transmitted	Recorded	
Goldstone	30	27,094	26,776	98.8
Woomera	31	32,663	31,317	95.9
Madrid	30	31,772	30,490	96.0
Total		91,529	88,583	96.9

Wide-Angle Frame 75 — Site IIS-5
Looking south on farside

1.5 MISSION EVALUATION

Lunar Orbiter II made significant additions to the accomplishments of Lunar Orbiter I as related to the techniques and data required to land a man on the Moon and return him safely to Earth. These accomplishments included but were not limited to:

- Provided large-area photographic coverage (including stereo photography) of 13 potential Apollo landing sites with a nominal 1-meter resolution capability.
- Demonstrated the techniques and feasibility of accurately positioning the spacecraft to obtain oblique photos of large areas of the lunar surface, including coverging telephoto stereo photographic coverage.
- Obtained high-quality oblique photos of both the near- and farside of the Moon which adds significant visibility for developing navigational methods and techniques, and the selection of landmarks for use by the Apollo astronauts.
- Verified the improvement in orbit determination and prediction accuracy obtained by incorporating the updated lunar mathematical model coefficients developed from the evaluation of the Mission I tracking and selenodetic data.
- Provided high-quality photos of the Ranger VIII impact area and identified the crater created by impact as one of two craters approximately 90 meters apart.
- Concurrent recording of Lunar Orbiter transmissions by two tracking sites provides data that may result in an improvement of resolution because of partial white noise cancellation in the areas of multiple recording.
- Obtained extensive data to fully analyze ranging as a data type throughout the mission.
- Recorded station time-check data to provide station clock synchronization to within 50 microseconds or better.

Mission II was considerably more complicated than Mission I in that all of the film-set photos were designated as secondary photo sites. This made a total of 30 sites to be photographed. Experience gained from Mission I enabled the operations team to prepare premission planning to provide the required control and look-ahead visibility while reducing the stress on the operating team. The addition of an off-line planning group was a significant factor in the smooth conduct of the mission. The overall effect was that, with minor exceptions, the total mission was conducted as planned.

The failure of the traveling-wave-tube amplifier on the last day of the photo mission prevented final readout of approximately one half of primary Site IIS-1 photos. Priority readout data of this site completed the wide-angle coverage of the site and provided sections from six of the eight telephoto frames, thus reducing the actual loss of data. All of the reconstructed photos were of usable quality and the telephoto coverage provided extensive and detailed visibility of the lunar surface approaching 1-meter resolution.

Lunar Orbiter II recorded three known micrometeoroid impacts over a 19-day period with no noticeable effect on the spacecraft performance. It is believed that these impacts may have been the result of the annual Leonid shower.

Spacecraft temperature control was smoothly integrated into the operational sequence. Thermal paint degradation was improved by the additional coating of S-13G, but the spacecraft had to be oriented off the sunline in a routine manner to maintain thermal control.

The overall performance of the spacecraft and the near completion of this complex mission as planned again demonstrates the extensive capability of the command and control concepts employed.

NASA-Langley, 1967 —— 31 CR-883